

UNCLASSIFIED

AD 401 458

*Reproduced
by the*

DEFENSE DOCUMENTATION CENTER

FOR

SCIENTIFIC AND TECHNICAL INFORMATION

CAMERON STATION, ALEXANDRIA, VIRGINIA



UNCLASSIFIED

NOTICE: When government or other drawings, specifications or other data are used for any purpose other than in connection with a definitely related government procurement operation, the U. S. Government thereby incurs no responsibility, nor any obligation whatsoever; and the fact that the Government may have formulated, furnished, or in any way supplied the said drawings, specifications, or other data is not to be regarded by implication or otherwise as in any manner licensing the holder or any other person or corporation, or conveying any rights or permission to manufacture, use or sell any patented invention that may in any way be related thereto.

63 3-2

ASD-TR-61-667
VOLUME III

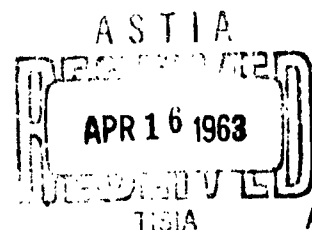
CATALOGED BY ASTIA
AS AD No. 401458

**ELASTO-PLASTIC ANALYSIS OF STRUCTURES
UNDER LOAD AND TWO-DIMENSIONAL
TEMPERATURE DISTRIBUTIONS**

**VOLUME III. EXPERIMENTAL EVALUATION
OF THE GENERAL TIME-DEPENDENT
ANALYSIS**

TECHNICAL REPORT No. ASD-TR-61-667, VOL. III

MARCH 1963



401 458

**FLIGHT DYNAMICS LABORATORY
AERONAUTICAL SYSTEMS DIVISION
AIR FORCE SYSTEMS COMMAND
WRIGHT-PATTERSON AIR FORCE BASE, OHIO**

Project No. 1467, Task No. 146701

(Prepared under Contract No. AF 33(616)-7738,
BPS No. 2(1-1367)-14002 by
Martin Marietta Corporation, Baltimore Division, Baltimore, Maryland
Author: R. J. Edwards.)

NOTICES

When Government drawings, specifications, or other data are used for any purpose other than in connection with a definitely related Government procurement operation, the United States Government thereby incurs no responsibility nor any obligation whatsoever; and the fact that the Government may have formulated, furnished, or in any way supplied the said drawings, specifications, or other data, is not to be regarded by implication or otherwise as in any manner licensing the holder or any other person or corporation, or conveying any rights or permission to manufacture, use, or sell any patented invention that may in any way be related thereto.

Qualified requesters may obtain copies of this report from the Armed Services Technical Information Agency, (ASTIA), Arlington Hall Station, Arlington 12, Virginia.

This report has been released to the Office of Technical Services, U.S. Department of Commerce, Washington 25, D.C., for sale to the general public.

Copies of this report should not be returned to the Aeronautical Systems Division unless return is required by security considerations, contractual obligations, or notice on a specific document.

Aeronautical Systems Division, Dir/Aeromechanics, Flight Dynamics Lab, Wright-Patterson AFB, Ohio.
Rpt Nr ASD-TR-61-667, Vol III. ELASTO-PLASTIC ANALYSIS OF STRUCTURES UNDER LOAD AND TWO-DIMENSIONAL TEMPERATURE DISTRIBUTIONS: Experimental Evaluation of the General Time-Dependent Analysis. Final report, Mar 63, 93 p. Incl illus., tables, 6 refs.

Unclassified Report
This report describes investigations performed to determine experimentally the validity of the time-dependent aspects of a time-dependent, elastoplastic stress and strain analysis method (published in ASD-TR-61-667, Vol. I "Elasto-Plastic Analysis of Structures Under Load and Two-Dimensional Temperature Distributions") for

structures exposed to complex load and two-dimensional elevated temperature environments. An experiment specifically designed to evaluate the accuracy of the theoretical method is presented. This consisted of a test of a long flat plate subjected to step functions of load randomly combined with several two-dimensional temperature distributions. Magnitude and duration of the test variables were such that plasticity, creep, and appreciable thermal stress systems were introduced. Comparisons are made of experimental total strains with analytical total strains calculated for conditions identical with the test. The degree of correlation achieved indicates verification of the analysis method within the range of test parameters selected.

1. Thermal Stress
2. Experimental Data
3. Aluminum Alloys
4. Plasticity
5. Creep
- I. AFSC Project 1467, Task 146701
- II. Contract No. AF33(616)7738, BPS No. 2(1-1367)-14002
- III. Martin Marietta Corp., Balto. Div., Baltimore, Md.
- IV. R. J. Edwards
- V. Secondary Rpt Nr RR-35
- VI. In ASTIA collection
- VII. Aval fr OTS

Aeronautical Systems Division, Dir/Aeromechanics, Flight Dynamics Lab, Wright-Patterson AFB, Ohio.
Rpt Nr ASD-TR-61-667, Vol III. ELASTO-PLASTIC ANALYSIS OF STRUCTURES UNDER LOAD AND TWO-DIMENSIONAL TEMPERATURE DISTRIBUTIONS: Experimental Evaluation of the General Time-Dependent Analysis. Final report, Mar 63, 93 p. Incl illus., tables, 6 refs.

Unclassified Report
This report describes investigations performed to determine experimentally the validity of the time-dependent aspects of a time-dependent, elastoplastic stress and strain analysis method (published in ASD-TR-61-667, Vol. I "Elasto-Plastic Analysis of Structures Under Load and Two-Dimensional Temperature Distributions") for

structures exposed to complex load and two-dimensional elevated temperature environments. An experiment specifically designed to evaluate the accuracy of the theoretical method is presented. This consisted of a test of a long flat plate subjected to step functions of load randomly combined with several two-dimensional temperature distributions. Magnitude and duration of the test variables were such that plasticity, creep, and appreciable thermal stress systems were introduced. Comparisons are made of experimental total strains with analytical total strains calculated for conditions identical with the test. The degree of correlation achieved indicates verification of the analysis method within the range of test parameters selected.

1. Thermal Stress
2. Experimental Data
3. Aluminum Alloys
4. Plasticity
5. Creep
- I. AFSC Project 1467, Task 146701
- II. Contract No. AF33(616)7738, BPS No. 2(1-1367)-14002
- III. Martin Marietta Corp., Balto. Div., Baltimore, Md.
- IV. R. J. Edwards
- V. Secondary Rpt Nr RR-35
- VI. In ASTIA collection
- VII. Aval fr OTS

FOREWORD

This report was prepared by the Martin Company under Contract AF33(616)-7738, BPS No. 2(1-1367)-14002.

The contract was sponsored by the Flight Dynamics Laboratory under Technical Area 750A, "Mechanics of Flight." It was initiated under Project 1367, "Structural Design Criteria" and was completed under Project 1467, "Structural Analysis Methods," Task 146701, "Stress-Strain Analysis for Structures Exposed to Creep Environment."

The work was administered under the direction of the Structures Branch by Mr. J. R. Johnson, Project Engineer. This report summarizes work performed during the period 15 February 1962 to 1 January 1963.

Significant contributions to this program were made by:

Dr. P. C. Huang	Research Project Director
Mr. R. J. Edwards	Principal Investigator, coordination and direction of the verification program.
Mr. J. Mason	Assistant to the author, performance of material control coupon tests, data reduction and analyses.
Mr. B. Josselyn Mr. J. Hughes	Facility modification, instrumentation installation and performance of large specimen tests.
Mr. E. Marsh	Instrumentation circuitry design, data collection for large specimen tests.

The author also wishes to thank Mr. C. Swanson, Mr. E. Mead, Jr., and Mr. D. Buttermore for their technical and administrative assistance.

This report was issued by the Martin Company as Research Report RR-35.

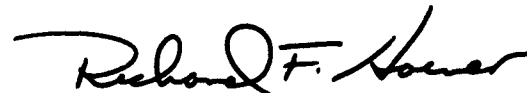
ABSTRACT

This report describes investigations performed to determine experimentally the validity of the time-dependent aspects of a time-dependent, elasto-plastic stress and strain analysis method (published in ASD TR-61-667 Vol. I "Elasto-Plastic Analysis of Structure Under Load and Two-Dimensional Temperature Distributions") for structures exposed to complex load and two-dimensional elevated temperature environments. An experiment specifically designed to evaluate the accuracy of the theoretical method is presented. This consisted of a test of a long flat plate subjected to step functions of load randomly combined with several two-dimensional temperature distributions. Magnitude and duration of the test variables were such that plasticity, creep, and appreciable thermal stress systems were introduced. Comparisons are made of experimental total strains with analytical total strains calculated for conditions identical with the test. The degree of correlation achieved indicates verification of the analysis method within the range of test parameters selected.

PUBLICATION REVIEW

This report has been reviewed and is approved.

FOR THE COMMANDER:



RICHARD F. HOENER
Chief, Structures Branch
Flight Dynamics Laboratory

CONTENTS

	Page
I. Introduction	1
II. Experimental Program	3
A. Basic Approach to Test Program	3
B. Specimen Design	3
C. Specimen Instrumentation	4
D. Test Conditions	5
E. Test Sequence	8
F. Data Handling Procedures	11
G. Strain Gage Calibration Data Analysis	12
H. Test Data Analysis, Large Specimen Test	14
I. Material Control Coupon Program	16
III. Evaluation of the Analytical Method	17
A. General Discussion	17
B. Preparation of Analytical Data	18
C. Evaluation of Experimental Strain Data	19
D. Correlation of Analytical and Experimental Re- sults	21
IV. Conclusions and Recommendations.	23
V. References	25

CONTENTS (continued)

	Page
Appendix I: Experimental Facility	27
I. General	27
II. Specimen Heating and Cooling	27
III. Specimen Loading	28
IV. Instrumentation Systems	30
A. Strain Gages	30
B. Thermocouples	31
V. MillisADIC Data Processing System	32
VI. Test Performance	33
Appendix II: Materials Section (Table LXXV)	35
I. Material Control Coupon Program-- General	35
II. Elevated Temperature Tension Coupon Tests	35
A. Test Procedures and Instrumentation	35
B. Data Reduction and Analysis	36
III. Elevated Temperature Creep Coupon Tests	37
A. Introduction	37
B. Planning the Experiment	38
C. Test Instrumentation	39
D. Test Procedures	40
E. Data Analysis	40
Appendix III: Tables and Illustrations	45

LIST OF TABLES

<u>Table</u>	<u>Title</u>	<u>Page</u>
1	Summary of Weldable Strain Gage Performance During Calibration and Environmental Test	46
2	Random Test Conditions for Material Control Coupon Program	47
3	Summary of Material Control Coupon Utilization	48

LIST OF ILLUSTRATIONS

<u>Figure</u>	<u>Title</u>	<u>Page</u>
1	Layout of Large Specimen and Material Control Coupons on Sheet Stock	49
2	Specimen Instrumentation Layout	50
3	Instrumented Specimen	51
4	Test Conditions, Nominal Temperature Distributions	52
5	Random Test Conditions	53
6	Actual Load and Temperature Spectrum Versus Time	54
7	Tuckerman Slope Versus Temperature	55
8	Strain Gage Sensitivity Versus Temperature	56
9	Apparent Strain Versus Temperature	57
10	Typical Actual Temperature Distributions	58
11	Total Strain Versus Time, Station X = 0 in.	59
12	Total Strain Versus Time, Station X = 4 in.	60
13	Total Strain Versus Time, Station X = 8 in.	61
14	Total Strain Versus Time, Station X = 12 in.	62
15	Total Strain Versus Time, Station X = 16 in.	63

LIST OF ILLUSTRATIONS (continued)

<u>Figure</u>	<u>Title</u>	<u>Page</u>
16	Total Strain Versus Time, Station X = 20 in.	64
17	Total Strain Versus Time, Station X = 24 in.	65
18	Total Strain Distributions, Station X = 0 in.	66
19	Total Strain Distributions, Station X = 4 in.	67
20	Total Strain Distributions, Station X = 8 in.	68
21	Total Strain Distributions, Station X = 12 in.	69
22	Total Strain Distributions, Station X = 16 in.	70
23	Total Strain Distributions, Station X = 20 in.	71
24	Total Strain Distributions, Station X = 24 in.	72
25	Test Facility Schematic	73
26	Overall View of Test Facility	74
27	Schematic of Load Control System	75
28	Typical Strain Gage Circuit	76
29	50-Channel Strain Gage Bridge Box	77
30	Typical Thermocouple Circuit	78
31	Thermal Coefficient of Expansion for 2024-T4 Bare Aluminum	79
32	Stress-Strain Coupon Test Setup	80
33	Modulus of Elasticity Versus Temperature for 2024-T4 Bare Aluminum Alloy	81
34	Nondimensional Stress-Strain Curve for 2024-T4 Bare Aluminum Alloy	82
35	Spectral Stress-Strain Curves for 2024-T4 Bare Aluminum Alloy	83

LIST OF ILLUSTRATIONS (continued)

<u>Figure</u>	<u>Title</u>	<u>Page</u>
36	Overall View of Creep Coupon Test Setup	84
37	Creep Coupon Test Instrumentation	85
38	Primary Slope m	86
39	Minimum Creep Rate a	87
40	Primary Creep Parameter K	88
41	Coefficients in $\text{Log } K = a_K + b_K \sigma$	89
42	Spectral Creep Curves for 2024-T4 Bare Aluminum Alloy (300° F)	90
43	Spectral Creep Curves for 2024-T4 Bare Aluminum Alloy (350° F)	91
44	Spectral Creep Curves for 2024-T4 Bare Aluminum Alloy (400° F)	92
45	Spectral Creep Curves for 2024-T4 Bare Aluminum Alloy (450° F)	93

I. INTRODUCTION

A hypersonic vehicle is subject to nonuniform heating and cooling which, associated with a nonuniform distribution of mass within the structural shell, induces uneven temperature patterns. These patterns continually change as vehicle flight conditions are altered, thereby subjecting each structural element to a spectrum of temperatures while simultaneously sustaining a spectrum of loads. At any particular instant, each structural element has a specific prior load-temperature history plus a current set of conditions to sustain; these include temperature level, stresses induced by external load, and thermal stresses induced by temperature variations. Stresses based on original structural geometry must be continually modified as load-temperature history is accumulated by accounting for changes in material stiffness and differential strains due to prior creep and plastic flow.

Time-dependent stress and strain analyses have been developed to provide solutions for the type of structural problem described above (Refs. 1, 2, 3, 4 and 6). The analysis described in Ref. 4 accounts for thermal stresses induced by temperature variations in the plane of a structural cross section and it takes into consideration both the elastic and plastic ranges of material behavior plus time-dependent effects of creep. The analysis of Ref. 4 was experimentally verified for the application of a one-dimensional temperature distribution only (variation in the plane of the cross section and approximately constant in the longitudinal direction).

In practice, temperature variations also occur in the longitudinal direction. For most structural configurations with an aspect ratio greater than 1.5, the above method of analysis can be adapted to account for the two-dimensional temperature variation. Accordingly, the analysis method described in Chapter II, Ref. 6, provides for the two-dimensional treatment of temperature. This method, programmed for the IBM 7094 digital computer, furnishes a rapid analysis tool which integrates all the factors discussed above and includes the calculation of shear stresses due to longitudinal temperature variations and transversely applied load. The time independent portion of the analysis of Ref. 6 (instantaneous stress distribution) was experimentally verified for the application of two-dimensional temperature distributions and for both elastic and plastic loads.

The program described in this report is the sixth in a series of analytical and experimental mechanics research programs dealing with elevated temperature behavior of structures. All these programs have utilized specially designed experiments to check newly developed analysis methods in which complex test variables were subject to discrete control and quantitative evaluation. This was made possible by

Manuscript released by the author January 1963, for publication as an ASD Technical Report.

the selection of simple, flat-plate specimens with known boundary conditions and with controlled load and temperature patterns applied. In the experimental phase of the first of this series (Ref. 1), the selected steady-state temperature distributions produced negligible thermal stresses, and the effect of the temperature-dependent variation of modulus and coefficient of thermal expansion was studied. In the experimental phase of the second of the series (Ref. 2), the selected steady-state temperature distributions produced thermal stresses of appreciable magnitude. The combined load-induced and thermal stress distributions for tension and compression loading were studied in both the elastic and plastic range. The influence of these stress distributions on buckling of the plate also was investigated. A cutout was the subject of the experimental investigation in the third program of the series (Ref. 3). Thermal stresses were of the same order of magnitude as those in the second program, but a centrally located cutout caused a redistribution of temperatures. Loading was in tension-producing stresses in the elastic and plastic range. In the fourth program (Refs. 4 and 5), a time-dependent structural analysis was verified. Step functions of load and temperature which produced thermal stresses of appreciable magnitude were applied to a flat-plate over an extended period of time. Elasto-plastic and creep effects were evaluated in terms of total strain. In the fifth program (Ref. 6), thermal stress patterns of appreciable magnitude were induced by subjecting the test specimens to various two-dimensional temperature distributions. Short-time tension loading at an approximately constant strain rate produced total stresses in the elastic and plastic range. Loading was accomplished at a relatively high strain rate to prevent the accumulation of significant creep strains.

Although the time-dependent analysis procedure presented in Chapter II, Ref. 6, is general in nature, the experimental program reported therein was specifically designed to determine the accuracy of only the time-independent aspects of the analysis, since the verification of the stress distribution was a logical first step in determining the validity of the complete theory.

The objective of the present (sixth) program was to determine experimentally the validity of the time-dependent aspects of the theoretical analysis of Ref. 6. The experiment consisted of a test of a long flat plate subjected to step functions of load randomly combined with several two-dimensional temperature distributions. Magnitude and duration of the test variables were such that plasticity, creep, and appreciable thermal stress systems were introduced.

A discussion of the experimental program and the correlation between analysis and experiment are presented in the body of this report. The details of the test program and the tables and illustrations are contained in the appendices.

II. EXPERIMENTAL PROGRAM

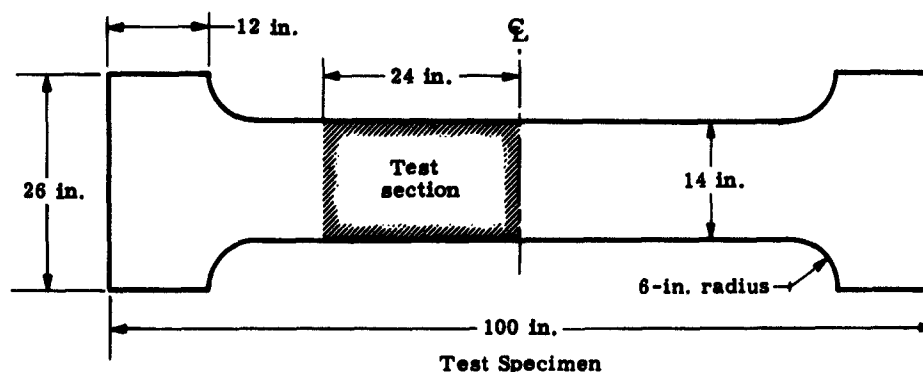
A. BASIC APPROACH TO TEST PROGRAM

The test program for evaluation of the time-dependent aspects of the theoretical analysis of Ref. 6 was not aimed at the duplication of design conditions for a particular vehicle. Rather, the interaction of the parameters included in the method of analysis was covered over a wide range of values. Load and temperature were applied to simulate some degree of typical environmental exposure. The temperature range of 200° to 450° F was selected to provide significant changes in the material properties of the test specimen. Load levels were selected such that in combination with the two-dimensional temperature distributions, significant total strains were produced in 24 hours of test time.

B. SPECIMEN DESIGN

Since specimen size is an important consideration in elevated temperature research, in the present program, as in past ones, large specimens are required to eliminate certain obvious difficulties. For example, thermal gradients are established by the temperature difference across the length or width of a specimen. If the specimen were too small, temperature sensing elements would, of necessity, be spaced very closely along the desired direction, with probable disturbance of the required gradient. In addition, excessively high gradients would be required, or temperature differences would be too small for accurate resolution by the instrumentation. Under such conditions, the range of temperature difference which could be used in the tests would be too narrow for complete verification of the method of analysis.

The geometry of the specimen for the present program is identical to that of the specimens used in previous programs (Fig. 1 and Refs. 1, 2, 3, 5 and 6).



The design was based on the following requirements:

- (1) A plate was selected to permit easy isolation of pertinent parameters and exclusion of all others.
- (2) A width of 14 inches was provided to obtain and adequately measure transverse temperature and strain variations.
- (3) With the width established, a length of 100 inches was provided to attain an aspect ratio (length-to-width) greater than 1.5 which minimized end effects in the instrumented region of the specimen where strain measurements were made to determine effects of two-dimensional temperature distributions.
- (4) The thickness of 0.25 inch was based upon a width-over-thickness ratio corresponding to a reasonable buckling stress level to prevent buckling under thermal stresses.
- (5) 2024-T4 bare aluminum alloy was chosen so that the required phenomena (e.g., modulus variation with temperature, plasticity) occur within a practical temperature and load range. This is of importance for reasons of instrumentation and equipment.

The specimens were manufactured to close tolerances on a numerical milling machine which utilized a punched tape program. The machining and drilling were done in conformance with the geometry of the four existing test fixture end plates by which the load is applied. This procedure reduced any moments due to eccentricity of axial loading to a minimum. The geometry of the instrumented test section for each specimen was such that only those thermal and load-induced stress systems pertinent to the analysis were measured.

C. SPECIMEN INSTRUMENTATION

Specimen temperatures were measured with iron-constantan, Y-calibration thermocouples; strains were measured with high temperature weldable strain gages (Type AL-E-5-A, manufactured by Microdot, Inc.). The analog output from both sets of instrumentation was recorded by the MilliSADIC Data Processing System (see Appendix I, Section V).

Since heating was symmetrical with respect to the center line, one half of the specimen was instrumented heavily so as to determine strain and temperature variations adequately (see Figs. 1 and 2). The specimen was instrumented with 50 strain gages on each side located

back-to-back along seven transverse sections. Each strain gage output was recorded separately for greater reliability. Specimen temperatures were recorded at nine transverse sections to determine accurately both the temperature distributions imposed and the strain gage temperatures. The latter are of great importance in performing an accurate in-place calibration and in the reduction of test data. The actual installation of the instrumentation on the large test specimen is shown in Fig. 3.

D. TEST CONDITIONS

The experimental program consisted of an environmental test of a long flat plate subjected to conditions of tension loading and two-dimensional temperature distribution varying with time. Random step functions of load were combined with various temperature patterns in which temperature varied in both the longitudinal and transverse directions. Arbitrary combinations of step functions were applied over a preselected time span. The arbitrary temperature patterns included two extremes of longitudinal temperature gradient.

The test was designed to check the validity of the analysis for the effects of individual and combined variations of load and temperature. Since the extension of the analysis method to two dimensions was the new feature being investigated, at least two extreme longitudinal temperature gradients had to be investigated before a definitive conclusion as to the validity could be warranted.

The following considerations governed the selection of parameters for the environmental test.

- (1) Duration of Test. It was determined that a test span of approximately 24 hours would be required to fully evaluate the analysis. Since the test requires skilled personnel constantly in attendance, and due to the limited number of key engineering personnel available, the test was conducted over a two-day period. The 24-hour test span was broken into four phases of 6 hours each. The first day of testing included a pretest room temperature strain gage calibration and phases one and two (12 hours). The second day of testing included an intermediate strain gage calibration (room temperature, 300° F, and 450° F) and phases three and four (12 hours).
- (2) Time Combinations. Time combinations were formed of whole hours adding up to the 6-hour duration of each test phase. Possible combinations are:

1-2-3	3-1-2	1-5
1-3-2	3-2-1	5-1
2-1-3	2-4	
2-3-1	4-2	

(The combinations 1-5 and 5-1 were deleted due to the large number of parameters to be investigated in the relatively short test span.)

- (3) **Temperature Distributions.** Since the longitudinal temperature gradient is a prime parameter to be considered, the following four distributions were chosen within the limitations of the test facility and time span of test and based on the experience gained under Ref. 6 (see Fig. 4).

Type Distribution	Longitudinal Temperature Difference (1) (° F)	Lateral Temperature Difference (2) (° F)
100° Tent	100	50
100° Recess	100	50
200° Tent	200	50
200° Recess	200	50

NOTE: (1) Temperature difference over 24-inch half-length of test section.

(2) Temperature difference over 7-inch half-width of test section.

- (4) **Load Levels.** Throughout the test there was an element of the center section of the beam at 450° F (station X = 0), Figs. 4 and 5. The maximum load that can be safely imposed on the beam was then dictated by the response of the center section to loading. There were two mechanisms which acted to keep the actual stress on the 450° F element lower than the nominal stress applied to the beam. The transverse temperature gradient served to create a compressive stress on the 450° F element for both the tent and recess type distributions.

The other mechanism was the redistribution of stress due to creep. The initial stress distribution was nonuniform. The fibers started to creep at various rates according to the stress levels; however, owing to the continuity of material, only a linear creep distribution over the cross section would satisfy the compatibility of strains. The stresses were redistributed in the course of creeping to be compatible with strains accumulated. Elements with the highest creep

rates lost effective stiffness in proportion to the relative creep rates of the other elements. This tendency to relax causes the redistribution stress.

- (5) Parameters for Random Selection of Test Conditions. The following combinations of load, temperature and time were assigned index numbers as a first step in selecting random test conditions.

<u>Index</u>	<u>Time Combination (hr)</u>	<u>Index</u>	<u>Axial Load (kips)</u>	<u>Index</u>	<u>Temperature Distribution</u>
1	1-2-3	1	96	1	100° Tent
2	1-3-2	2	92	2	100° Recess
3	2-3-1	3	85	3	200° Tent
4	2-1-3	4	77	4	200° Recess
5	3-1-2	5	70		
6	3-2-1				
7	2-4				
8	4-2				

- (6) Random Test Conditions. In obtaining the random test conditions (Fig. 5) the previously assigned index numbers were read from a table of random numbers in the following order: (1) time at load, (2) time at temperature, (3) load level, (4) temperature distribution. In selecting the random spectrum, a parameter was passed over in the table of random numbers after an average number of occurrences in order to evenly distribute the parameters. Once the random spectrum was obtained, a preliminary analysis was performed utilizing the IBM 7094 digital program and using the material properties input from Ref. 5. The preliminary analysis was performed to determine whether the selected random spectrum could be imposed without failure of the specimen.

<u>Phase</u>	<u>Time at Load</u>		<u>Load</u>		<u>Time at Temperature</u>		<u>Temperature Distribution</u>	
	<u>Index</u>	<u>Δ Hr</u>	<u>Index</u>	<u>Kips</u>	<u>Index</u>	<u>Δ Hr</u>	<u>Index</u>	<u>Distribution</u>
1	1				5			
		1	3	85		3	1	100° Tent
		2	2	92		1	2	100° Recess
		3	4	77		2	4	200° Recess

<u>Phase</u>	<u>Time at Load</u>		<u>Load</u>		<u>Time at Temperature</u>		<u>Temperature Distribution</u>	
	<u>Index</u>	<u>Δ Hr</u>	<u>Index</u>	<u>Kips</u>	<u>Index</u>	<u>Δ Hr</u>	<u>Index</u>	<u>Distribution</u>
2	3				2			
		2	2	92		1	3	200° Tent
		3	3	85		3	1	100° Tent
		1	2	92		2	4	200° Recess
3	7				7			
		2	1	96		2	2	100° Recess
		4	5	70		4	4	200° Recess
4	5				4			
		3	1	96		2	3	200° Tent
		1	5	70		1	2	100° Recess
		2	4	77		3	1	100° Tent

E. TEST SEQUENCE

The large test specimen was subjected to a 24-hour environmental test during which various load levels and two-dimensional temperature gradients were imposed on the specimen in random order. Prior to the final test, the 100 weldable strain gages were calibrated in place against the Tuckerman optical strain gage under conditions of elevated temperature and elastic loading. The detailed test sequence was as follows:

(1) Strain gage stabilization

The specimen was soaked at 460° F for 30 minutes because the need for stabilization cycling prior to the calibration of strain gages was indicated by coupon tests. The apparent strain versus temperature relationship for the first heating cycle generally differed from that recorded on subsequent cycles. (Subsequent cycles are repeatable within certain limits.)

(2) Heating and cooling checkout

Immediately following the strain gage stabilization, the heating and cooling checkout was performed. Each of the four nominal temperature distributions to be used in the environmental test was imposed on the specimen to determine instrument settings, lamp bank and cooling bank alignments, and operational procedures for the final test.

(3) Nominal strain gage sensitivity settings (room temperature)

The nominal sensitivities and zero offsets for the weldable strain gages were as follows:

Strain Gages Number	Zero Offset Z_o (cts)	Sensitivity S_w (μ -in./in./ct)
1 to 16	50	13.0
17 to 32	50	10.0
33 to 44	50	7.5
45 to 60	50	7.5
61 to 72	100	7.5
73 to 84	100	7.5
85 to 100	100	7.5

A nominal sensitivity was set by balancing the gages at zero counts and then maintaining a load of 50 kips on the specimen. The Tuckerman gages were read, and the proper number of nominal calibration counts (Z_{cal}) to be set on each channel was computed by:

$$\text{Calibration Counts } (Z_{cal}) = \frac{\text{Tuckerman Strain } (\epsilon_T) \text{ at 50 kips}}{\text{Strain Gage Sensitivity } (S_w)} \quad (1)$$

After the sensitivity had been set, each channel was offset the number of counts (Z_o) indicated in the table above. The gages were offset to allow for a negative apparent strain and/or negative drift.

(4) Room temperature strain gage calibration

After setting the strain gage sensitivities and offsetting the gages, a room temperature strain gage calibration was performed. The specimen was loaded to 100 kips in 10-kip increments. At each load increment the Tuckerman strain, weldable strain, MillisADIC load and monitor load were recorded. During the unload cycle, readings were taken at odd increments, i.e., 95, 85, 75, etc.

(5) Elevated temperature strain gage calibration

The 100 weldable strain gages were then calibrated against the Tuckerman optical strain gage under conditions of elastic loading and elevated temperature. The large test specimen was subjected to uniform

temperatures of 200° F, 300° F, 350° F, 400° F and 460° F. At each temperature level the specimen was subjected to incremental loading. Data were recorded at each increment as in the RT calibration (including MillisADIC temperatures). The load cycles were as follows:

Temperature Level (°F)	Maximum Load (kips)	Load Increment (kips)	Maximum Nominal Stress (ksi)
RT	100	10	27.7
200	50	5	13.8
300	50	5	13.8
350	50	5	13.8
400	40	5	11.1
460	25	5	6.9

In order to keep the time at temperature to a minimum, no readings were taken during the unload cycles. While making the transition from one temperature level to another, a 10-kip load was kept on the specimen. When the desired temperature level was reached, the 10-kip load was reduced to zero. Loads, strains, and temperatures were recorded at the zero load condition and at each load increment.

(6) Environmental creep test

The environmental creep test consisted of four phases of six hours each. The testing was governed by the detailed test conditions discussed in Section D of this chapter.

Phases I and II were conducted on the first day. Just prior to the initiation of Phase I, a RT strain gage calibration was performed in which the specimen was subjected to a 100-kip load cycle in increments of 10 kips. Loads, strains and temperatures were recorded on the up cycle only.

Phases III and IV were conducted on the second day. Just prior to the initiation of Phase III another RT strain gage calibration was performed as described above. The RT calibration was followed by calibration cycles at 300° F and 460° F. These cycles were performed in the same manner as those described above.

Detailed test procedures were drafted and were reviewed in detail prior to the initiation of testing. Selected strain gages and thermocouples were monitored throughout the test as well as loads and load beam deflections. Detailed test logs were prepared for the recording of these data.

During the final phase of testing, a series of radiant lamp failures hampered the test effort and ultimately resulted in termination after completing 21 of the 24 planned test hours, Fig. 5. (The actual test span, including transient heating time, was 26 hours, Fig. 6.) At the completion of 20 nominal hours of testing and while making the transition from a 200° tent distribution to a 100° recessed distribution there was a failure of two lamps located in the bottom longitudinal lamp bank. The lamps were successfully replaced during a shutdown of approximately one hour and testing was resumed. At the completion of 21 nominal hours (26 actual hours) of testing, the last temperature distribution was imposed on the specimen and load was applied. After seven minutes under stabilized conditions, three lamps failed in the center longitudinal bank. Since this bank is inaccessible without removal of the entire heating assembly, and it was reasonable to expect that more lamp failures were imminent, the test was terminated after a careful review of the available raw data was made to assure that sufficient data had been obtained. The maximum total strain had been reached, since the remaining load levels were low and the creep strain yet to be accumulated was expected to be small. The lamp failures were attributed to overheating of the end seals. The lamp bank assembly which supports the radiant lamps and focuses the heat onto the specimen also served to confine the end seals in a relatively severe environment for long periods which eventually resulted in their failure.

F. DATA HANDLING PROCEDURES

The MilliSADIC Data Processing System (Appendix I) was used for the collection, analog-to-digital conversion, and storage of the digital output from the strain gages, load monitoring bridges, and thermocouples. This system converts and stores as many as 400 channels of information at a sampling rate of up to 200 channels per second. The MilliSADIC system stores the data on magnetic tape from which it is read into an IBM 523 punch unit with 20 channels in parallel. The IBM cards were listed in tabular form for editing purposes. Each card represents a single datum point for each of 20 channels. Superfluous cards were removed and the data checked for consistency. Four sets of cards (MilliSADIC output cards, control cards, strain gage data cards and thermocouple data cards) were combined and reduced to strains, loads, and temperatures by means of an IBM 7094 digital computer program prepared for this purpose. The IBM 7094 output was in tabulated form with the option of obtaining printed plots directly from the computer and/or punched cards for use in plotting with the BOSCAR Plotter, a slower, but more reliable and versatile means of plotting. This procedure for reduction of the test data from the large specimen was almost fully automatic; however, the very lengthy method of strain gage calibration adopted for this program, together with the already large number of data channels, made the overall data reduction effort a

considerable undertaking. Although the strain gage calibration data reduction procedure was tedious and time-consuming, the resulting strain data justified the extra effort in terms of accuracy, consistency and reliability. The overall data reduction procedure proved to be efficient and highly accurate.

G. STRAIN GAGE CALIBRATION DATA ANALYSIS

Experience gained in past investigations (Refs. 3 and 5) indicated that calibration of strain gages by means of shunting procedures could lead to errors of undue magnitude. Other sources of error in utilizing conventional calibration techniques include wide scatter and nonrepeatability of gage factor and apparent strain versus temperature curves for a given lot of gages. The use of a single plot of gage factor versus temperature to describe the change in sensitivity with temperature of a given lot of gages is not consistent with the degree of precision required in experimental programs of this nature. It was discovered during the in-place strain gage calibration performed under Ref. 6 that the variation of apparent strain with temperature was of a greater magnitude than was claimed by the strain gage manufacturer. Of even more significance, however, was the lack of repeatability and wide scatter of the apparent strain versus temperature relationship from gage to gage. (The apparent strain versus temperature relationship was repeatable for an individual gage.) A technique of direct in-place calibration of strain gages against a known standard (Tuckerman optical strain gage) was therefore adopted for this program and a potentially large source of error thus was negated.

The 100 weldable strain gages on the large specimen were calibrated against two Tuckerman optical strain gages under conditions of elastic loading and elevated temperature. Prior to the environmental test, the specimen was subjected successively to approximately uniform temperatures of room temperature, 200° F, 300° F, 350° F, 400° F and 450° F. At each temperature level, an elastic load cycle was imposed in even increments. Loads, strains and temperature were recorded at each increment of load. During the shutdown between the first and second day of testing, an intermediate strain gage calibration was performed successively at approximate temperature levels of room temperature, 300° F and 460° F.

The first step in the evaluation of the data was to reduce the thermocouple data collected at the various temperature levels by means of the MilliSADIC Digital Data Reduction Program. Average strain gage temperatures for a given run then were determined by interpolation of average temperatures of adjacent thermocouples. A least squares

correlation analysis of MilliSADIC load versus raw strain gage data (counts) was performed at each temperature level for each of the weldable strain gages. A correlation of MilliSADIC load versus the strain obtained from the two Tuckerman gages also was performed at each temperature level, from which a plot of Tuckerman slope versus temperature was constructed (Fig. 7).

The equation of best fit was determined by means of an IBM Bi-Variate Correlation Analysis which utilized linear, quadratic, cubic, quartic, semi-log and log-log fits by the method of least squares.

The sensitivity (S_s in microinch per inch per count) of each strain gage at a particular temperature level was then obtained by:

$$S_s = B_T/B_c \quad (2)$$

where

B_T is equal to the slope (microinch per inch per kip) of the linear regression equation ($Y = A + BX$) obtained from the load versus Tuckerman strain correlation analysis. (The Tuckerman slope used in this computation was the Tuckerman slope at the particular strain gage temperature and was obtained from the plot of Tuckerman slope versus Tuckerman temperature.) B_c is equal to slope (counts per kip) of the linear regression equation obtained from the load versus raw strain channel counts correlation analysis. The variation of strain gage sensitivity with temperature then was plotted for each strain gage.

The apparent strain versus temperature relationship for each strain gage was actually determined in terms of apparent MilliSADIC strain channel counts, A_c , since this method was much more adaptable to digital data reduction procedures. Apparent counts for each strain gage were determined for each temperature level by means of the linear regression equation obtained from the load versus raw strain gage data correlation analysis. The intercept (A_c in counts) of the line of regression represents the zero load condition. A plot of apparent counts versus temperature then was constructed for each strain gage.

Average strain gage temperatures for the two-dimensional, steady-state temperature distributions imposed on the test specimen during the various test phases were determined from the thermocouple data. The elevated temperature sensitivity and the apparent strain correction for each gage were obtained from the above mentioned plots.

Examples of the variation of strain gage sensitivity and apparent strain with temperature are presented in Figs. 8 and 9. In this program as in the program of Ref. 6, the apparent strain correction for some gages approximated, in some instances, the strains induced by thermal stress. To attempt to apply a uniform apparent strain versus temperature correction to such data would give wholly unsuitable and unintelligible results. From an evaluation of the strain gage calibration data, it was determined that 83 of the 100 strain gages performed satisfactorily. The 17 strain gages that did not perform satisfactorily can be summarized as shown in Table 1.

Of the 17 strain gages that were lost during the various stages of testing, 16 were exposed either to direct radiant heating or air cooling. It should be noted that only two pairs of strain gages were lost (gages 13 to 14 and gages 83 to 84), and since the gages were installed back-to-back, there was a complete loss of data at only two of the 50 strain gage locations.

H. TEST DATA ANALYSIS, LARGE SPECIMEN TEST

The analog output of all instrumentation (load, strain and temperature) was processed through the MilliSADIC Data Processing System, appearing in digital form (0 to 999) on punched cards with 20 channels per card. All data associated with the large specimen, including load beam and strain gage calibrations, were contained in approximately 34,000 punched cards.

For the thermocouple channels, the sensitivity was known in terms of millivolts per count (see Appendix I for calibration procedure) and the temperature was computed by:

$$E = S_T Z \quad (3)$$

and

$$T = f(E) \quad (4)$$

where

E = millivolt output of thermocouple

S_T = thermocouple sensitivity (millivolt per count)

Z = MilliSADIC output

$f(E)$ = temperature conversion curve for iron-constantan, Y-calibration thermocouples.

Loads were computed by:

$$P = (Z - Z_0) S_p \quad (5)$$

where

P = load (kip)

Z_0 = MilliSADIC counts at zero load

S_p = load beam bridge sensitivity obtained from the load beam calibration (kip per count).

Total strains were obtained from:

$$\epsilon_{tot} = (Z - Z_0) S_s - AS \quad (6)$$

where

ϵ_{tot} = strain associated with thermal and/or load induced stress plus accumulated creep plus thermal expansion (inch per inch)

S_s = strain gage sensitivity (inch per inch per count)

AS = $\epsilon_A - \alpha \Delta T$ = fictitious apparent strain

ϵ_A = $S_s \times A_c$ (see Chapter IIG) = apparent strain (inch per inch)

$\alpha \Delta T$ = free thermal expansion.

The strain gage sensitivity used in the above calculation was obtained from an individual plot of strain gage sensitivity versus temperature constructed from the data of the in-place strain gage calibration. The apparent strain was calculated from an individual plot of apparent strain channel counts versus temperature constructed from the data of the in-place strain gage calibration (see Figs. 8 and 9).

The weldable strain gages used in this program were compensated for aluminum alloy and, therefore, indicated total strain minus thermal expansion ($\alpha \Delta T$). For short-time testing, this indicated strain is meaningful as it is associated with stress. Under creep conditions, however, this indicated strain has no meaning, and total strains are required. In order to obtain total strains with the existing IBM 7094 program, a fictitious apparent strain (AS) was used, as indicated above.

The final test was conducted according to the nominal environmental conditions outlined in Chapter II D and illustrated in Fig. 5. A sampling of the actual temperature distributions imposed on the specimen are shown in Fig. 10. Figure 6 is a summary of the actual load and temperature spectrum versus time.

In reducing the data from this test, the procedure was as follows:

- (1) The strain gage calibration data were reduced (as discussed in Chapter II G) to yield sensitivity and apparent strain versus temperature curves for each gage.
- (2) The MilliSADIC data cards from the final test were reduced by means of the IBM 7094 to yield specimen temperatures versus time at the thermocouple locations.
- (3) By interpolation of adjacent thermocouples, strain gage temperatures were determined during the various test phases.
- (4) With strain gage temperatures known, values were obtained for strain gage sensitivity and apparent strain.
- (5) The MilliSADIC data cards were run through the IBM 7094 again to obtain load and strain versus time, both tabulated and plotted.

I. MATERIAL CONTROL COUPON PROGRAM

In an experimental program such as this, the values for material properties are test parameters that must be known with a degree of accuracy consistent with the objective of evaluating the analysis. The present program included the testing of twelve material control coupons to obtain elastic and plastic stress-strain data over a range of temperature from room temperature to 450° F. An additional 46 coupons were tested at temperature levels of 200° F, 300° F, 350° F, 400° F and 460° F and over a wide range of stresses to obtain tension-creep data. Use was also made of coefficient of thermal expansion data collected under a past program (Ref. 5) of a similar nature. The details of the material control coupon program are presented in Appendix II.

III. EVALUATION OF THE ANALYTICAL METHOD

A. GENERAL DISCUSSION

The objective of this experimental program was to provide test data with which the reliability of the theoretical method of Ref. 6 (programmed for the IBM 7094 computer) could be ascertained. In particular, the time-dependent aspects of the analysis were to be evaluated since the time-independent features of the analysis (instantaneous stress distribution) had been verified previously (Ref. 6).

Because of the presence of creep strain, the strains associated with stress for general time-dependent conditions cannot be measured directly by experiment. Since the stress affects the creep rate exponentially, it was advisable to conduct a time-independent program wherein the stress distribution could be verified prior to undertaking an evaluation of the general time-dependent analysis.

The computer programmed analysis of Ref. 6 is a general procedure for determining the time-dependent nonlinear stress and strain behavior of an elevated temperature structure under bending and/or axial load conditions. The structure may be subjected to a wide variety of exposure conditions, including combinations of load and thermal stress produced by two-dimensional temperature distributions which vary with time. Stress and strain distributions may be determined in both the elastic and plastic ranges. The effects of creep are determined by the use of either the time-hardening or strain-hardening rules for material creep behavior.

To verify such a broad general theoretical method experimentally over a full range of its potential applications would require many complex tests. These tests would have to include a full range of parameter combinations and variations. Since such a series of tests is not economically feasible, a single complex tension test was conceived with random combinations of axial load and two-dimensional temperature distributions applied to a long plate. The aim was to produce significant measurable time-dependent effects in the plate in a test period of approximately 24 hours (see Section D, Chapter II for the detailed discussion of the test conditions and the considerations which governed the selection of the test parameters).

The environmental test thus selected covered a complex range of time-dependent interactions of load and temperature effects. Of particular interest was the inclusion of the longitudinal temperature gradient, since this was a new feature of the analysis. Longitudinal temperature differences of 100° F and 200° F were incorporated in the four two-dimensional temperature distributions selected (Fig. 4). By

applying the theoretical method to the actual test conditions, a check was made of its engineering accuracy by directly comparing analytical and experimental results. Total strain versus time was selected as the most important measurable parameter for comparison. The assumption was made that if the analysis proved sufficiently accurate to predict the strain history within reasonable tolerances ($\pm 10\%$) then the general time-dependent theoretical method was verified in total over the range of test parameters selected.

Individual techniques for handling various factors in the analysis have known deficiencies. A good example is the treatment of material properties. Only the effects of temperature level in defining the environmental stress-strain curves are utilized. Actual environmental effects would result in an infinite number of curves. Also, the stress-strain curves and creep parameters which are part of the material properties input to the theoretical program are normalized data derived from a sampling of the test specimen sheet stock. The actual local material behavior can be expected to be somewhat different. The thermal coefficient of expansion data (also material properties input) was determined under a past program from different sheet stock. Another possible source of analytical error is the idealized treatment of creep by either the strain-hardening or time-hardening rules. In addition, this analysis was based on the uniaxial flow law while the two-dimensional temperature distributions actually give rise to a biaxial stress state.

The nature of the analysis is that of a life-span evaluation of the structure. This means that all effects of environment on the structure start with time zero, and a running summation must be kept to account for conditions of the structure at any finite time thereafter. One feature of this type of procedure is that small unaccounted for errors and inaccuracies in assumptions in both the analytical and test values accumulate by these summations. A degree of divergence between analytical and experimental values is therefore not unexpected as time of exposure increases.

B. PREPARATION OF ANALYTICAL DATA

For purposes of determining its accuracy, the analytical method was applied to the actual test conditions of Fig. 6. The overall procedure for analysis with the theoretical computer program was:

- (1) The material properties (stress-strain, tension creep and thermal coefficient of expansion) were prepared for IBM 7094 input.

- (2) Average thermocouple temperatures were computed for each stabilized condition at each of the 7 instrumented cross sections. The beam cross sections were divided into 17 elements, and element temperatures were determined by interpolation.
- (3) Average loads were computed for each stabilized condition.
- (4) The time for each input phase at which conditions were stabilized was determined. Subsequently, times were selected during each input phase for which theoretical analyses were desired.
- (5) Transient conditions were simplified as follows:
 - (a) At the beginning of the test, during the majority of the temperature changes and in restarting the test after shutdown, transient conditions were approximated by 10 kip load and stabilized temperature.
 - (b) Changes from one input phase to the next were simplified by assuming stabilized conditions from the previous phase to continue constant until the next input phase had stabilized.
- (6) The analysis was performed twice, once for the strain-hardening rule and again for the time-hardening rule.

C. EVALUATION OF EXPERIMENTAL STRAIN DATA

The experimental total strains were obtained by the data reduction procedures described in Sections G and H of Chapter II. Before comparing the experimental results with those predicted by theory, an evaluation of the strain data was conducted to determine the degree of reliability.

The strain gage data exhibited an obviously linear trend across the width of the specimen which agrees with the assumption that plane sections remain plane in a time-dependent elasto-plastic state of deformation. A linear regression analysis was performed on the experimental data from the center station of the beam (station $X = 0$ in., Fig. 2). Throughout the test span, this section of the beam was the hottest (400° to 450° F, nominal). In addition, the outboard strain gages at this station were under a transverse lamp bank and the inboard gages were under a transverse cooling tube. With the severe temperature environment and the exposure to direct radiant heating or air cooling, it was not surprising that the gages at this cross section exhibited the maximum

scatter. While the maximum strain also occurred at the center station of the beam, it must be concluded that the severity of the operating conditions to which the gages were subjected had more effect on the reliability of the strain data than did the strain level, since the section which exhibited the second greatest amount of scatter (station X = 24 in.) underwent the least amount of strain. The gages at station X = 24 in. were also subjected to direct radiant heating and air cooling, but the maximum nominal temperature was 350° F. The overall strain gage performance is measured statistically by the standard error of estimate (zero for no scatter) as shown below.

<u>Time</u>		<u>Load</u> (kip)	<u>Nominal Temperature</u>		<u>Standard Error, All Gages</u> (μ - in./in.)	<u>Standard Error, Inboard Gages Only</u> (μ - in./in.)
<u>(sec)</u>	<u>(hr)</u>		<u>Center</u> (°F)	<u>Edge</u> (°F)		
13,620	3.78	91.4	450	400	193	126
34,980	9.72	91.4	450	400	340	241
58,600	16.28	95.5	400	450	260	153
94,010	26.11	96.1	400	450	299	181
100,130	27.81	0	RT	RT	Mean = 267	Mean = 167

The overall scatter for all gages (outboard and inboard) at the center station is approximately 250 μ - in./in. If only the inboard strain data is considered (those gages subjected only to air cooling), the scatter drops to approximately 150 μ - in./in. In view of the fact that these maximum deviations are acceptable, and indeed the strain gages at the other six stations exhibited even less scatter, it was concluded that the overall strain gage performance was entirely satisfactory. (The linearity of the experimental total strain distributions at the seven instrumented cross sections can be seen in Figs. 18 through 24.)

Another check on the strain gage performance was provided by the measurement of the room temperature residual strain at the end of the test by the Tuckerman optical strain gage. Two Tuckerman gages were installed at station X = 4 in. The residual strain obtained with the Tuckerman gage agreed closely with the strain gage data at that station (see Fig. 19).

D. CORRELATION OF ANALYTICAL AND EXPERIMENTAL RESULTS

Both analytical and experimental results are plotted in Figs. 11 through 24. In Figs. 11 through 17, total strain is plotted against time for the individual datum points from selected strain gages as well as the analytical curves for both the strain-hardening and time-hardening rules. The seven figures represent theoretical and experimental total strains versus time for each of the seven instrumented cross sections of the test specimen. Each figure consists of two plots representing total strain versus time for an element above and an element below the specimen centerline (roughly at the quarter points). At all stations except the center station the average strain from back-to-back gages is plotted.

In Figs. 18 through 24, selected distributions of total strain across the specimen are shown for the seven instrumented stations. The experimental results are plotted as individual datum points and the analytical results are shown as bands bounded by the solutions from the time-hardening and strain-hardening rules. These bands actually should be wider, since each of the two solutions is based on mean material properties and, therefore, does not include a statistical evaluation of the material input data.

From a study of Figs. 11 through 17 (total strain versus time) the following may be concluded:

- (1) The analysis is very effective at predicting total strain increments due to changes in load and temperature distribution. This is especially evident in Figs. 13 through 17 where the accumulated creep strain is small and there is little divergence between the experimental and theoretical values with time.
- (2) The analytical strain rates generally are in agreement with the experimental rates. In this comparison, where deviations occur (Figs. 11 and 12) the analysis somewhat overestimates the strain rates.
- (3) Deviations between theory and experiment are cumulative. The deviations between the analytical and experimental strain rates are accumulated over the test span causing a growing divergence with time between theory and experiment (Figs. 11 and 12). The maximum deviation between theory and experiment occurred, as expected, at the center section of the test beam (station $X = 0$, Fig. 11), since the maximum total strain (approximately 12,000 μ -in./in.) occurred at this section. At the maximum strain condition

(time = 26.11 hours) the deviation between the time hardening rule and the mean experimental strain was 750 μ -in./in. (Fig. 18). This represents an error of only 6.3%, a deviation well within acceptable engineering tolerances since a tolerance of $\pm 10\%$ is generally accepted for the variance in material properties.

A study of the total strain distributions of Figs. 18 through 24 results in the following conclusions:

- (1) The moderate time-dependent divergence between theory and experiment noted for selected elements at a cross section in Figs. 11 and 12 is exhibited for the entire cross section in Figs. 18 and 19.
- (2) The experimental strain distributions across the specimen width exhibit a distinctly linear trend with a minimum of scatter, indicating reliable strain gage performance.
- (3) There is a rotation of the cross section due to the actual temperature distributions not being perfectly symmetrical about the longitudinal centerline. In general, the experimental and theoretical data followed the same trend.

IV. CONCLUSIONS AND RECOMMENDATIONS

This report presents an experimental program for determining the accuracy of a previously developed computer-programmed, time-dependent, elasto-plastic stress and strain analysis for plates and beam-type structures subjected to load and two-dimensional temperature variations.

The general trends of total strain versus time predicted by the analysis correlate very satisfactorily with experiment. Minor deviations between analytical and experimental strain rates can be ascribed to the normalized creep parameters which are part of the material properties input to the theoretical analysis, as well as to assumptions made in the analytical method (Section A, Chapter III). Maximum quantitative differences between theory and experiment are well within the $\pm 10\%$ tolerance generally accepted for the variance in material properties. It is concluded therefore that the theoretical method is valid within the range of test and material parameters utilized in the experiment. Moreover, since the experiment had a maximum number of variables integrated together, i. e., the effects of creep, elasto-plasticity, thermal stresses, two-dimensional temperature distribution inputs, etc., it is believed that the basic analytical method has been proven feasible for general engineering applications.

In a previous time-dependent experimental program (Ref. 5) conducted in a similar manner with one-dimensional temperature distributions (variation in the plane of a cross section and approximately constant in the longitudinal direction), a satisfactory correlation was achieved for the same basic analysis method being evaluated in this report. Since the deviation between theory and experiment was within $\pm 10\%$ for both experimental programs while, in the present program, a longitudinal temperature gradient was introduced, it was concluded that the effect of the longitudinal gradient was negligible. The analysis is considered applicable for structures with an aspect ratio (length-to-width ratio) greater than 1.5. As was pointed out in Chapter II, Ref. 5, the effect of the longitudinal temperature gradient may become important when the aspect ratio is smaller.

The following recommendations and observations are made as a result of this program.

- (1) Although the strain-gage performance was very satisfactory during this program (due to the direct, in-place calibration procedures adopted), more reliable strain gages are needed at higher temperatures. Strain gage properties such as gage factor and apparent strain should

be more uniform for a particular lot of gages. If consistency in strain gage properties could be attained for a given lot of gages, a direct, in-place calibration need be performed for all gages only at room temperature and for a sampling of gages at elevated temperature. Present scatter in gage properties requires individual calibrations of each gage over the full temperature range anticipated during test. Strain gage rosettes for use at elevated temperature are also desirable.

- (2) Methods of direct, in-place calibration of strain gages against a known standard should be more widely applied as they appear to hold great promise toward more reliable strain data collection.
- (3) More reliable strain instrumentation is needed for elevated temperature material properties coupon testing. SR-4 type extensometers in current use are subject to drift, which can be a source of significant error as the test duration increases. Extensometer systems utilizing variable permeance-type transducers have been utilized in long term creep testing, and improvements have been noted in the long term stability of this type of system over other electronic means of strain measurement, but this method of measurement is still not completely satisfactory. The Tuckerman optical strain gage was utilized during the creep testing with very satisfactory results, but since readings must be taken manually, data were obtained only during the day shift. It is believed that a photographic system could be developed by which Tuckerman readings could be taken at desired intervals. Such a system would provide a permanent strain record and would allow the Tuckerman gage to be used in instances where strains change rapidly with time and human limitations preclude its use.
- (4) The similarity between nondimensional stress-strain curves obtained independently under four separate programs (the present program and Refs. 3, 5 and 6) verifies the validity of the procedure for synthesizing stress-strain data for 2024-T4 bare aluminum alloy. This technique of normalizing data should be considered for other materials to which the general time-dependent analytical method may be applied by future users.
- (5) The technique for normalizing tension creep properties data described in Appendix III of this report and in Ref. 5 was found to be very satisfactory for aluminum and should be given consideration for other materials by future users of the computer programmed theoretical analysis.

V. REFERENCES

1. Sprague, G. H., and Huang, P. C., "Analytical and Experimental Investigation of Stress Distribution of Long Flat Plates Subjected to Longitudinal Loads and Transverse Temperature Gradients," WADC TR 55-350, ASTIA AD 97319, September 1956.
2. Huang, P. C., and Van Der Maas, C. J., "Combined Effects of Axial Load, Thermal Stress, and Creep in Flat Plates," WADC TR 57-442 and Supplement 1, March 1958.
3. Huang, P. C., and Van Der Maas, C. J., "Theoretical and Experimental Studies of the Stresses and Strains Around Cut-outs in Loaded, Unevenly Heated Plates," WADC TR 59-2, March 1959.
4. Huang, P. C., "Elasto-Plastic Bending Analysis for Structures Under Arbitrary Load-Temperature Environments--Part I, Analysis Development and Digital Program," WADD TR 60-541, 1960.
5. Van Der Maas, C. J., "Elasto-Plastic Bending Analysis for Structures Under Arbitrary Load-Temperature Environments--Part II, Experimental Verification," WADD TR 60-541, 1960.
6. Huang, P. C., and Edwards, R. J., "Elasto-Plastic Analysis of Structures Under Load and Two-Dimensional Temperature Distributions--Volume I: Analysis, Development and Experimental Program--Volume II: Summary of Test Data," ASD TR 61-667, April 1962.

APPENDIX I

EXPERIMENTAL FACILITY

I. GENERAL

The test facility utilized in this program (see Figs. 25 and 26) was designed to provide precise control of both input parameters and measured variables. It is equally suitable for both time-dependent and time-independent elevated temperature testing. The facility, in its present form, is the result of new requirements of the present program and practical modifications arising from previously sponsored Air Force research contracts (reported in Refs. 1, 2, 3, 5 and 6). Details of the test facility are described in the following discussion.

II. SPECIMEN HEATING AND COOLING

The two specimens tested were heated on one side (outboard) by radiation from T-3 quartz infrared lamps and air cooled on the other side (inboard). The radiant lamp assemblies and slotted air-cooling tubes were mounted back-to-back along the longitudinal centerline and along three vertical sections (see Fig. 25). This arrangement made it possible to achieve two-dimensional heat-flow and temperature distributions which varied from a recessed type, through nominally constant, to a tent-type (Figs. 4 and 10). Nominal test temperatures varied from 200° F to 450° F.

The reflecting surfaces of the assemblies in which the lamps were enclosed were of 0.10-inch polished aluminum reflector sheet. The lamp assemblies were mounted approximately 1/8 inch from the specimen to concentrate heat input into one-inch wide strips painted black for high absorption of radiant heat. Positive temperature control was achieved by having the heating override any cooling effects.

The five temperature control channels consisted of three ignitron power controllers (manufactured by Research, Inc. (RI)) and two saturable reactors (manufactured by General Electric (GE)). The three longitudinal lamp banks were each independently controlled by an ignitron controller. The two vertical lamp banks at each end of the specimen gage section were controlled by a GE controller;

the vertical lamp bank on the specimen centerline was controlled by the second GE controller. The power supplied by an ignitron controller to a lamp bank was determined by the difference between the input signal from an RI function generator and a feedback signal from one of the control thermocouples mounted on the specimen. While the GE controllers do not utilize function generators, they do have the capability of automatically maintaining a specific surface temperature. In imposing a distribution on the specimen, the heating rates of the GE controllers were synchronized with the heating rates programmed on the function generators of the ignitron controllers by manually following preplotted curves on temperature recorders. When the desired temperature was reached, all five controllers were placed on automatic hold. In switching from one temperature distribution to another, the specimen was cooled at a controlled rate, proper control thermocouples were selected, and the new distribution was imposed.

When the five control channels reached the desired temperature levels, the air cooling was adjusted to obtain the optimum temperature distribution and the most efficient operation. Advantages of this method of temperature control were:

- (1) Rapid changes in temperature distribution.
- (2) Positive control of heating rates during changes.
- (3) Accurate control of maximum specimen temperatures.
- (4) No separate air cooling servo system.

The objective of linear temperature distributions could not be fully attained because of: (1) the finite width of the black lines needed for adsorption of radiant heat, (2) the radiant and convective losses between the radiant lamp assemblies and, (3) the convective and conductive losses at the inboard side of the specimen. The linearity of the distribution was also affected by the proximity to the specimen of the radiant lamp assembly and cooling assembly. The deviations of the actual temperature distributions imposed on the specimen from the planned distributions were not of significant concern.

III. SPECIMEN LOADING

Loads were applied at a rate corresponding to that used in the material control coupon program (approximately 12,000 psi/min). Changes in load and temperature (Fig. 6) were such that there was a minimum of creep deformation. This circumstance is desirable,

since in the theoretical analysis, transient test conditions must be approximated. As a result, loads were reduced to 10 kips during temperature changes, except for three instances. At 5, 9 and 17 hours, loads were maintained, since the change in temperature distribution resulted only in an increase or decrease in the longitudinal gradient (e. g., from 100° recess to 200° recess at 5 hours).

The pin-supported beams transferred the load from the jacks to the specimen (Figs. 25 and 26). Each beam was instrumented with four strain gages on the tension side and four strain gages on the compression side, a total for both beams of 16 strain gages. These were wired in four-arm bridge circuits, each of the two beams contributing one tension and one compression gage to the bridge. Two of these bridge circuits were used for data collection on MilliSADIC channels 142 and 143, and another was used for the load monitor. The fourth bridge furnished the feedback signal for the load control system. To reduce friction losses to a minimum, the load beam support plates rested upon needle bearing assemblies that were free to move in the direction of loading.

The load control system is shown schematically in Fig. 27. The feedback signal from one of the four load beam bridge circuits was compared with the command signal from the load control dial. The error signal was amplified ($\approx 300,000$) to operate a hydraulic servo-valve which, in turn, controlled the hydraulic loading jacks. It is seen in Fig. 27 that the circuit allows both for balancing and calibration. A parallel monitoring system utilized the output from the fourth load beam bridge circuit which was recorded on a Leeds and Northrup recorder. In applying or changing loads during test, the procedure was to manually operate the load control dial so that a preplotted load versus time curve was followed as accurately as possible. During sustained load conditions, the L and N recorder was calibrated and read at regular intervals to make sure that the load was not subject to unanticipated changes.

The load monitoring beams were calibrated using two 50-kip capacity SR-4 load cells which had been calibrated previously against a primary standard. The high coefficient of correlation obtained from the load beam calibration data indicated that the data was of a high degree of linearity, and the low standard error of estimate was an indication of the degree of consistency and repeatability. On the basis of standard errors, the MilliSADIC accuracy is much better than 1% over the total load range (100 kip).

During the course of the test program, the load beam bridge on MilliSADIC channel 142 exhibited erratic behavior; however, the performance of the bridge on MilliSADIC channel 143 remained consistent throughout. In reducing the large specimen test data, a

sensitivity of 0.1229 kip per count was used for MilliSADIC channel 143.

IV. INSTRUMENTATION SYSTEM

The large specimen was equipped with the following instrumentation:

- (1) One hundred high temperature weldable strain gages for data collection.
- (2) Seventy-three iron-constantan thermocouples for data collection.
- (3) Fifteen iron-constantan thermocouples for temperature control by the ignitron units and the GE saturable reactors.
- (4) Fifty iron-constantan thermocouples for monitoring on three temperature recorders.
- (5) Four Tuckerman optical strain gages for calibration and monitoring.

The data collection instrumentation will be discussed.

A. STRAIN GAGES

High temperature weldable strain gages, Microdot-type AL-E-5A, 60 ohm (compensated for aluminum alloy), were used. A detailed discussion of the installation of these gages is presented in Appendix II, Ref. 6, and calibration procedures are discussed in the main body of this report. The circuit for recording the strain gage output on the MilliSADIC is shown in Fig. 28. The inactive arms of each bridge circuit consisted of noninductively wound wire resistors with the nominal resistances and tolerances shown. To facilitate the installation of the strain gage circuitry, two permanent 50-channel bridge boxes were constructed (Fig. 29). Each bridge box consisted of five banks of ten bridges each; each bridge circuit was wired to a female cannon plug for connection to the MilliSADIC Data Processing System.

The active gauge connection was accomplished through permanently installed lead wires from the bridge boxes to the two test facility terminal boards. The instrumented specimen was connected to the terminal boards after installation in the test fixture. This design resulted in a simple connection of all components of the strain gauge circuits and allowed maximum use of existing circuits from a past program (Ref. 6).

It is seen that the circuit of Fig. 28 represents considerable deviations from the conventional Wheatstone bridge. Experience gained in past programs indicated that shunt calibration procedures could lead to errors of undue magnitude, e. g., analyses performed under Ref. 5 indicated that errors of 3% to 4% could be expected for shunting at B, and errors ranging to 22% could be expected when the shunting was performed at A. Shunting at A corresponded to calibration in the MilliSADIC trailer while shunting at B corresponded to calibration at the bridge box.

These and other considerations have led to the adoption of the present procedure for direct in-place calibration of all gages against the Tuckerman optical strain gage under conditions of elastic loading and elevated temperature.

B. THERMOCOUPLES

All temperature measurements were made with iron-constantan, type Y thermocouples which were spot welded to the test specimen with wires parallel and no more than 1/32 inch apart. This method of attachment permitted actual surface temperatures to be obtained at a highly localized area between the welded junctions. This technique ensured that the points at which temperatures were measured were known accurately--an essential feature when temperature gradients must be determined. Thermocouples exposed to direct radiant heating were protected with aluminum oxide paint to prevent heat absorption. The circuit for recording the thermocouple output on the MilliSADIC is shown in Fig. 30.

Three permanent, 25-channel cold junction boxes were used in the data collection thermocouple circuitry. Each cold junction box consisted of a bank of five wide-mouth thermos bottles. A total of 11 glass tubes were inserted through the rubber stopper of each thermos bottle and embedded in a crushed ice and water bath. The 11 glass tubes contained the following types of junctions, each immersed in oil:

- (1) Five constantan-copper junctions.
- (2) Five iron-copper junctions.
- (3) One iron-constantan junction.

Each thermos assembly contained five data channels and one channel for monitoring the reference junction temperature. The assembly was wired permanently from input terminals, through individual iron and constantan wires to the glass tubes, and from there through copper wires to female Cannon plugs. This provided for a simple insertion of the cold junction box in the overall thermocouple circuit.

The thermocouples were calibrated as follows (refer to Fig. 30):

- (1) The preamplifier, A, was adjusted for an initial count of one with the preamplifier inputs open circuited, i. e., time sharing control unit off.
- (2) For each thermocouple channel, the connecting or shunt resistor for the bridge balance circuit was removed from the top of the channel attenuation pad, B, to avoid cross talk.
- (3) A pyrotest potentiometer (Technique Associates, Model 9B) was connected to the test jacks of the channel to be calibrated.
- (4) A millivolt source was connected across the 1-ohm resistor, B.
- (5) The millivolt source was adjusted such that the potentiometer was nulled at 15 millivolts.
- (6) The potentiometer leads were removed from the test jack and the channel being calibrated was connected to the preamplifier, A, and converter via the time-sharing unit.
- (7) The channel attenuation pad, B, was adjusted so that the MilliSADIC converter read 1000 counts.
- (8) The millivolt source was removed and the initial count observed. This initial count represented the ambient temperature of the active junction referenced to the cold junction displayed as 0.015 millivolts per count.
- (9) The preamplifier was rechecked as in step (1) above. If necessary, it was readjusted and steps (3) through (9) were repeated.

V. MILLISADIC DATA PROCESSING SYSTEM

The MilliSADIC Data Processing System, used for recording time, load beam, strain gage, and thermocouple data, is capable of converting and storing up to 400 channels of information at an average sampling rate up to 200 channels per second. It accepts analog voltage inputs from the thermocouples, from the load beam bridges and from the strain gage bridges and places them into the 100-channel preamplifier. From here, the signals pass through a high speed commutator into an amplifier. The stability, linearity, and accuracy of this amplifier are better than $\pm 0.1\%$ to 5000 cps.

The converter receives analog voltage signals from the amplifier and converts them into trains of pulses. A pulse train is produced from each sample taken. The input voltage is sampled, and a proportional train of pulses is produced at the output in 500 microseconds. The maximum sample repetition rate is 1000 per second. Each sample is initiated by an external sample trigger pulse. Full-scale input is 99.9 volts; full-scale output is 999 pulses. Thus, each pulse corresponds to a 100-millivolt increment of input signal. Full-scale accuracy of conversion is greater than $\pm 0.2\%$.

The pulse trains emitted by the converter are translated into a digital code for recording by the counter-register which accumulates the pulses in three decades of electronic counters. The resultant code is transferred to temporary electronic storage from which the decimal-coded digits may be sequentially transferred to magnetic tape by means of blocking oscillator output. In addition, the time-register accumulates and stores digital time information in six decimal time digits which may be sequentially transferred to magnetic tape by means of blocking oscillators.

The decimal digit outputs from the counter-register and time-register are in time series on magnetic tape. However, punched cards are required, and the digital information must be made available in time parallel. This is accomplished by storing the sequential data, as read from the magnetic tape, on a magnetic recording drum. The stored information is read from the drum to an IBM 523 punch, 20 channels in parallel. The punched cards, thus obtained, form a permanent record of each test and can be used in conjunction with the IBM 7094 digital computer for analysis of the test data.

VI. TEST PERFORMANCE

Data obtained from the experimental program include loads, temperatures, and total strains as a function of time.

The technique of using localized radiant heating on one side of the specimen combined with air cooling on the opposite side, and of depending on thermal conductivity for distribution has proven to be a satisfactory method of imposing various shapes of temperature distribution on the specimen (Refs. 5 and 6). A variety of distributions can be obtained easily without a change in the heating installation, and only a portion of the test instrumentation must be exposed to direct radiant heating. The temperature distributions actually obtained did not meet the test objective of linear gradients; however, of greater importance in a program of this nature is the desirability of knowing accurately the actual temperatures. This was accomplished, and although non-linear gradients were encountered, these deviations from the nominal

distributions were of no special concern in verifying the theory, since theoretical analyses were performed using actual test conditions. The spot welding of thermocouples proved to be a reliable and easily installed instrumentation method for temperature measurement.

The strain gage instrumentation gave results that were highly satisfactory. The problems associated with accurate measurement of strains at elevated temperatures are many and varied. It had been verified during a past program (Ref. 5), (see Chapter VI), that conventional shunt calibration procedures were inadequate for programs of this nature, and that reliable strain data could be obtained only by providing sensitivity calibrations under test conditions against a known standard. The in-place strain gage calibration procedure used under the present program (see Chapter II F) provided for a determination of the individual variation of both strain gage sensitivity and apparent strain correction with temperature, and with time. The calibration was performed over a range of temperature from ambient to 450° F using two Tuckerman optical strain gages as the known standard.

Data handling procedures which were practically fully automatic were utilized for all instrumentation (load, temperature, and strain). The data collection and reduction procedures proved highly efficient and resulted in great savings of manpower and time and in an increase in accuracy and reliability. This is particularly noteworthy in view of the large number of strain gages and thermocouples involved, and the lengthy method of strain gage calibration.

APPENDIX II

MATERIALS SECTION (TABLE LXXV)

I. MATERIAL CONTROL COUPON PROGRAM--GENERAL

Material properties are test parameters that must be known with a degree of accuracy consistent with the objective of evaluating the analysis. It is not sufficient to use values for the material properties obtained from handbooks or the general literature. The material properties data are inputs to the theoretical method programmed for the IBM 7094 digital computer and, as such, must be synthesized into a spectral format to cover the range of parameters encountered in the environmental test of the large specimen. The present program included the testing of 12 material control coupons to obtain tension stress-strain data over a range of temperature from room temperature to 460° F. An additional 46 coupons were tested at the temperature levels of 200° F, 300° F, 350° F, 400° F and 450° F and over a wide range of stresses to obtain tension-creep data. Use was also made of material properties data collected under a past program of a similar nature. The variation of the coefficient of thermal expansion with temperature (Fig. 31) was taken from Ref. 5.

All tests involving load (coupon stress-strain, coupon creep and random loading of the large specimen) were conducted at the same stress rate of 12,000 psi/min, the approximate rate achieved automatically by the Baldwin lever arm creep machines used for creep testing. This was done so that any creep strain accumulated during loading was automatically accounted for in the stress-strain curves.

The layout of the 72 material control coupons on the large specimen sheet stock was as shown in Fig. 1. Tables 2 and 3 summarize coupon test conditions and utilization.

II. ELEVATED TEMPERATURE TENSION COUPON

A. TEST PROCEDURES AND INSTRUMENTATION

Twelve coupons were tested in tension over a range of temperature from room temperature to 460° F. All coupons were loaded into the plastic range to a strain level greater than two per cent. Strains were measured with the Tuckerman optical strain gage and with an SR-4 high temperature extensometer. The Tuckerman strain readings were synchronized with test machine loads at preselected intervals while the

extensometer strain was recorded continuously on a strip chart recorder. Temperatures were measured with two iron-constantan thermocouples on each coupon at the extremities of the gage section.

The temperature level at which each coupon was tested was assigned randomly. In addition, the order in which the coupons were tested was obtained from a table of random numbers (Table 2). The test setup is shown in Fig. 32.

B. DATA REDUCTION AND ANALYSIS

The nondimensional procedure reported in Refs. 2, 5, and 6 was used for synthesis of the tension stress-strain data. In order to nondimensionalize the coupon data, the variation of modulus of elasticity with temperature and the strain at 0.2% offset had to be known.

The variation of modulus with temperature is shown in Fig. 33. Supplemental modulus data obtained with a Tuckerman optical strain gage was available from the tension creep study. The individual values of modulus were obtained with an IBM correlation analysis which established a linear line of regression by the method of least squares. Values of the correlation coefficient very close to unity verified the linearity of the data. Low values of the standard error of estimate indicated that the scatter of the individual data points about the line of regression was small. The resulting variation of modulus with temperature was obtained by analyzing the modulus versus temperature data by means of an IBM Bi-Variate Correlation Analysis which utilized linear, quadratic, cubic, quartic, semilog, and log-log fits. The quadratic regression equation of Fig. 33 had a higher correlation coefficient and a lower standard error of estimate than the other available fits.

The test data from the tension coupon program were converted into nondimensional form using values of strain at 0.2% offset and modulus of elasticity at elevated temperatures. The results are plotted in Fig. 34 along with the exponential curves fitted to the data by the method of least squares. The expressions for the fitted curves are:

$$y = 0.900 x^{-0.137} \quad \begin{array}{l} 0.4 < x < 0.743 \\ \text{for } 0.938 \leq \bar{y} \leq 1.0 \end{array}$$

Standard error of y on x = 0.036

Correlation coefficient = 0.503

$$y = 0.710 x^{-0.937} \quad \begin{array}{l} x > 0.743 \\ \text{for } y < 0.938 \end{array}$$

Standard error of y on x = 0.029

Correlation coefficient = 0.991

where

x = strain per strain at 0.2% offset

y = secant modulus per modulus of elasticity at elevated temperature.

The results obtained in Refs. 2, 5, and 6 are expressed by:

$$y = 0.725 x^{-0.923}$$

$$y = 0.717 x^{-0.909}$$

$$y = 0.712 x^{-0.924}$$

These expressions are associated with tests performed on different sheet stock and utilizing different instrumentation. It can be assumed, therefore, that this procedure for synthesizing stress-strain data is valid.

The nondimensional stress-strain curve of Fig. 34 was converted to the spectral stress-strain curves of Fig. 35 by using the regression curve of Fig. 34 and a mean value of 0.006810 in./in. for the strain at 0.2% offset.

III. ELEVATED TEMPERATURE CREEP COUPON TESTS

A. INTRODUCTION

The specific objective of this study was to obtain the tension creep characteristics of the sheet material utilized for the large specimen test. The coupons were laid out as indicated in Fig. 1. A total of 46 of these coupons were tested in tension creep and the results reported herein.

Certain assumptions are necessary for this study to be compatible with the requirements of the contract. One of these is that total strains are measured from stabilized temperature conditions, thus eliminating a variation in free thermal expansion with time. For purposes of determining creep properties, by definition, total strain is expressed by:

$$\epsilon_{TOT} = \epsilon_{LD} + \epsilon_{CR}$$

where

ϵ_{LD} = initial load strain

ϵ_{CR} = creep strain

Effectively, this means that by definition, creep encompasses all time-dependent strain variations.

B. PLANNING OF THE EXPERIMENT

Some of the variables which enter into coupon testing programs are sheet stock, coupon location in the sheet stock, testing machine, load and temperature control, operator, time of test, etc. To evaluate each and every one of these variables would require an extremely large test program. The obvious reason for not conducting a program of this nature is, of course, high cost. At least as important, however, is the consideration that the general effect of most of the variables is not required a priori but only to the specific extent in which they affect the desired results, i. e., spectral creep strain versus time. A solution is to design the test as follows:

- (1) Conduct a factorial experiment with the primary variables of stress and temperature.
- (2) Randomly sample the universe of secondary variables.

With this approach, the stress-temperature effects are obtained in a conventional manner, while the effects of the secondary variables may be evaluated statistically. In this study, the effects of the secondary variables were not evaluated, since this procedure for obtaining tension creep characteristics of 2024-T4 bare aluminum was proven reliable under a similar past program (Ref. 5). For an indication of the effects of some of these secondary variables, see Appendix IV, Ref. 5.

The detail design of the experiment was accomplished as follows (see Table 2):

- (1) A table of index numbers (1 through 60) versus actual coupon number (601 through 660) was prepared.
- (2) A table of five columns was set up with headings: number, coupon number, temperature, stress, and machine number. The first column was numbered 1 through 60, consecutively.
- (3) A table of random numbers was entered and the second column (coupon number) was filled with the index numbers 1 through 60 as they occurred in the random table. Upon completion, the table of random numbers was marked where the last number occurred.
- (4) The random index numbers obtained under (3) were converted to actual coupon numbers using the table of (1).

- (5) The following were assigned in sequence: 15 coupons for static stress-strain testing, 45 coupons for tension creep testing, and the remaining 12 coupons were held as spares (a total of 72 coupons).
- (6) To the 45 creep coupons, 5 temperatures were assigned in random order, starting in the table of random numbers at the previous end point (Item 3).
- (7) Creep machine numbers 1 through 3 were assigned randomly in a similar manner.
- (8) For each of the 5 temperatures, stress levels were assigned as follows:
 - (a) The minimum stress (significant creep strain in 100 hours) was estimated from the data of Ref. 5.
 - (b) The maximum practical stress (about 1% total strain in 0.5 hour) was estimated similarly.
 - (c) The coupons were divided as evenly as possible over the established stress interval.
- (9) The spare coupons were assigned test conditions as the occasions arose.

Table 2 is the direct result of the application of the above procedure. Table 3 is a summary of material control coupon utilization in order of coupon number.

C. TEST INSTRUMENTATION

Tests were conducted utilizing 20,000-lb Baldwin creep machines. Three of these machines were reserved specifically for use on this program and provided with identification numbers 1 through 3. Loads were imposed on the test coupons by dead weight through a 40:1 lever system while the application of the load was accomplished automatically at a nearly constant rate. The load systems of these machines were monitored by load links which were calibrated in an FGT machine which, in turn, was calibrated against NBS certified load rings.

The test coupons were heated in 1800° F Marshall furnaces, (2-1/2 inches ID by 16 inches). Furnace temperatures were controlled by Series 60 Leeds and Northrup Controllers and recorded on Speedomax G instruments. The coupons were machined to standard configuration and instrumented with two iron-constantan thermocouples. The thermocouples were spotwelded to the coupon, one on each side of the gage length.

Strains were measured by both the Martin developed extensometer-translator system and the Tuckerman optical strain gage. The Tuckerman gage was also used to calibrate the extensometer system before each test.

Thermocouple, load-link, and extensometer readings were taken by the Martin 10-channel digital recorder. A line voltage regulator was used in the power supply lines to the 10-channel recorder and the extensometer systems. The test setup is shown in Figs. 36 and 37.

D. TEST PROCEDURE

After installation of the coupon and hookup of the strain and temperature instrumentation, the coupon was heated and stabilized at the desired temperature. An extensometer system calibration against the Tuckerman optical strain gage was performed for each coupon after it was brought to temperature and before the start of a creep test. Each creep coupon was tested for either 100 hours or until the total strain level reached one per cent. Strain readings were taken at preselected intervals during the application of load. For the first five minutes after loading, readings were taken at 30-second intervals and thereafter at intervals of five minutes for the first hour. Readings were then taken at 30-minute intervals for the remainder of the test except for the Tuckerman gage which was read during the day shift only.

E. DATA ANALYSIS

The primary purpose of this creep coupon program is to obtain spectral creep curves representative of the material used in the large specimen tests. These spectral creep curves are to be used as material properties input to the time-dependent, elasto-plastic analysis which is to be evaluated. In order to reduce the mass of individual test points into spectral curves, certain simplifying assumptions must be made. From a literature study conducted under Refs. 4 and 5, it was decided that enough evidence was available to warrant the conclusion that the creep laws:

$$\epsilon_p = Kt^m \quad (7)$$

for the primary stage, and

$$\epsilon_s = at + b \quad (8)$$

for the secondary stage are representative of the actual physical phenomena. In these expressions,

- t = time (hr)
 K = primary creep parameter (in. /in.)
 m = primary slope
 a = minimum creep rate (in. /in. /hr)
 b = offset of the secondary stage (in. /in.).

Equation (8) can be rewritten in terms of the coordinates of the secondary point (t_2 , ϵ_2):

$$\epsilon_s = a (t - t_2) + \epsilon_2 \quad (9)$$

The creep rates follow from Eqs (7) and (9):

$$\dot{\epsilon}_p = Km t^{m-1} \quad (10)$$

$$\dot{\epsilon}_s = a \quad (11)$$

At the secondary point, the primary and secondary creep rates are identical so that

$$t_2 = \left(\frac{a}{mK} \right)^{\frac{1}{m-1}} \quad (12)$$

Using the above relationships, all the creep data were analyzed systematically to obtain spectral creep curves:

- (1) The creep strain versus time plot was edited and an estimate made of the primary stage range. The data cards corresponding to this range were submitted to the IBM-7094 computer for a correlation analysis. In this program, Eq (7) was fitted to the data by the method of least squares, resulting in values for m , K , standard error and correlation coefficient.
- (2) The creep strain versus time plot was edited and an estimate made of the secondary stage range. The data cards corresponding to this range were submitted to the IBM-7094 for a correlation analysis, such that Eq (8) was fitted to the data by the method of least squares. Results were values for a , b , standard error and correlation coefficient.

(3) The primary slopes m obtained under item (1) were evaluated as follows:

(a) When m was plotted against stress at each of the five temperature levels, it became evident that, in general, m is invariant with stress and scatters about an average value.

(b) For each temperature, the mean of the m data was computed.

(c) A summary plot of the m data is presented in Fig. 38.

(4) The minimum creep rates " a " obtained under item (2) were evaluated as follows:

(a) For each of four temperatures, the equation

$$\text{Log } a = P' + Q' \sigma \quad (13)$$

was fitted to the data by the method of least squares to obtain the auxiliary parameters P' and Q' . This operation was not performed for the 300° F data because of the restricted range of the datum points (difference between maximum and minimum test stresses is small).

(b) The mean slope Q was computed by

$$Q = \frac{\sum N_T Q'}{N} \quad (14)$$

where N_T is the number of data points corresponding to each Q' and N is the total number of data points.

(c) A least squares analysis was performed to obtain P in

$$\text{Log } a = P + Q \sigma \quad (15)$$

using the mean slope Q obtained under (b).

(d) A summary plot of the a data and the fitted curves is presented in Fig. 39.

(5) The secondary point t'_2 was computed by Eq (12) using raw test data for K and fitted curves for a and m . In addition, t''_2 was estimated from each experimental creep curve. Plots of log time versus stress at constant temperature show good

correlation between t'_2 and t''_2 , indicating that the procedure was consistent up to this point.

- (6) The semilog plots of t_2 versus stress show a distinctly linear trend for the stress and temperature range investigated. The expression:

$$\text{Log } t_2 = p + q\sigma \quad (16)$$

was fitted to the data by the method of least squares to obtain the auxiliary parameters p and q .

- (7) The primary creep parameter K was then computed by:

$$K = \frac{a}{mt_2^{m-1}} \quad (17)$$

so that compatible creep rates were obtained at the secondary point (the values of t_2 used in this calculation were from Eq (16)).

- (8) The test data and computed curves for K were plotted on a semilog scale. The computed curves were extrapolated beyond the range of linearity such that the best possible fit to the test data was obtained. The results are shown in Fig. 40.
- (9) The spectral creep curves are being developed for use in an IBM-7094 program. In order to ensure proper interpolation for intermediate temperatures, a sufficient number of K -curves must be given. Intermediate K -curves were obtained in the following manner:
- (a) The data from the five K -curves determined by experiment were fitted to the equation (by the method of least squares)

$$\text{Log } K = a_K + b_K \sigma \quad (18)$$

- (b) A plot was made of the parameters a_K and b_K versus temperature, Fig. 41.
- (c) Values of a_K and b_K were obtained from the above plot at the desired intermediate temperatures.

- (d) Intermediate K-curves were obtained by substitution of these parameters in Eq (18).
- (10) Typical spectral creep curves were computed using the fitted m, K and a curves (Figs. 38, 40 and 39, respectively). The results, as well as a sampling of raw test data are presented in Figs. 42, 43, 44 and 45.

APPENDIX III

Tables and Illustrations

TABLE 1
**Summary of Weldable Strain Gage Performance During
Calibration and Environmental Test**

<u>Station</u>	<u>Gage No.</u>	<u>Outboard</u>	<u>Inboard</u>	<u>Under Lamp Banks</u>	<u>Under Cooling Banks</u>	<u>Comment</u>
X = 0	5	x		x		Out during installation of specimen
	7	x		x		Out during 2nd day of testing-erratic
	13	x		x		Out during pretest calibration
	14		x		x	Out during 1st day of testing
X = 4	17	x		x		Erratic
	23	x		x		Out during 2nd day of testing
	32		x		x	Out during 1st day of testing
	33	x		x		Out during intermediate calibration - erratic
X = 12	41	x				Out during 1st day of testing
	43	x		x		Out during pretest calibration
	52		x		x	Out during 2nd day of testing-erratic
	53	x		x		Out during 1st day of testing-erratic
X = 16	None					
X = 20	74		x		x	Out during pretest calibration
	83	x		x		Out during installation of specimen
	84		x		x	Out during installation of specimen
X = 24	86		x		x	Out during 1st day of testing

TABLE 2
Random Test Conditions for Material Control Coupon Program

Index No.	Coupon No.	Tempera- ture (°F)	Stress (ksi)	Machine No.	Index No.	Coupon No.	Tempera- ture (°F)	Stress (ksi)	Machine No.
1	614	RT	EL-PL	FGT	31	620	350	30.00	2
2	621	RT	EL-PL	FGT	32	656	300	48.50	1
3	622	200	EL-PL	FGT	33	603	350	37.00	1
4	617	300	EL-PL	FGT	34	609	400	18.01	3
5	646	325	EL-PL	FGT	35	605	300	28.00	1
6	647	350	EL-PL	FGT	36	655	450	16.00	3
7	608	375	EL-PL	FGT	37	606	300	46.51	3
8	629	400	EL-PL	FGT	38	628	200	53.00	3
9	624	420	EL-PL	FGT	39	604	200	51.00	2
10	657	440	EL-PL	FGT	40	618	450	20.00	1
11	645	450	EL-PL	FGT	41	627	200	55.00	3
12	639	460	EL-PL	FGT	42	654	400	22.00	3
13	659	←	Spare	←	43	638	400	26.00	3
14	640	←	Spare	←	44	607	450	20.00	3
15	625	←	Spare	←	45	633	400	30.00	3
16	601	200	47.50	1	46	635	400	28.00	3
17	613	350	22.00	3	47	648	450	26.00	1
18	612	400	9.98	3	48	632	400	34.00	1
19	634	300	32.00	1	49	619	450	30.00	3
20	650	300	42.49	1	50	652	300	42.50	2
21	660	400	14.00	1	51	611	400	32.00	1
22	630	200	49.69	3	52	615	400	36.00	1
23	610	350	26.00	1	53	602	200	54.00	2
24	649	300	32.00	2	54	651	350	18.00	2
25	643	450	4.01	2	55	636	450	24.00	2
26	641	450	7.99	3	56	616	350	46.00	2
27	623	300	38.60	2	57	626	450	22.00	2
28	644	300	44.50	2	58	642	450	18.00	2
29	631	450	11.99	2	59	637	350	43.00	1
30	658	350	34.00	1	60	653	350	40.00	2

TABLE 3
Summary of Material Control Coupon Utilization

Coupon No.	Temperature (°F)	Stress (ksi)	Machine No.	Index No.	Coupon No.	Temperature (°F)	Stress (ksi)	Machine No.	Index No.
601	200	47.50	1	16	637	350	43.00	1	59
602	200	54.00	2	53	638	400	26.00	3	43
603	350	37.00	1	33	639	460	EL-PL	FGT	12
604	200	51.00	2	39	640	← Spare →			
605	300	28.00	1	35	641	450	7.99	3	26
606	300	46.51	3	37	642	450	18.00	2	58
607	450	20.00	3	44	643	450	4.01	2	25
608	375	EL-PL	FGT	7	644	300	44.50	2	28
609	400	18.01	3	34	645	450	EL-PL	FGT	11
610	350	26.00	1	23	646	325	EL-PL	FGT	5
611	400	32.20	1	51	647	350	EL-PL	FGT	6
612	400	9.98	3	18	648	450	26.00	1	47
613	350	22.00	3	17	649	300	32.00	2	24
614	RT	EL-PL	FGT	1	650	300	42.49	1	20
615	400	36.00	1	52	651	350	18.00	2	54
616	350	46.00	2	56	652	300	42.50	2	50
617	300	EL-PL	FGT	4	653	350	40.00	2	60
618	450	20.00	1	40	654	400	22.00	3	42
619	450	30.00	3	49	655	450	16.00	3	36
620	350	30.00	2	31	656	300	48.50	1	32
621	RT	EL-PL	FGT	2	657	440	EL-PL	FGT	10
622	200	EL-PL	FGT	3	658	350	34.00	1	30
623	300	38.60	2	27	659	← Spare →			
624	420	EL-PL	FGT	9	660	400	14.00	1	21
625	← Spare →				661	← Spare →			
626	450	22.00	2	57	662	← Spare →			
627	200	55.00	3	41	663	← Spare →			
628	200	53.00	3	38	664	← Spare →			
629	400	EL-PL	FGT	8	665	← Spare →			
630	200	49.69	3	22	666	← Spare →			
631	450	11.99	2	29	667	450	20.0	3	
632	400	34.00	1	48	668	← Instrumentation Checkout →			
633	400	30.00	3	45	669	← Instrumentation Checkout →			
634	300	32.00	1	19	670	← Instrumentation Checkout →			
635	400	28.00	3	46	671	← Instrumentation Checkout →			
636	450	24.00	2	55	672	← Instrumentation Checkout →			

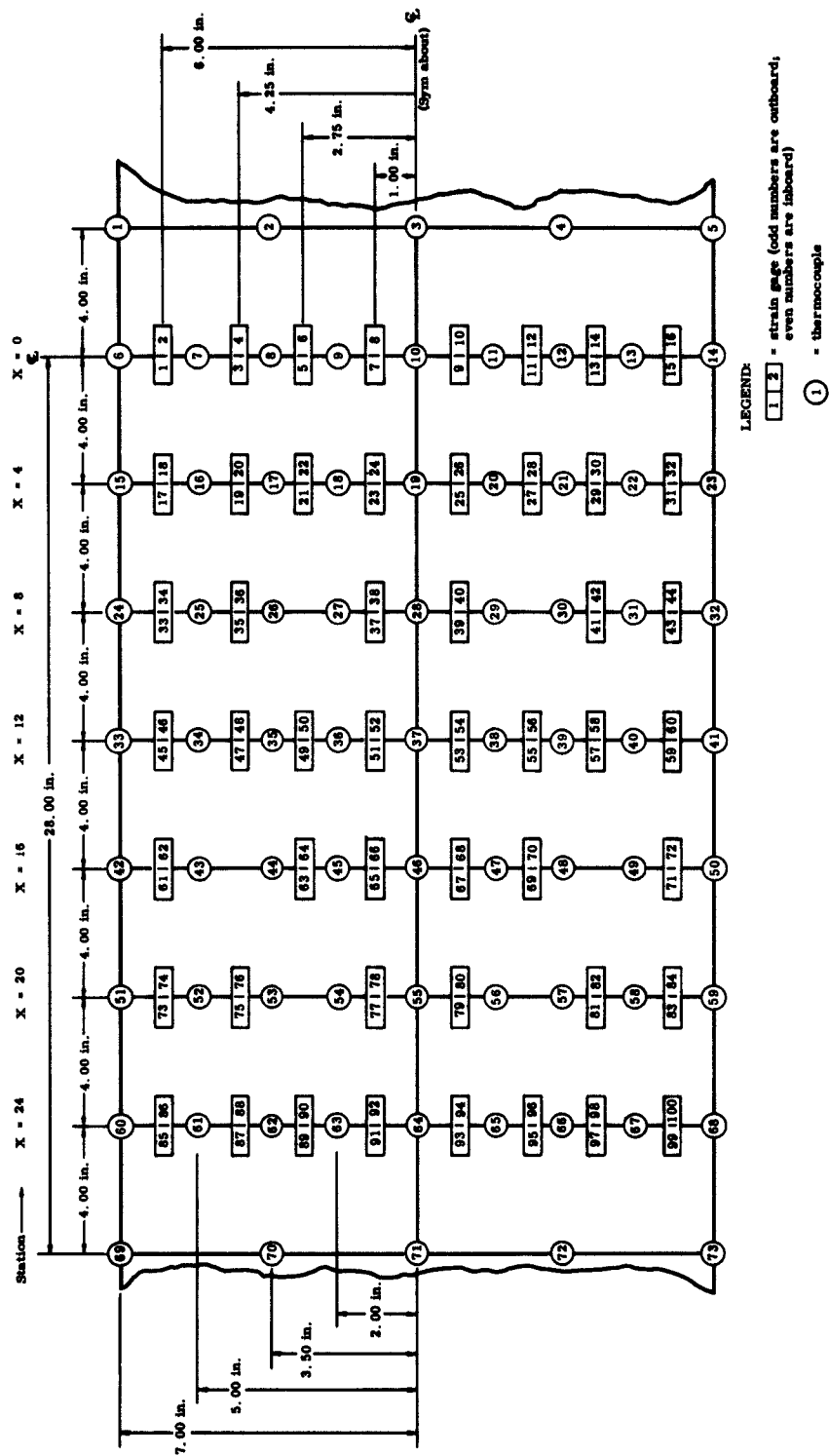


Fig. 2. Specimen Instrumentation Layout



Fig. 3. Instrumented Specimen

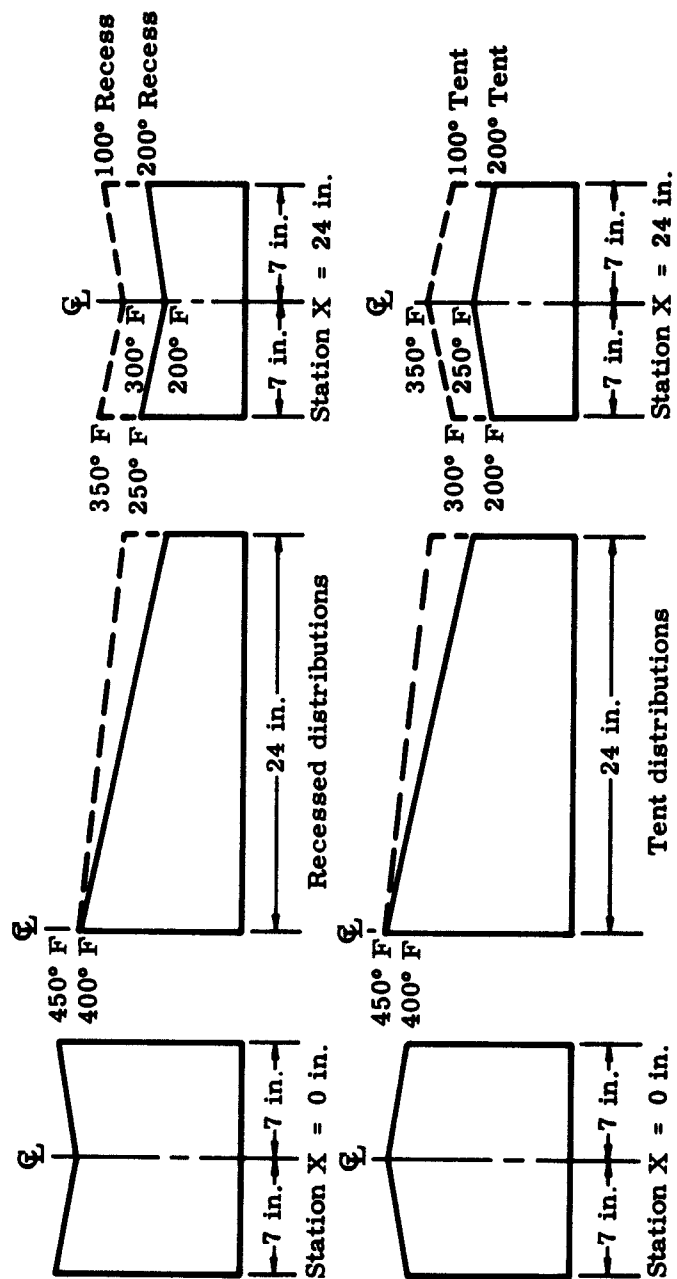


Fig. 4. Test Conditions, Nominal Temperature Distributions

LEGEND:

- Horizontal σ_x temperatures at Stations X = 0 and X = 24
 - - - - Edge temperatures at Stations X = 0 and X = 24

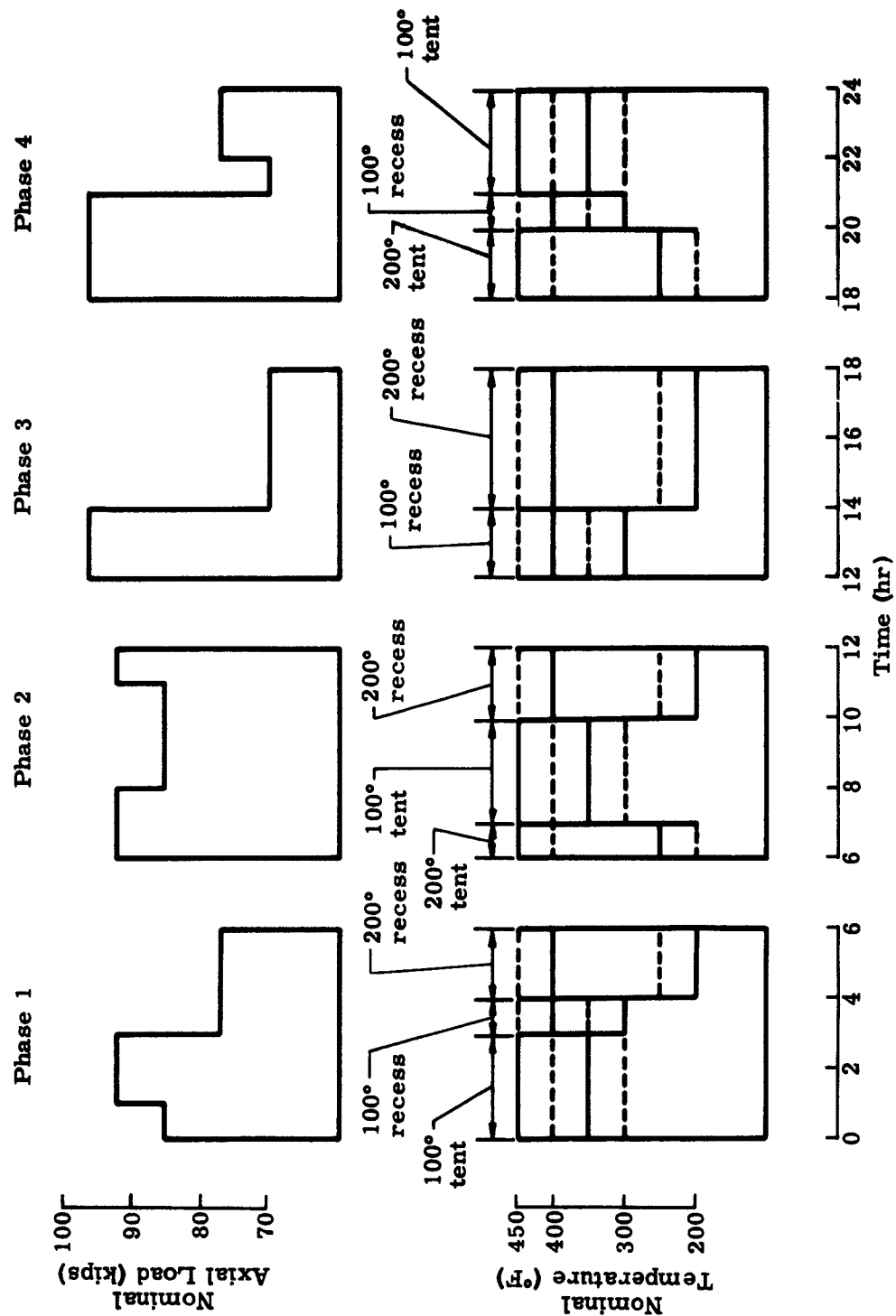


Fig. 5. Random Test Conditions

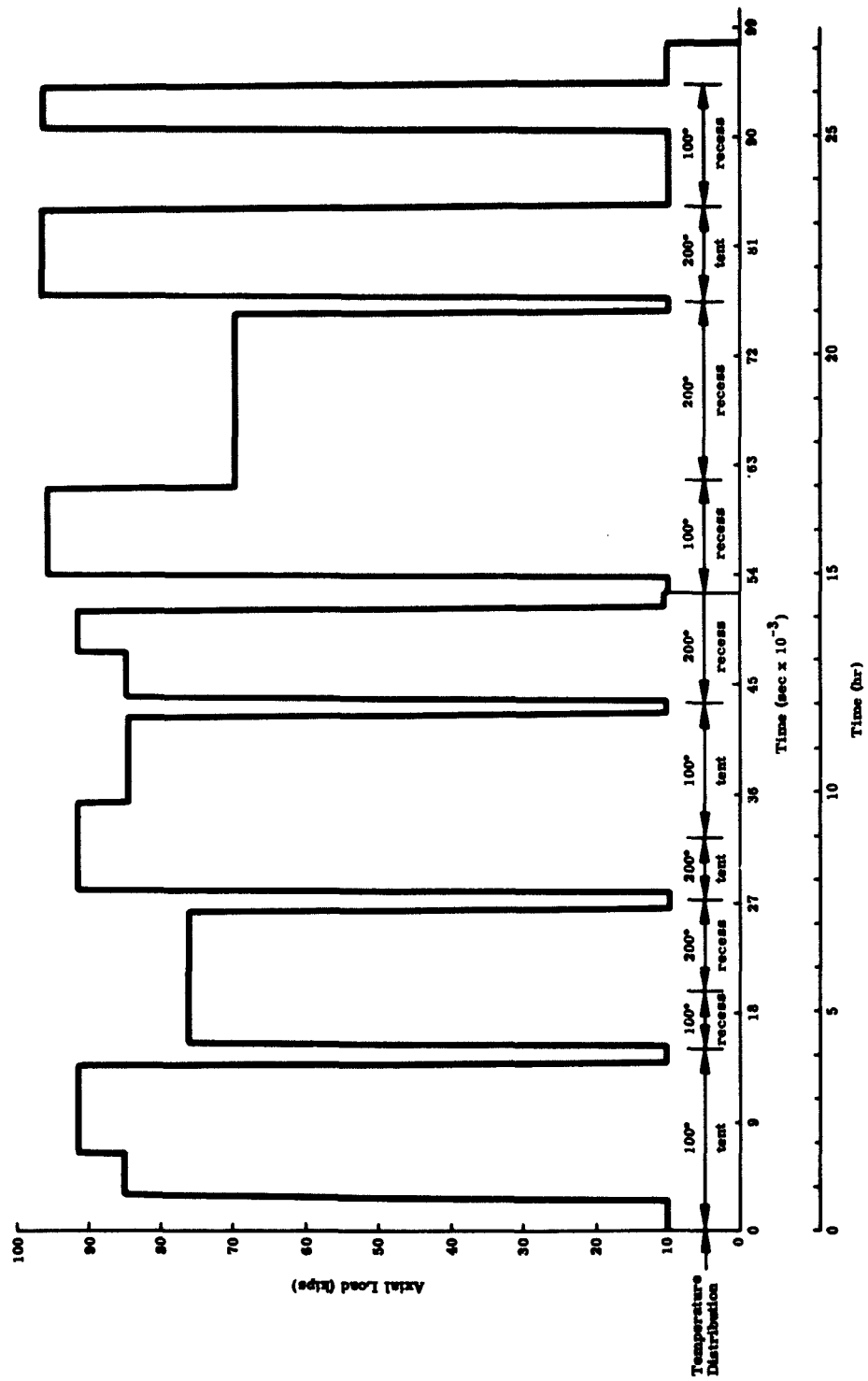


Fig. 6. Actual Load and Temperature Spectrum Versus Time

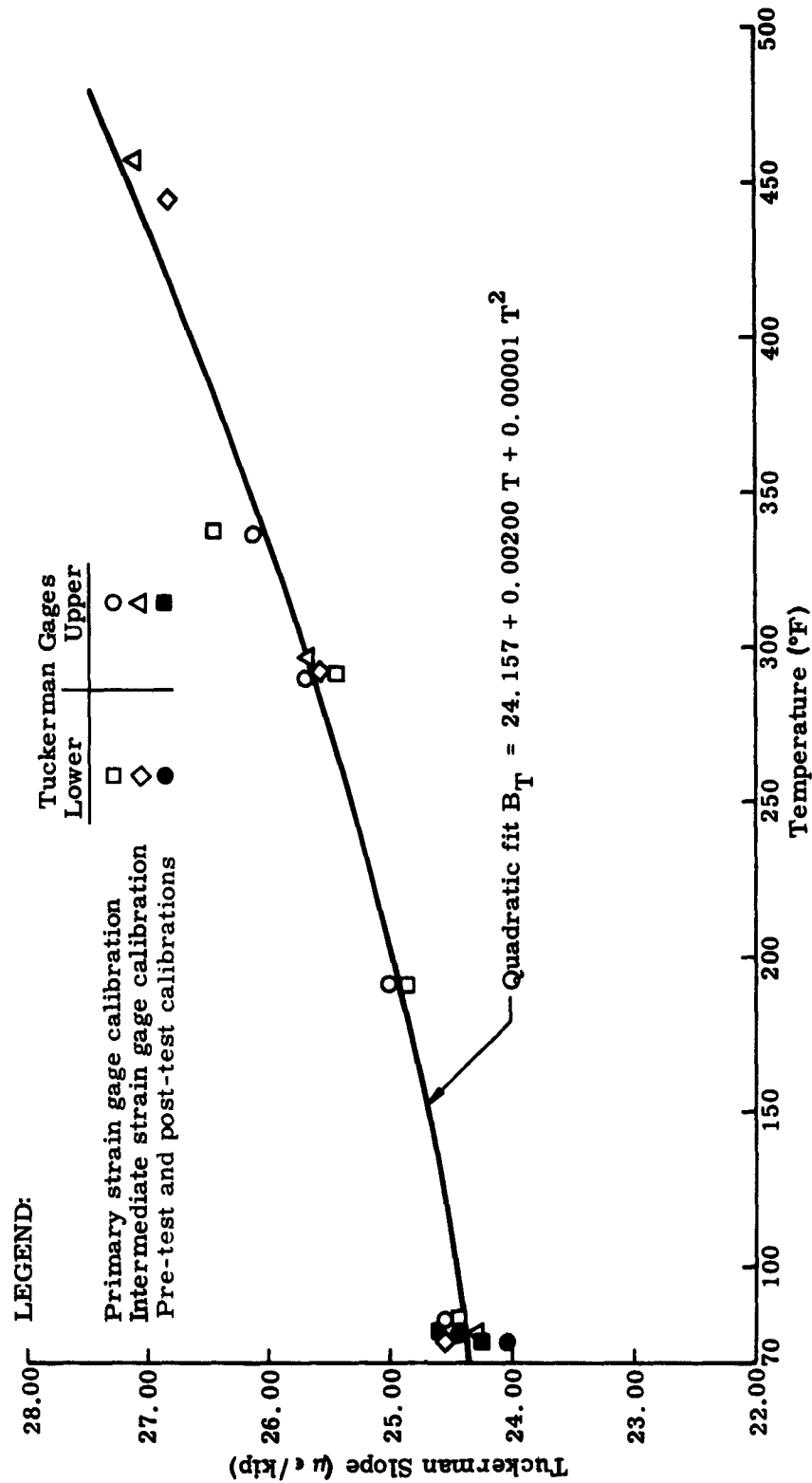


Fig. 7. Tuckerman Slope Versus Temperature

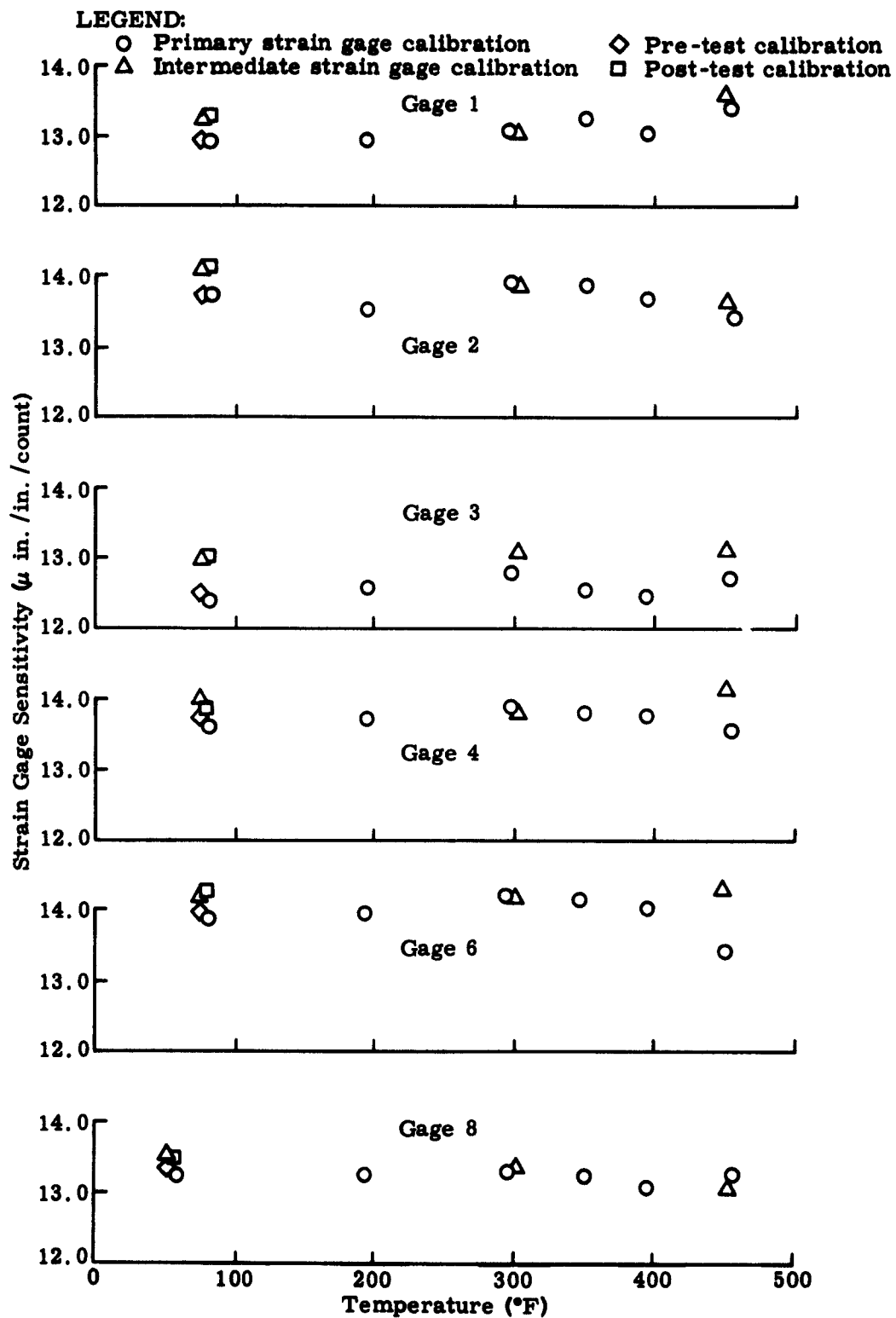


Fig. 8. Strain Gage Sensitivity Versus Temperature

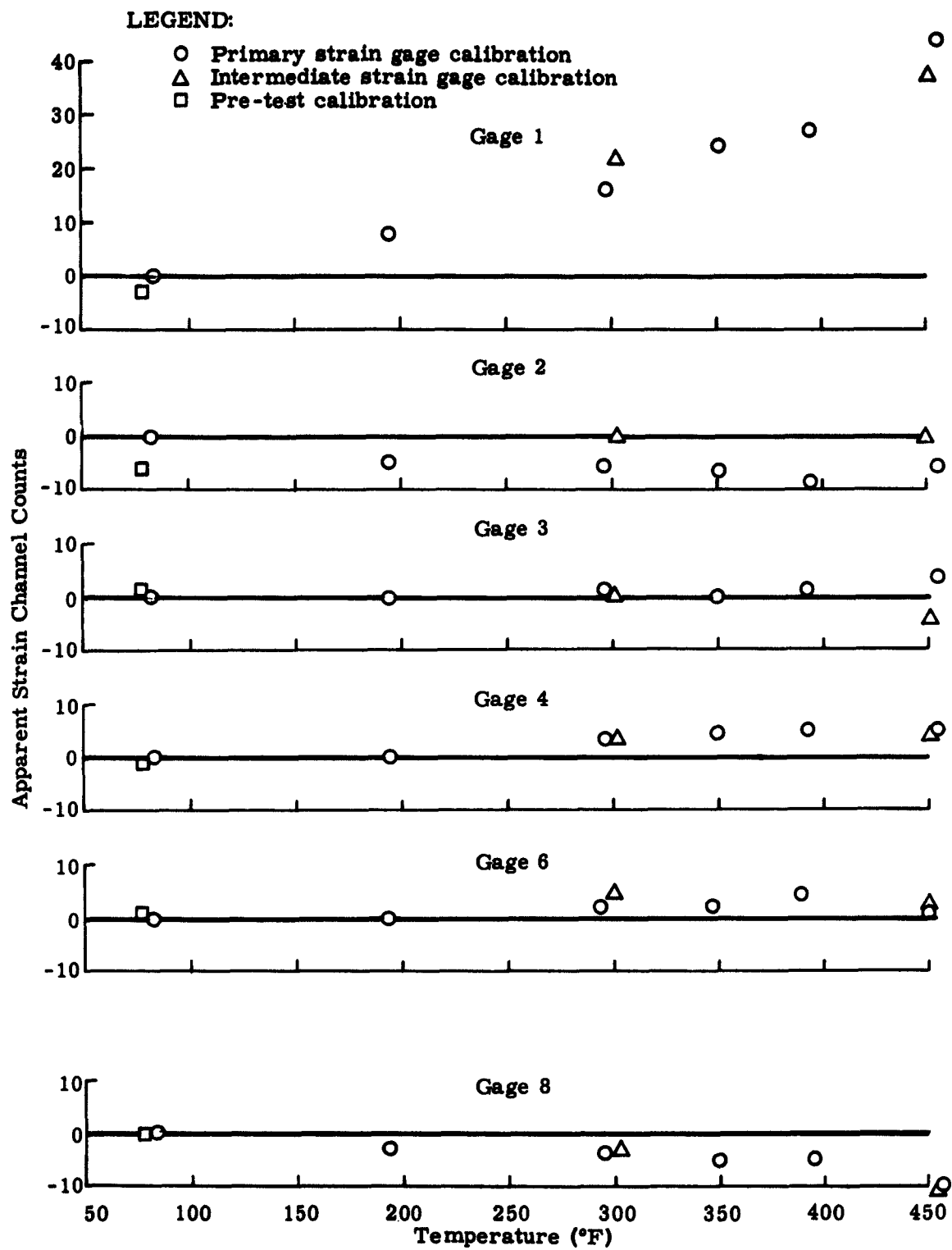


Fig. 9. Apparent Strain Versus Temperature

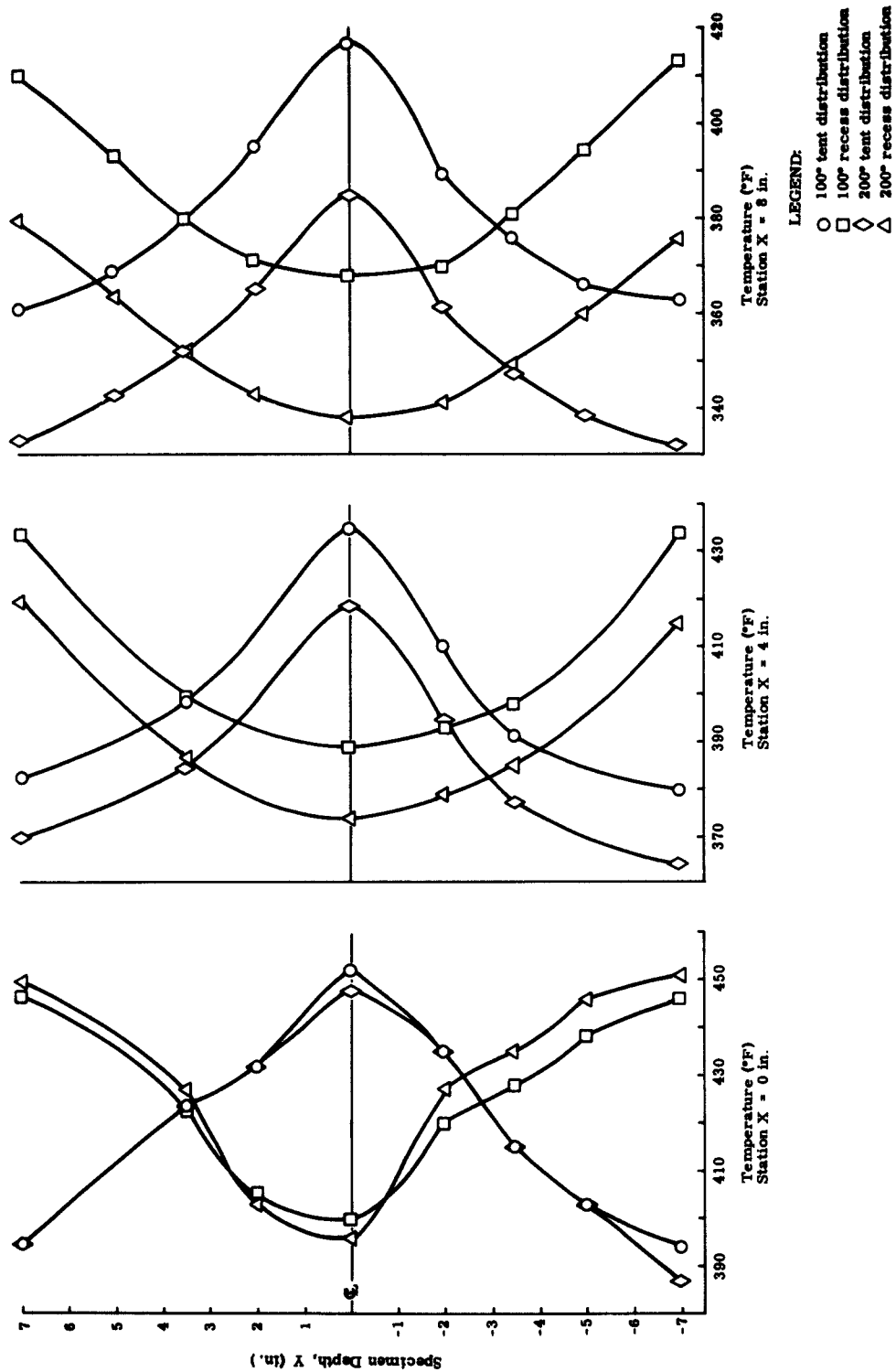


Fig. 10. Typical Actual Temperature Distributions

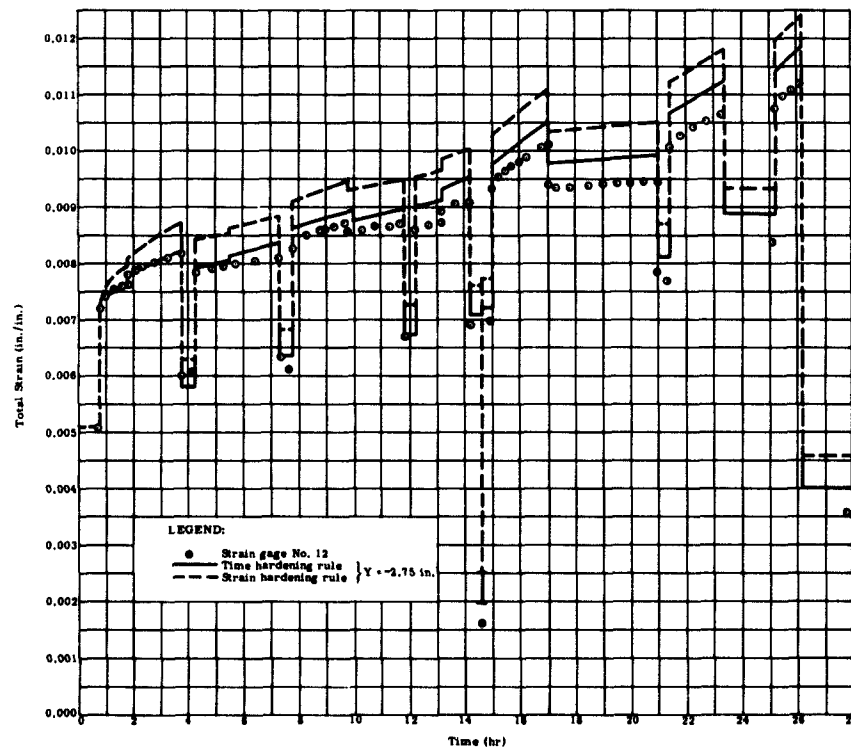
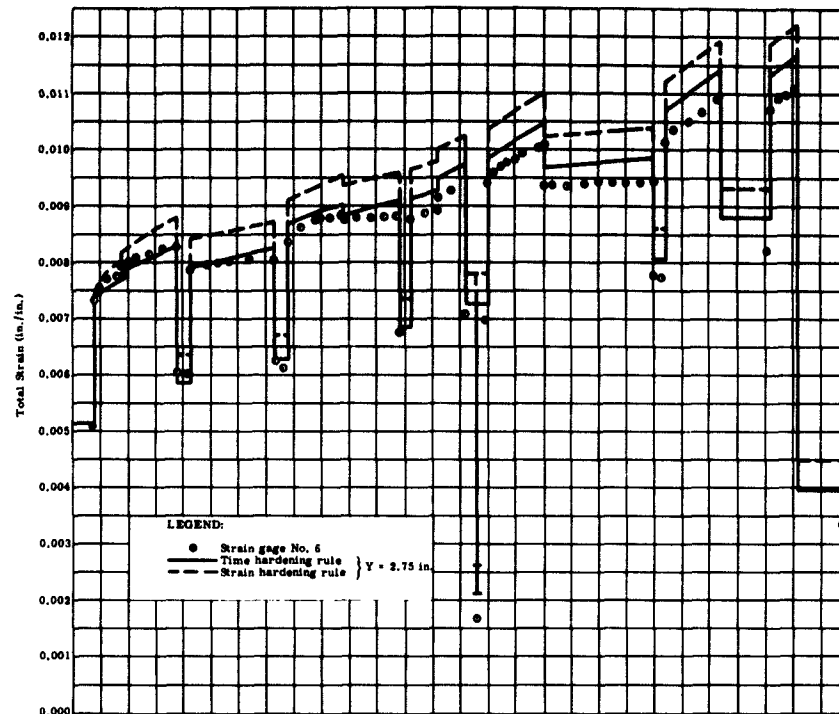


Fig. 11. Total Strain Versus Time, Station $X = 0$ In.

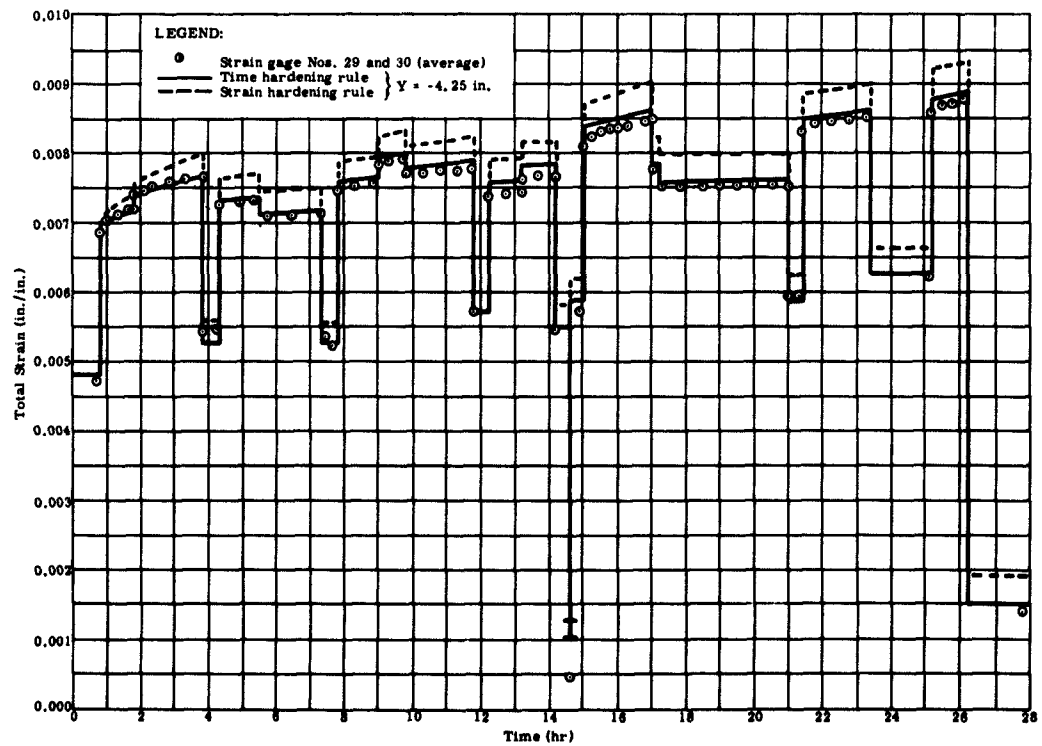
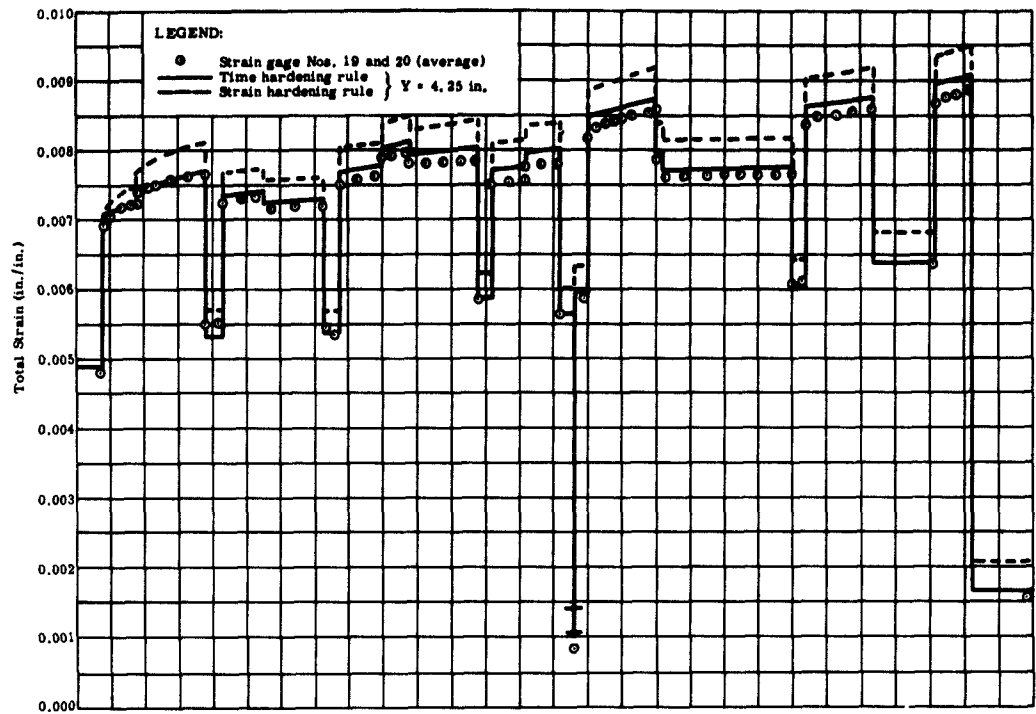


Fig. 12. Total Strain Versus Time, Station $X = 4 \text{ in.}$

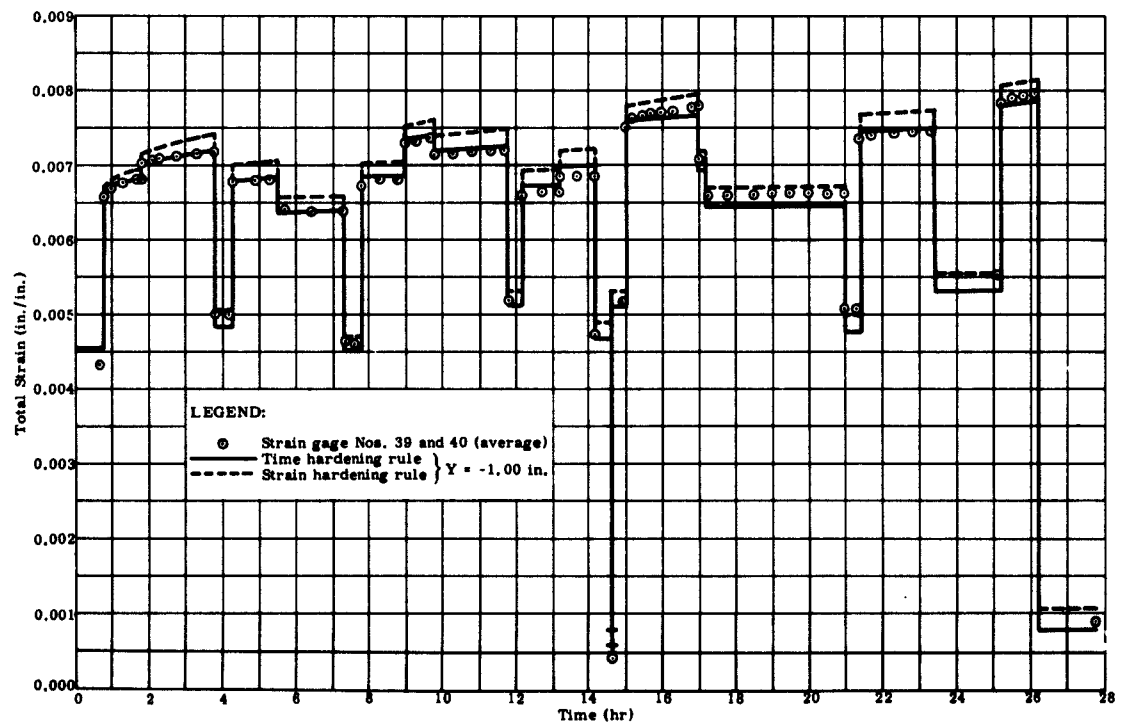
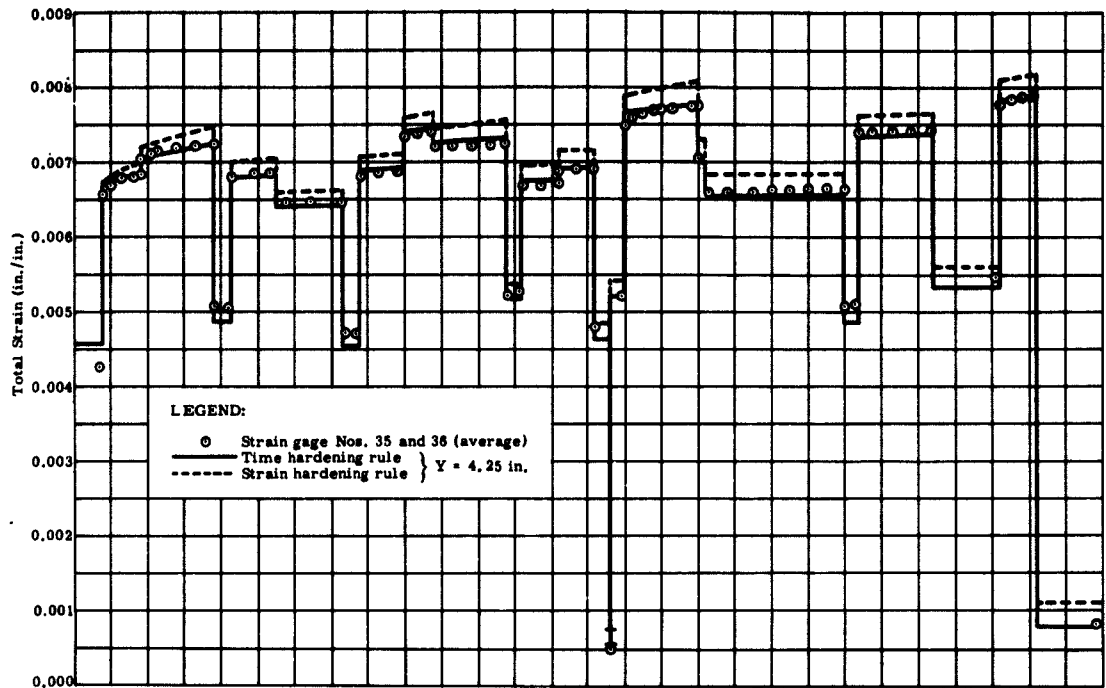


Fig. 13. Total Strain Versus Time, Station X = 8 In.

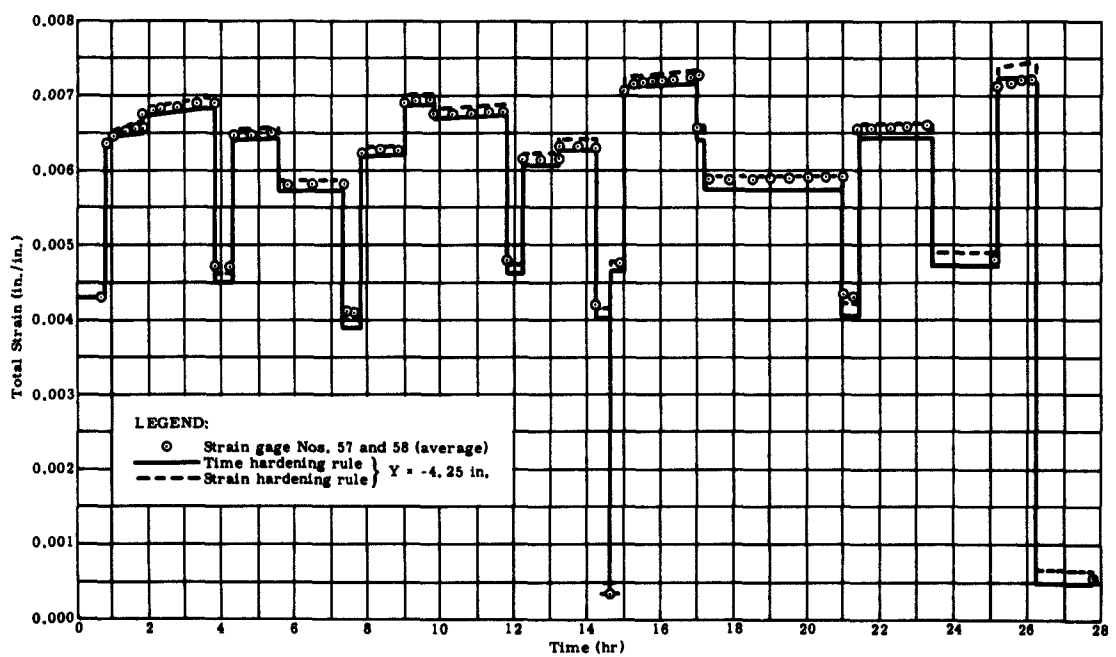
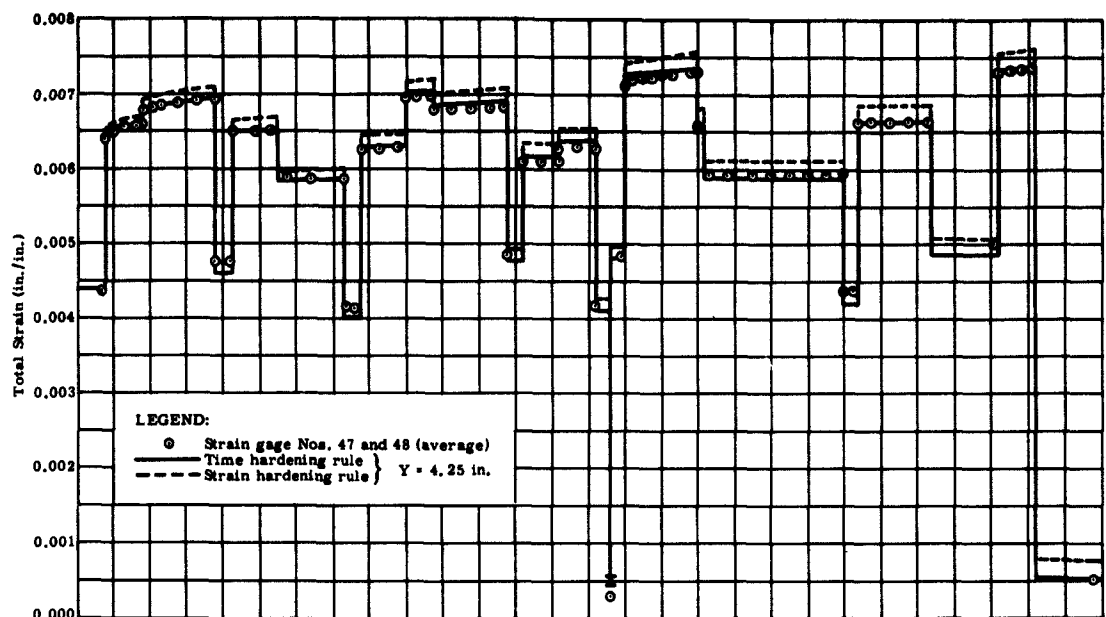


Fig. 14. Total Strain Versus Time, Station X = 12 in.

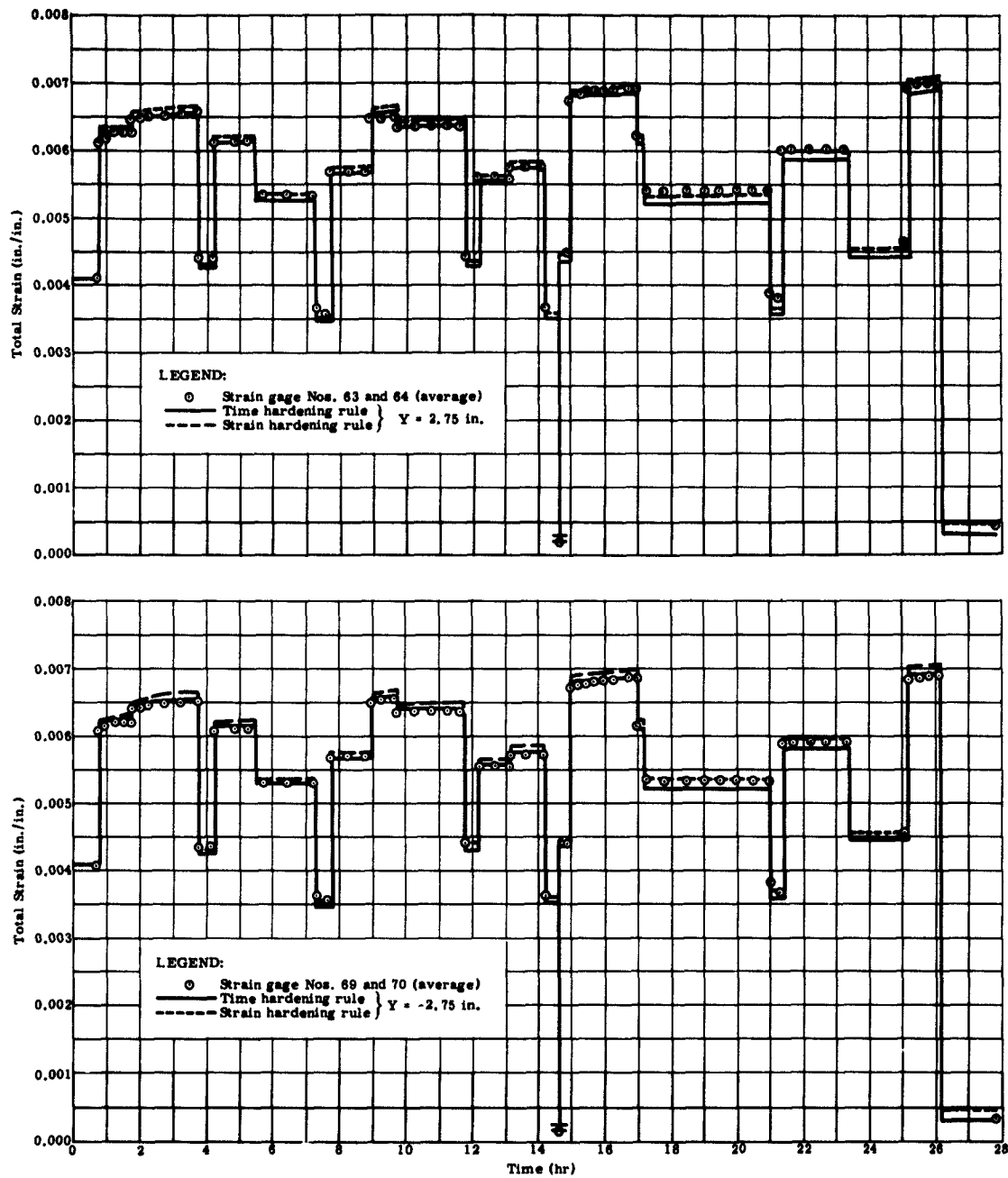


Fig. 15. Total Strain Versus Time, Station X = 16 In.

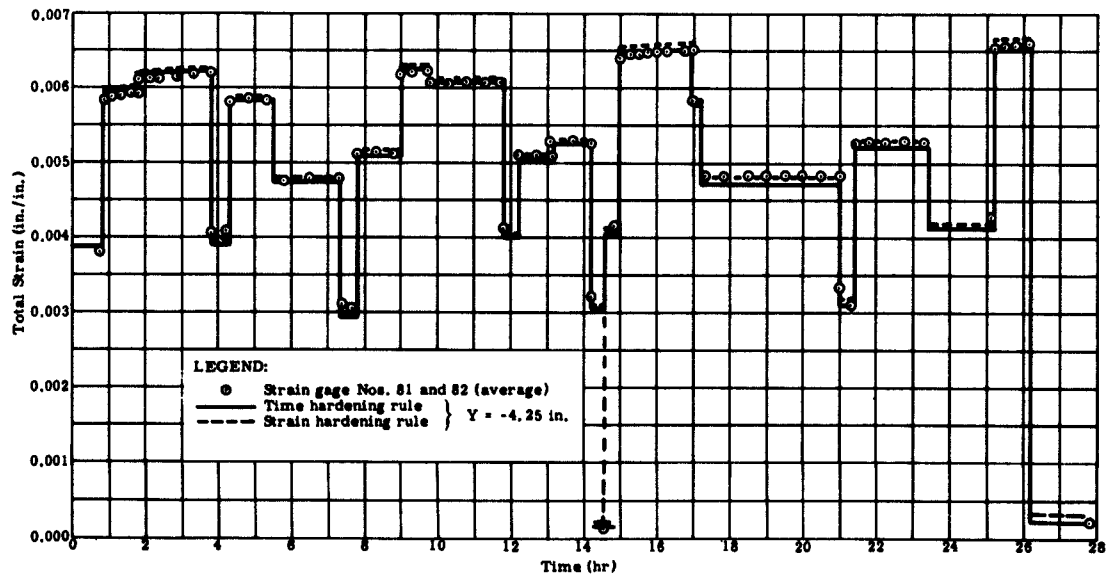
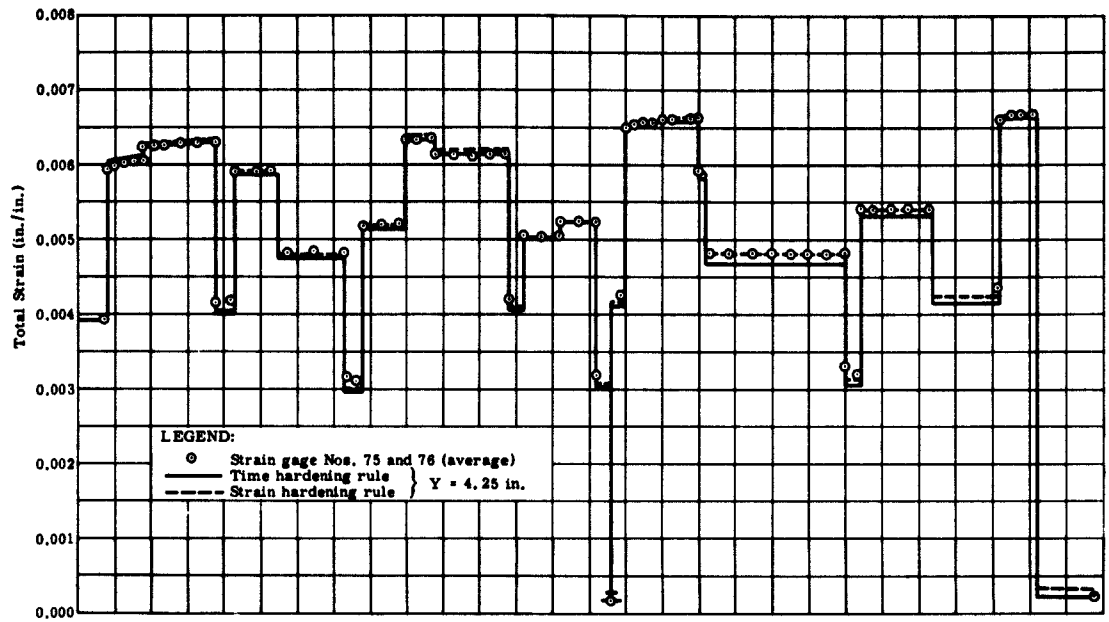


Fig. 16. Total Strain Versus Time, Station X = 20 In.

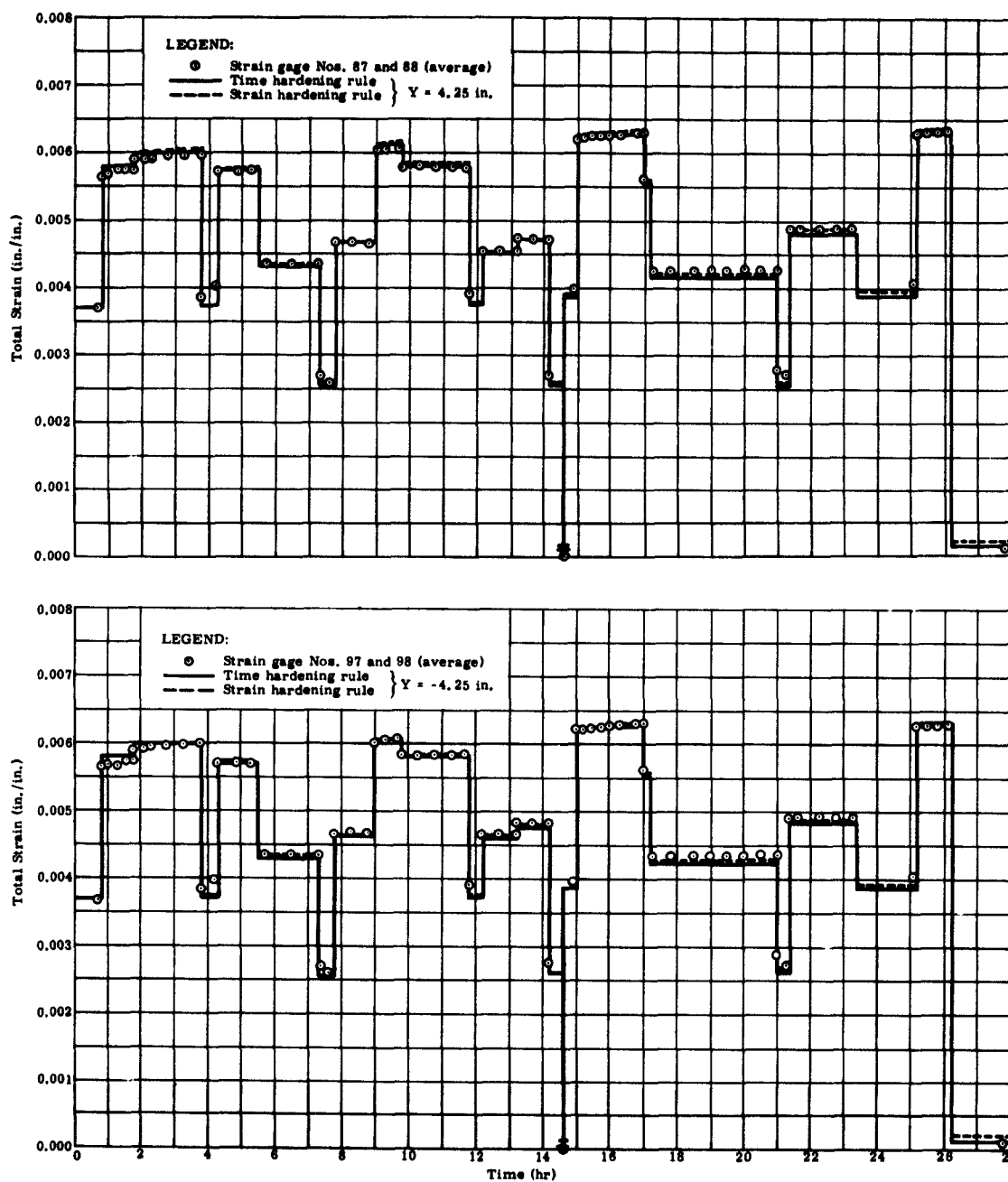


Fig. 17. Total Strain Versus Time, Station X = 24 In.

LEGEND:

- Experimental strain outboard
- Experimental strain inboard
- Mean regression of strain gage data
- Analytical strain--strain hardening rule
- Analytical strain-time hardening rule
- * Room temperature residuals at end of test

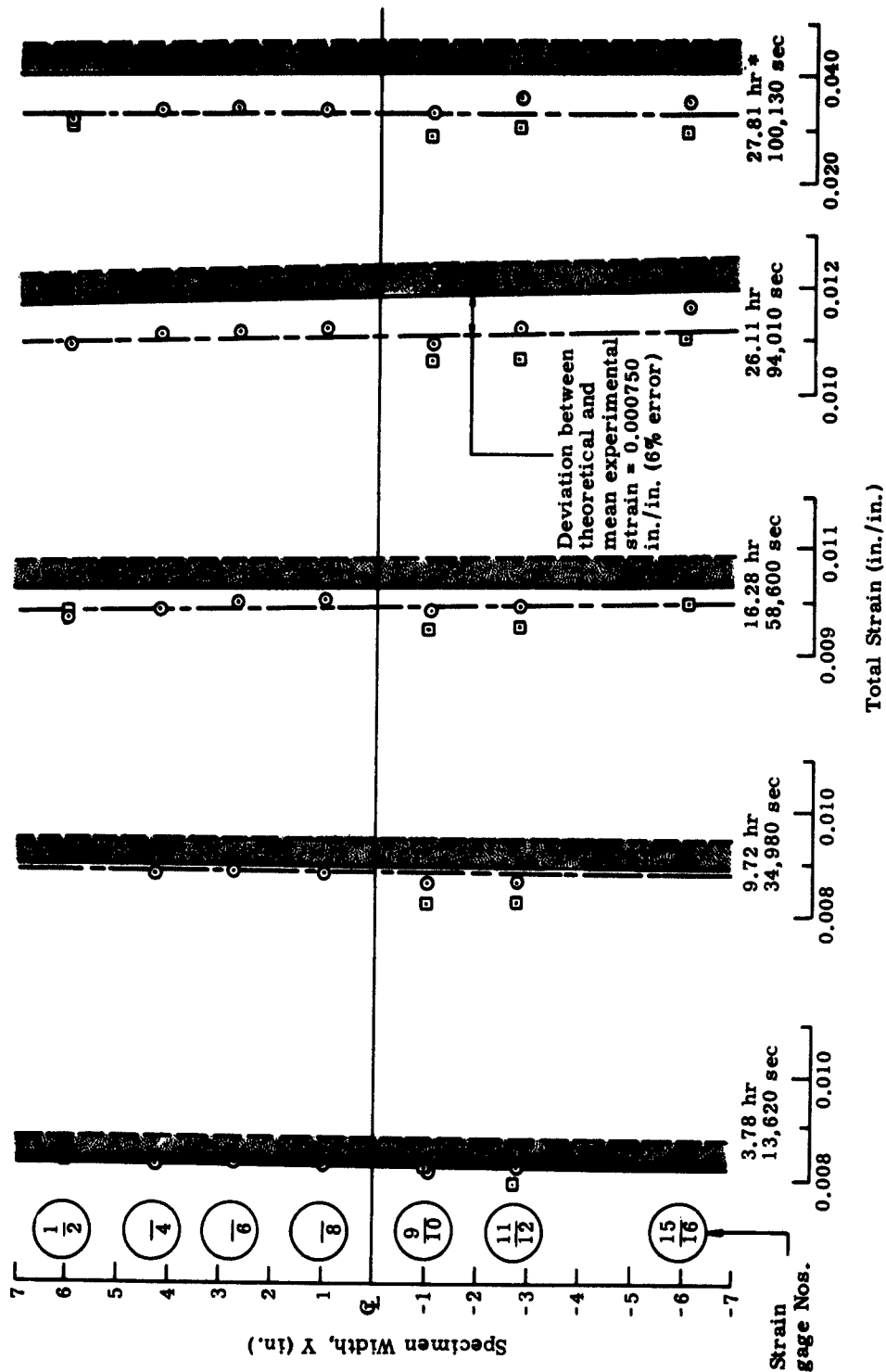


Fig. 18. Total Strain Distributions, Station X = 0 in.

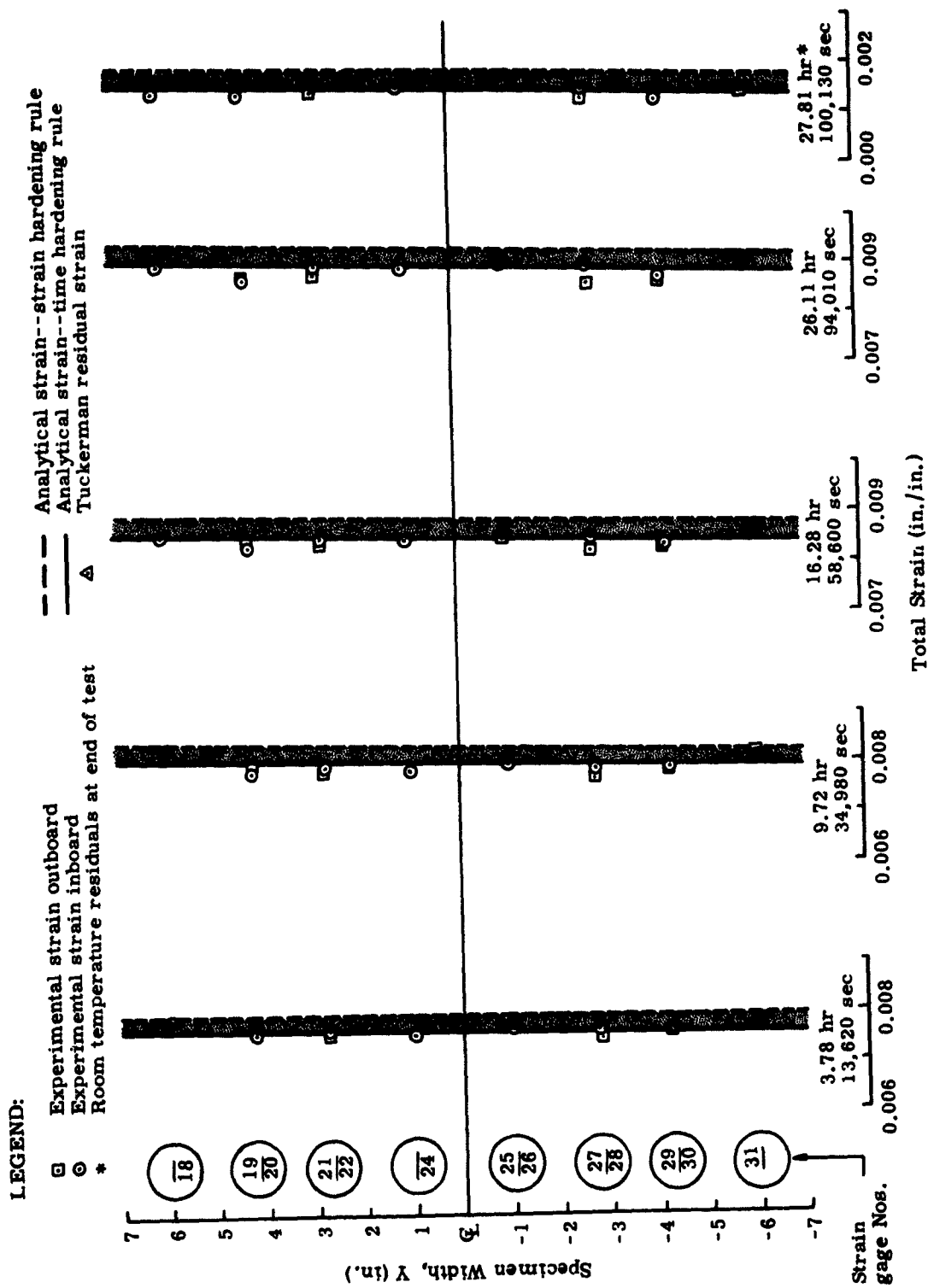


Fig. 19. Total Strain Distributions, Station X = 4 in.

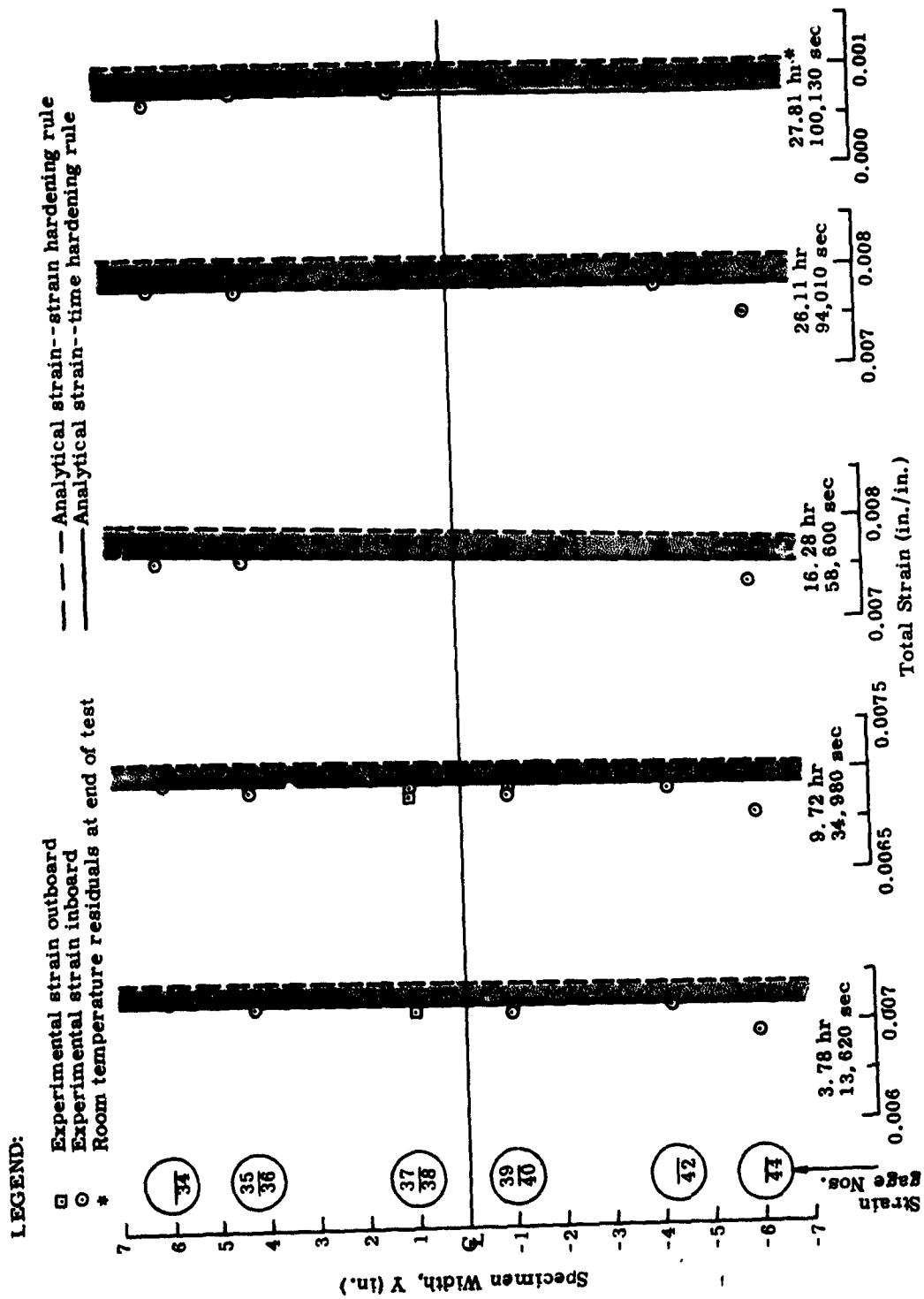


Fig. 20. Total Strain Distributions, Station X = 8 In.

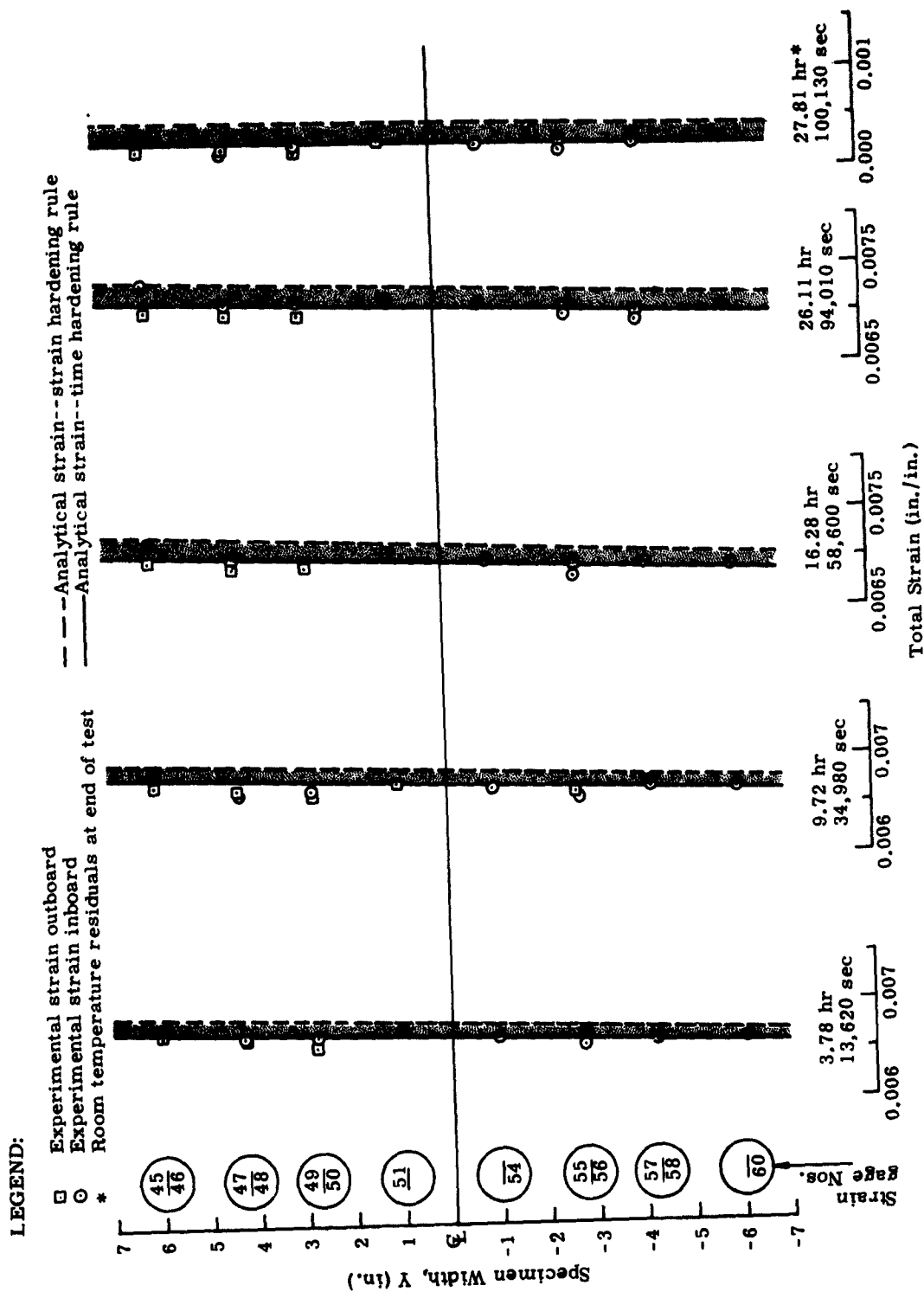


Fig. 21. Total Strain Distributions, Station X = 12 in.

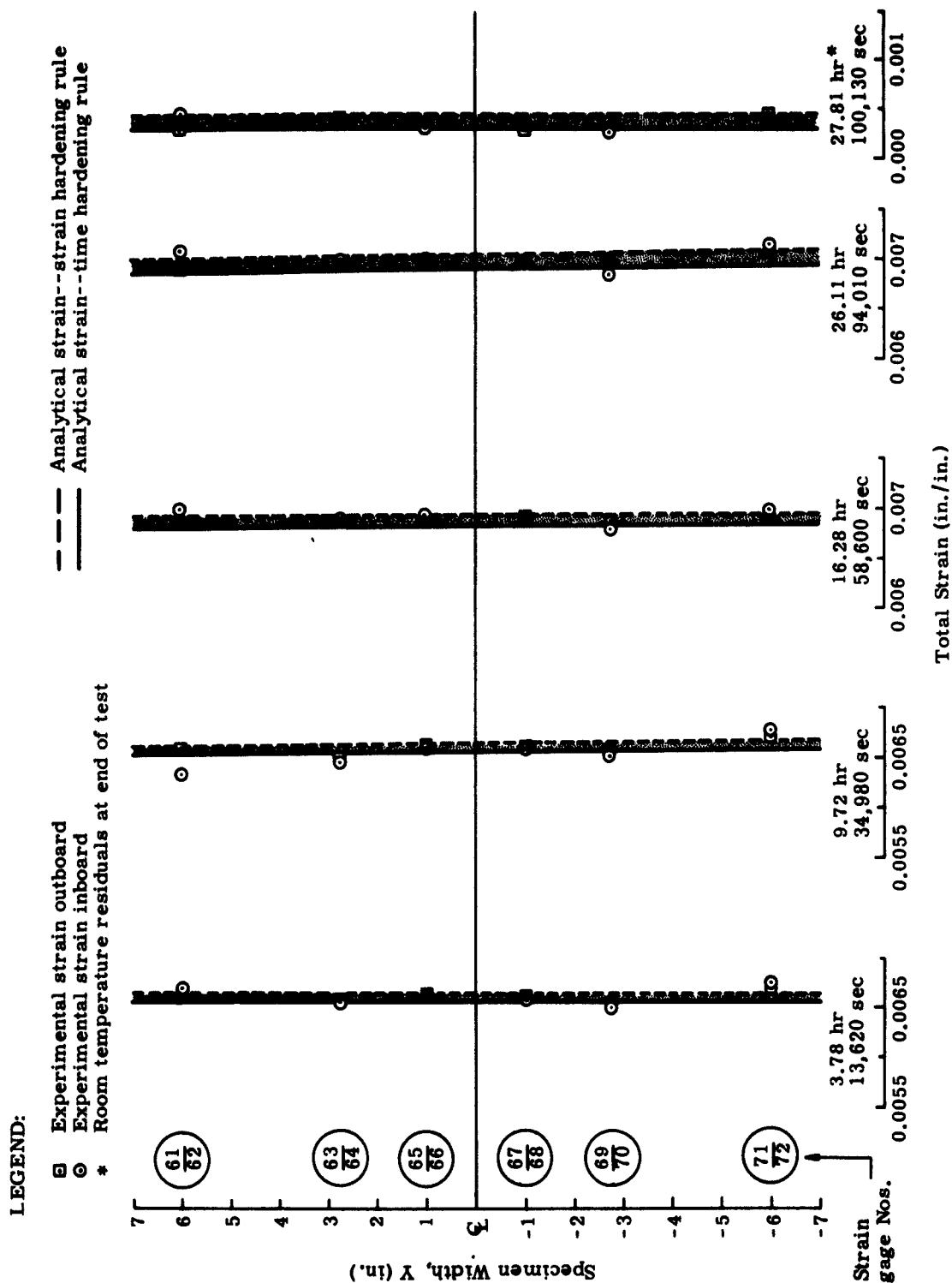


Fig. 22. Total Strain Distributions, Station X = 16 in.

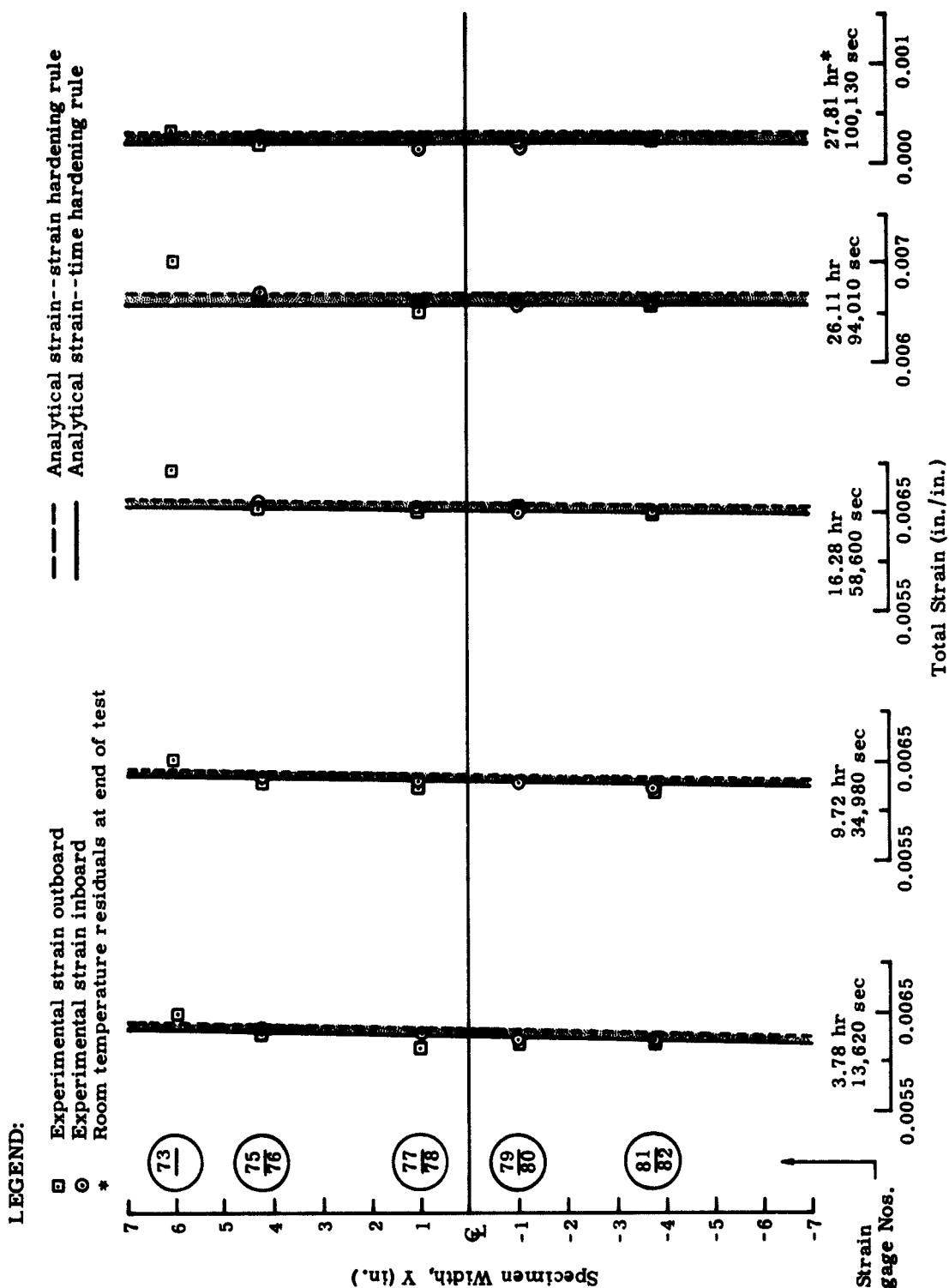


Fig. 23. Total Strain Distributions, Station X = 20 In.

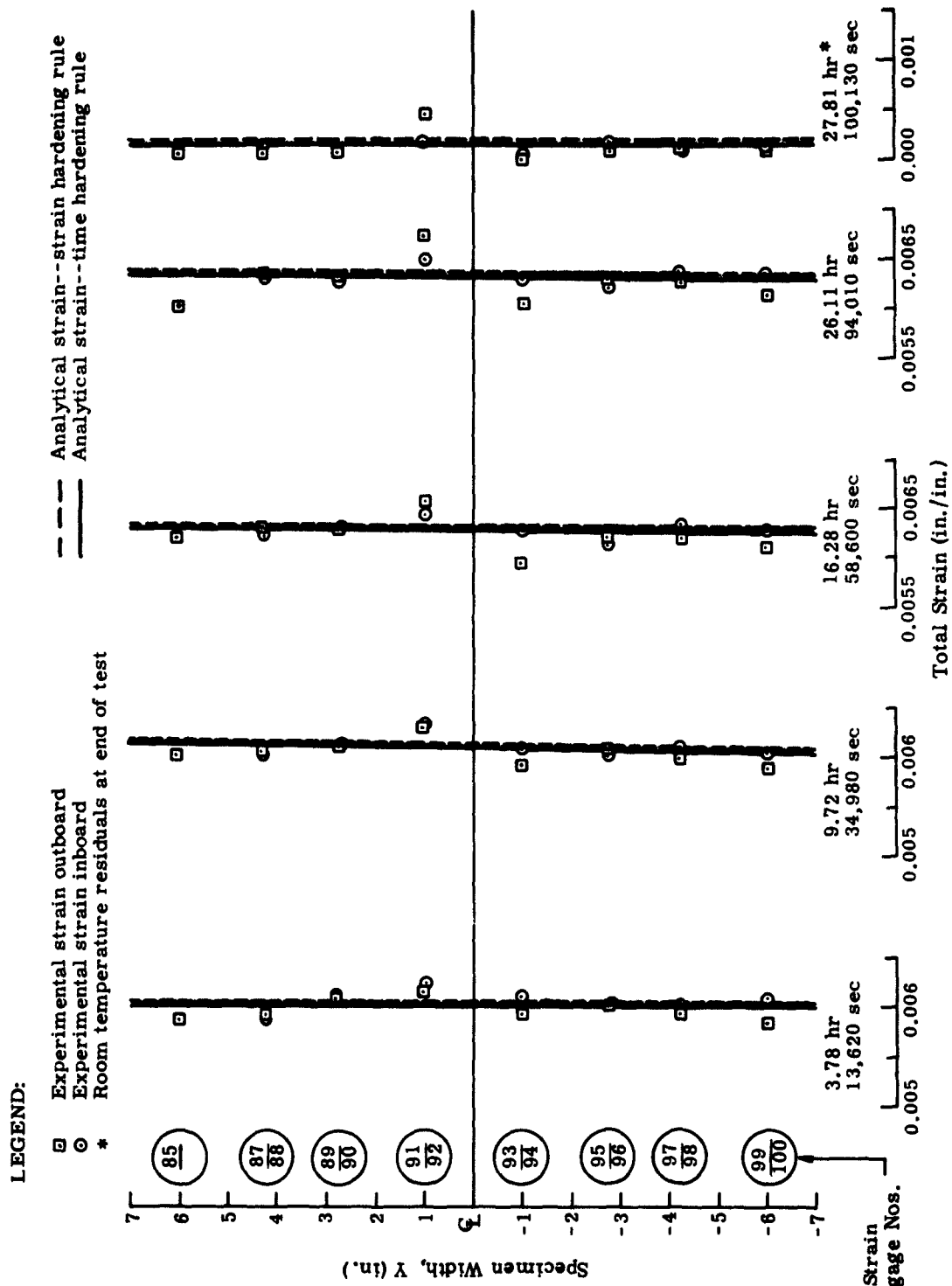


Fig. 24. Total Strain Distributions, Station X = 24 In.

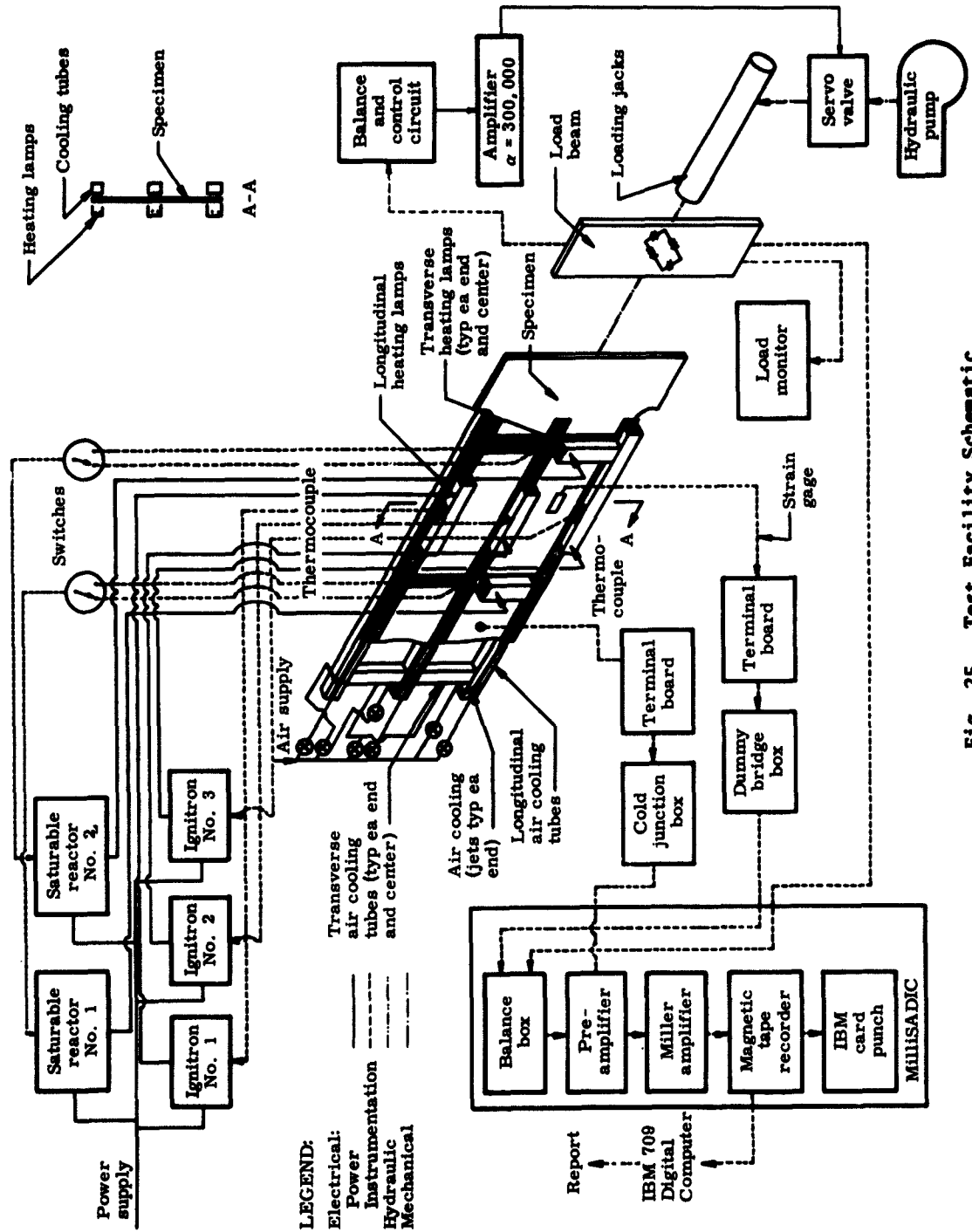


Fig. 25. Test Facility Schematic



Fig. 26. Overall View of Test Facility

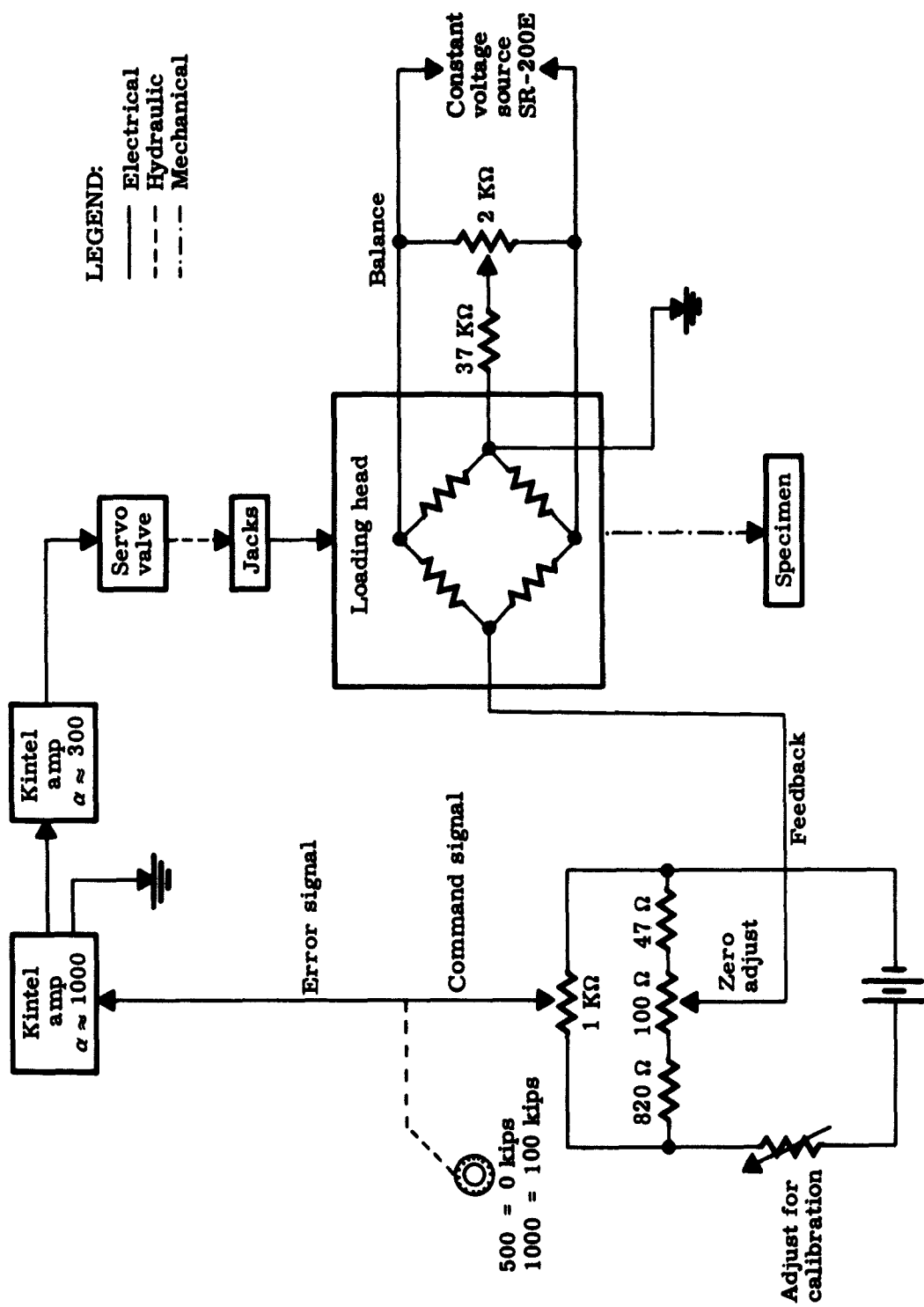


Fig. 27. Schematic of Load Control System

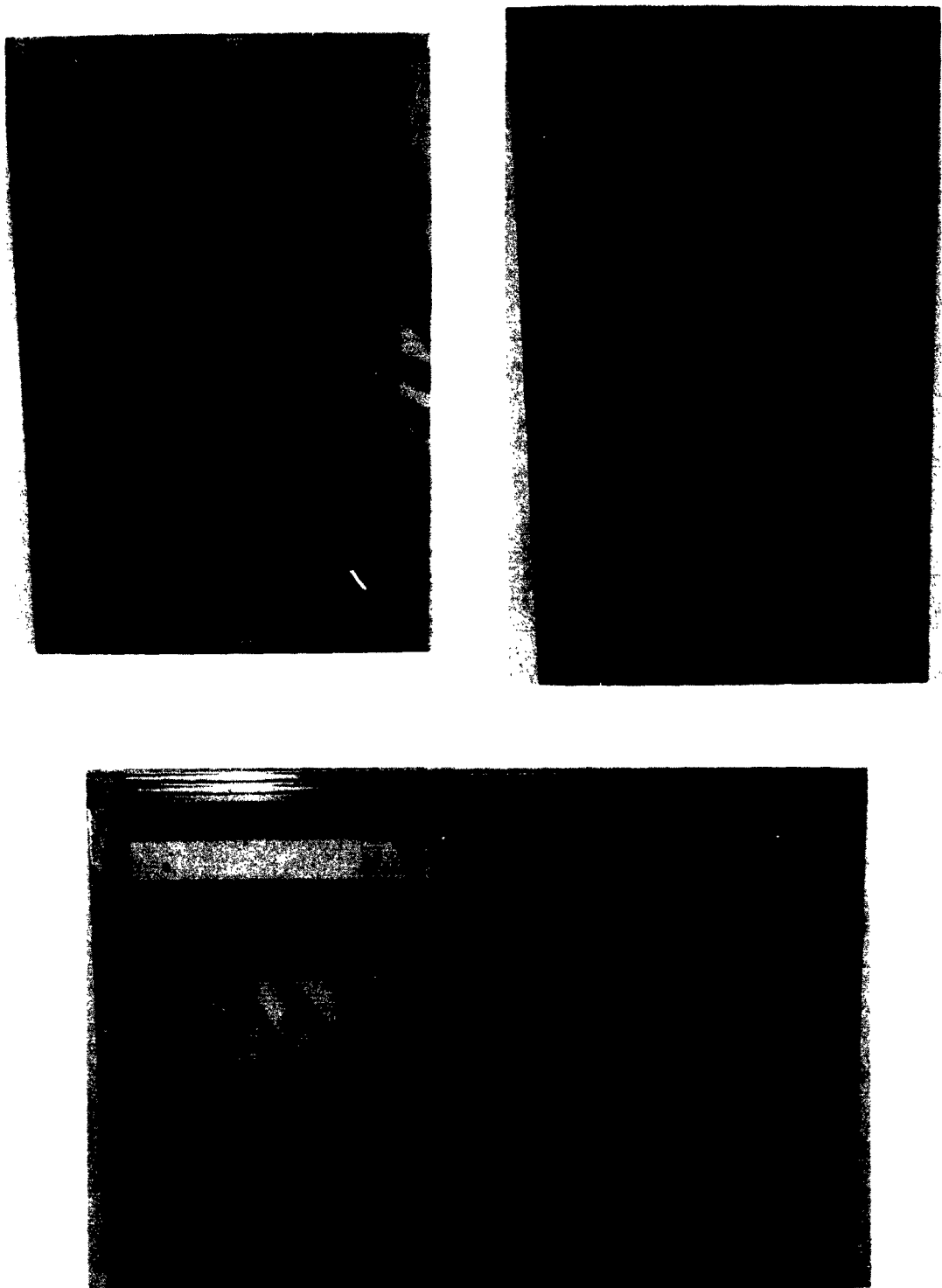


Fig. 29. 50-Channel Strain Gage Bridge Box

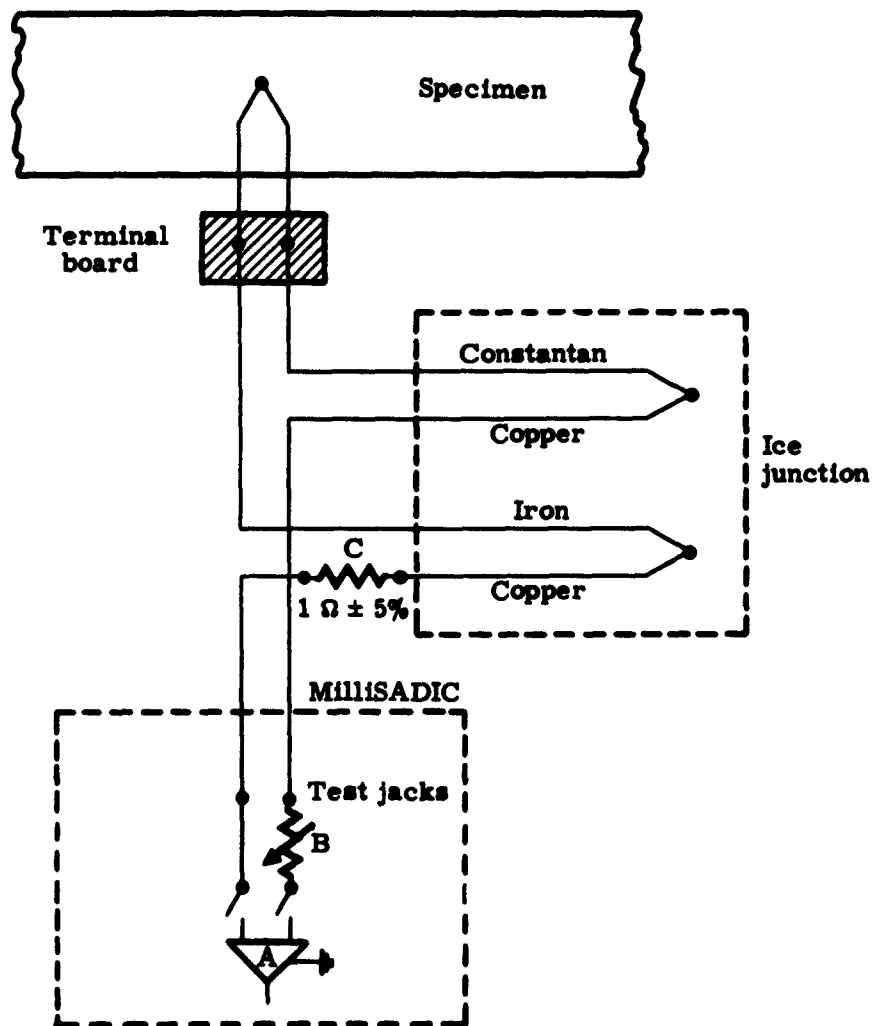


Fig. 30. Typical Thermocouple Circuit

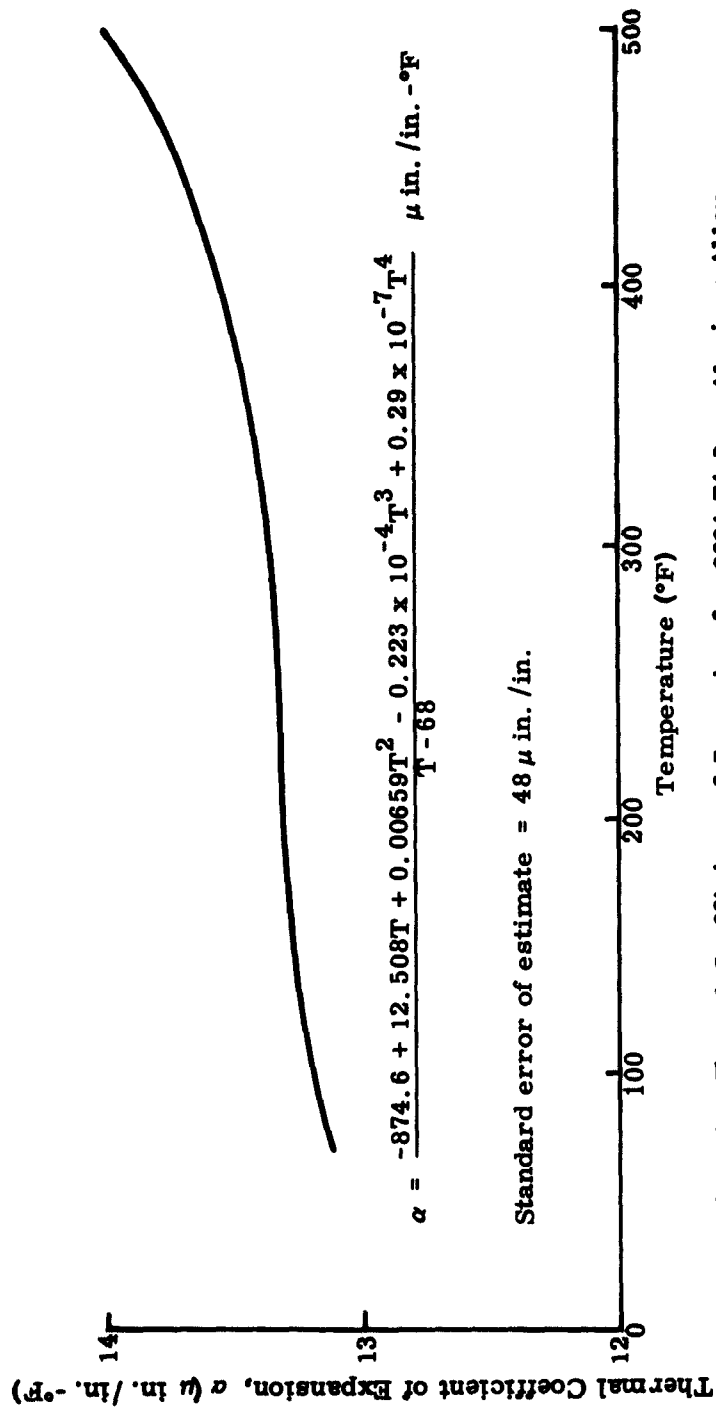


Fig. 31. Thermal Coefficient of Expansion for 2024-T4 Bare Aluminum Alloy

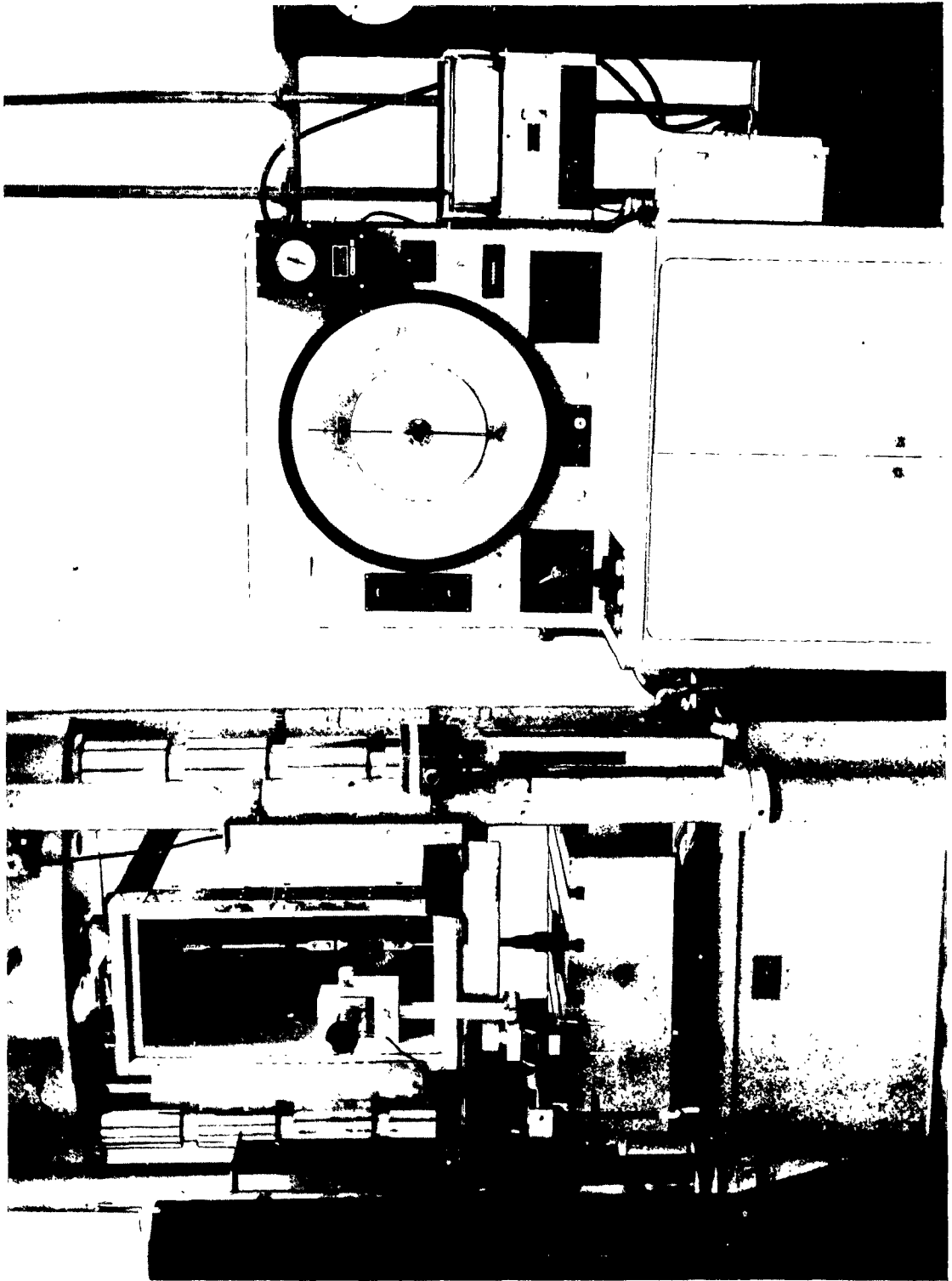


Fig. 32. Tension Coupon Test Setup

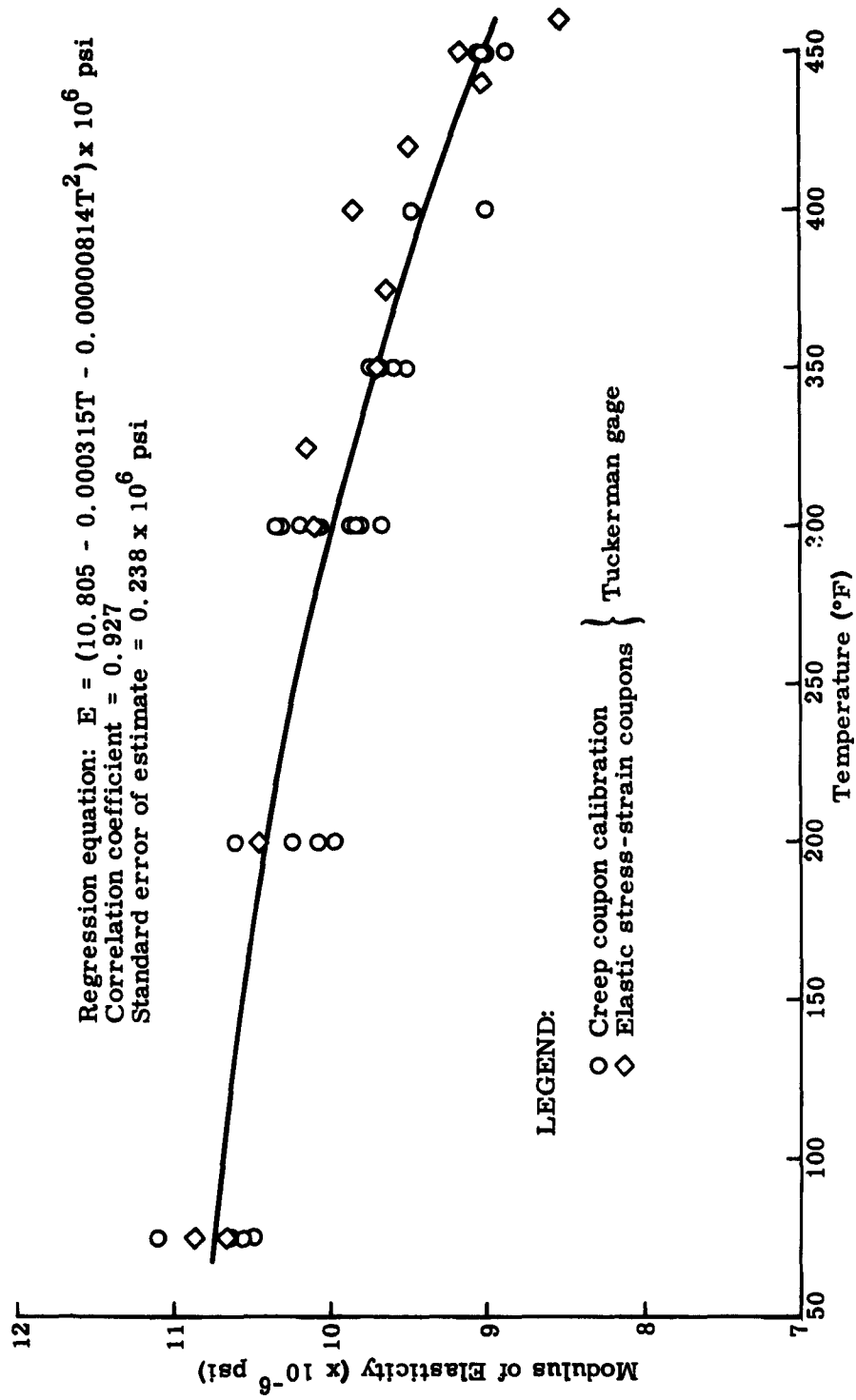


Fig. 33. Modulus of Elasticity Versus Temperature for 2024-T4 Bare Aluminum

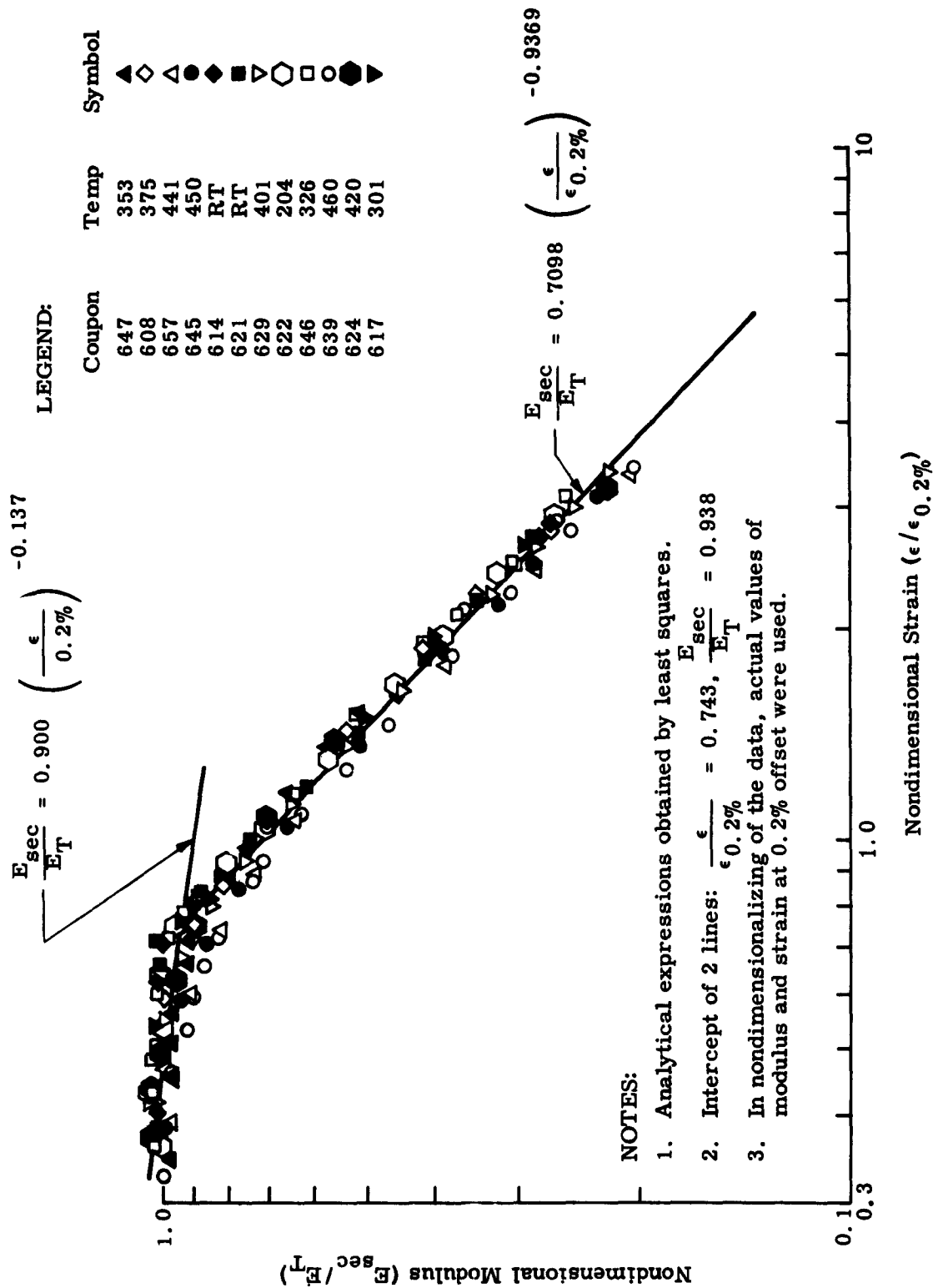


Fig. 34. Nondimensional Stress-Strain Curve for 2024-T4 Bare Aluminum Alloy

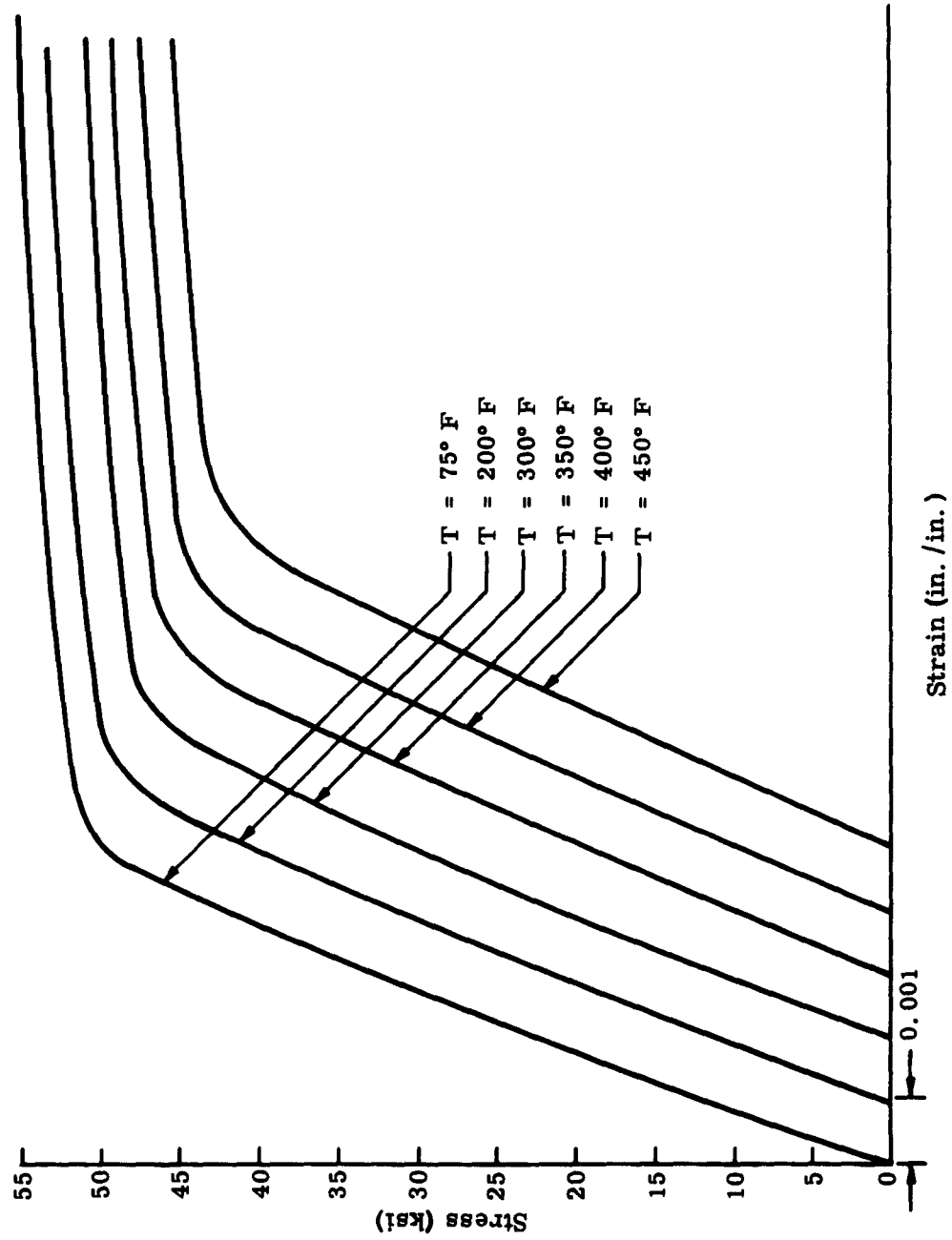


Fig. 35. Spectral Stress-Strain Curves for 2024-T4 Bare Aluminum Alloy

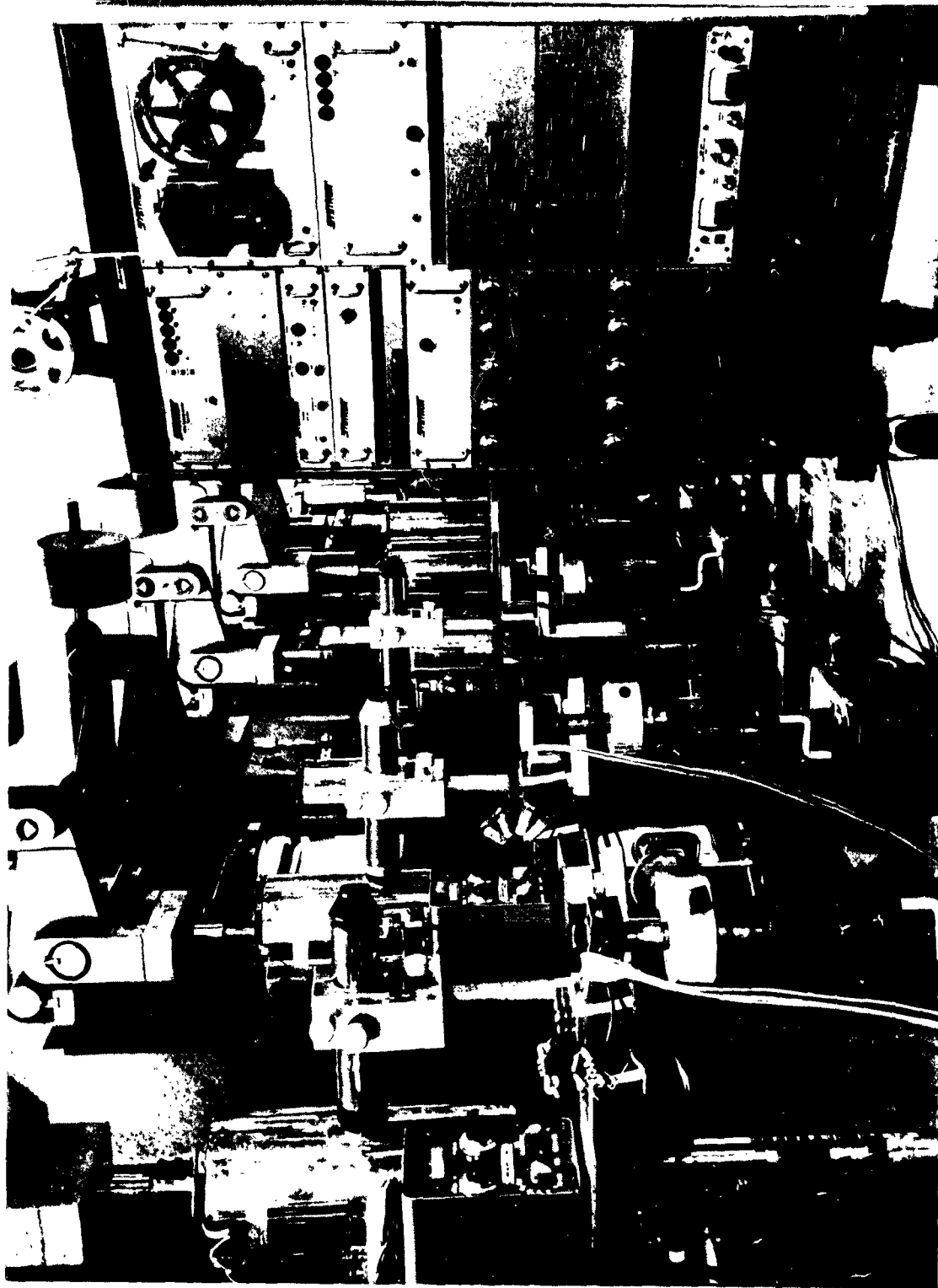


Fig. 36. Overall View of Creep Coupon Test Setup

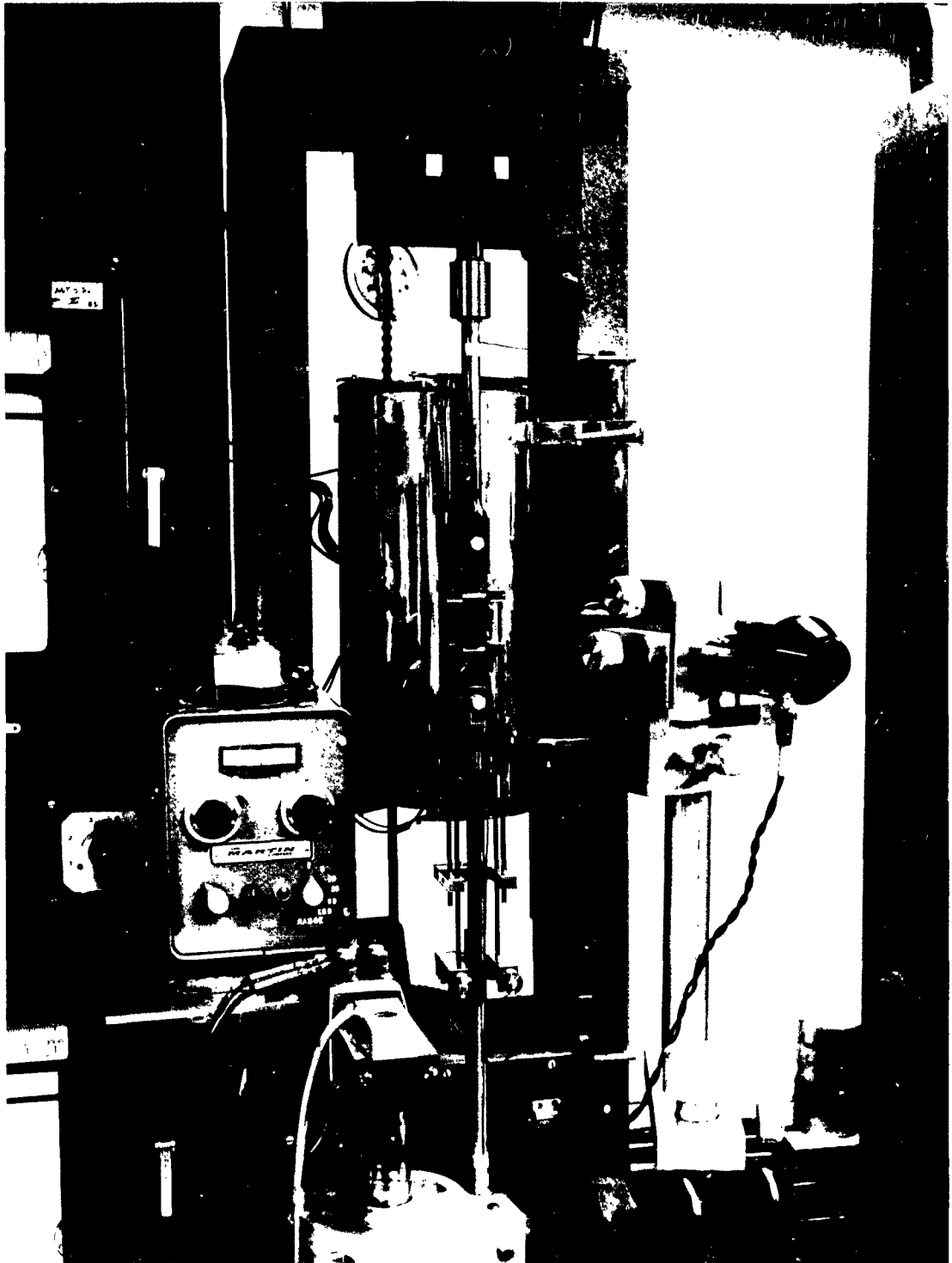


Fig. 37. Instrumented Creep Coupon

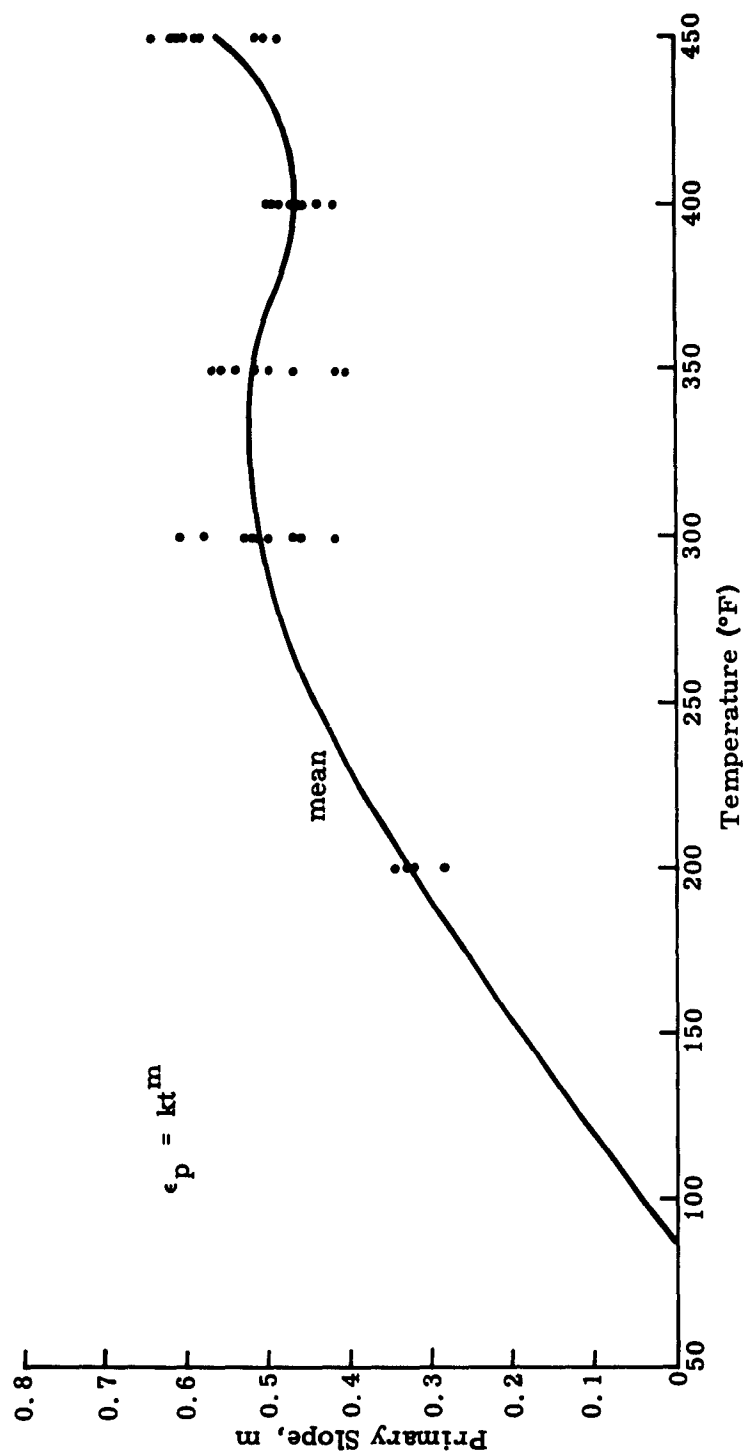


Fig. 38. Primary Slope, m

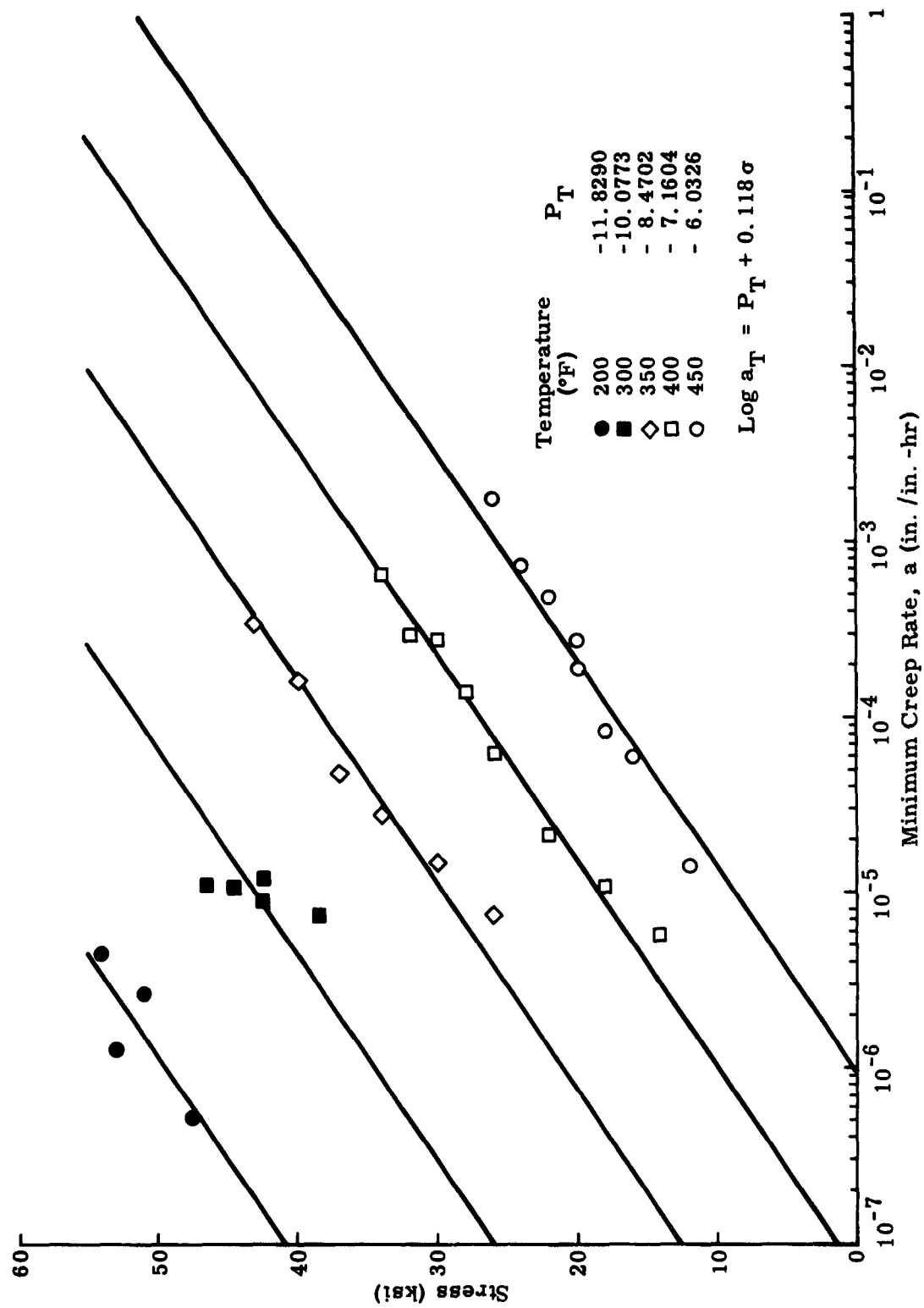


Fig. 39. Minimum Creep Rate a

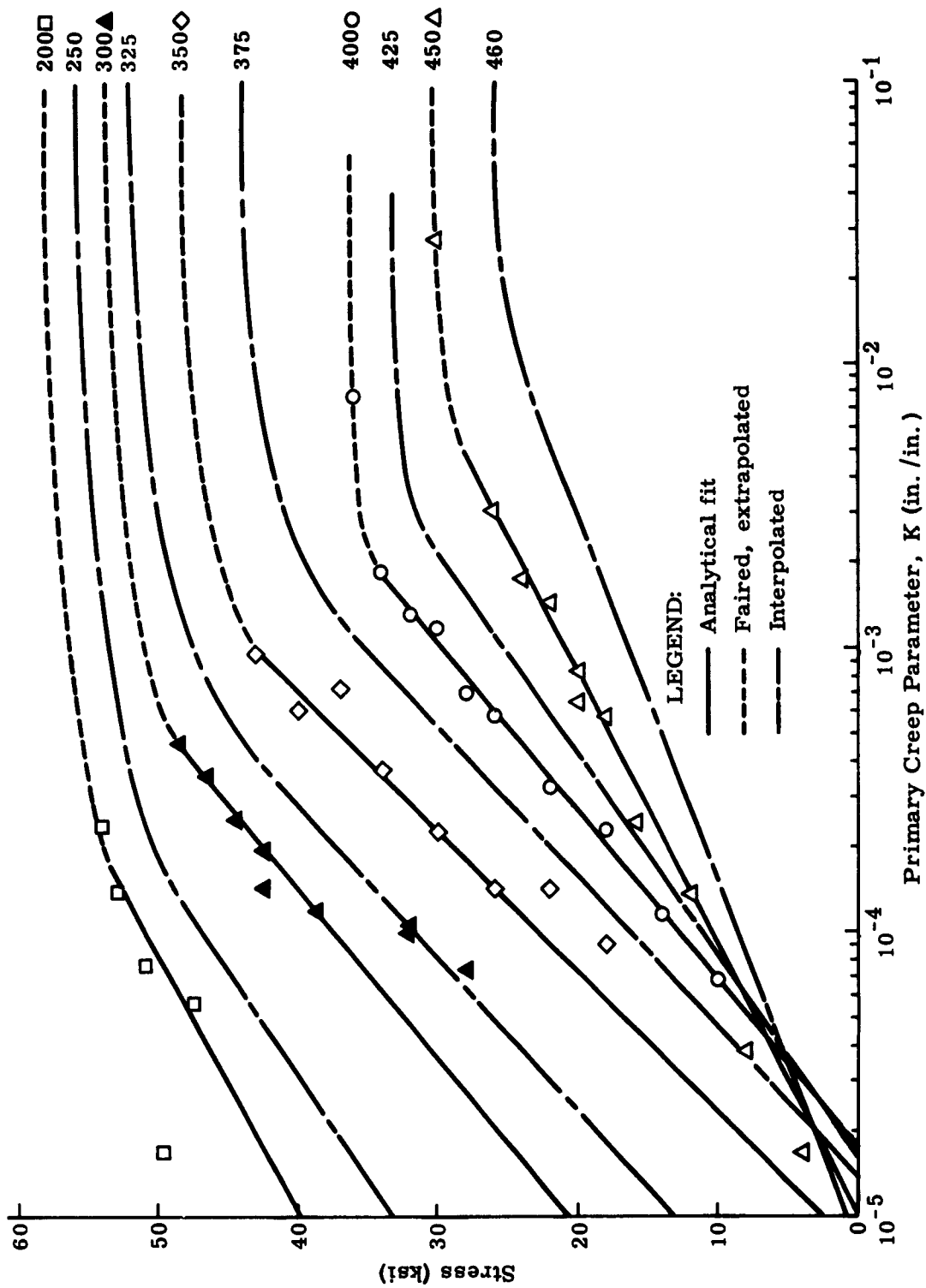
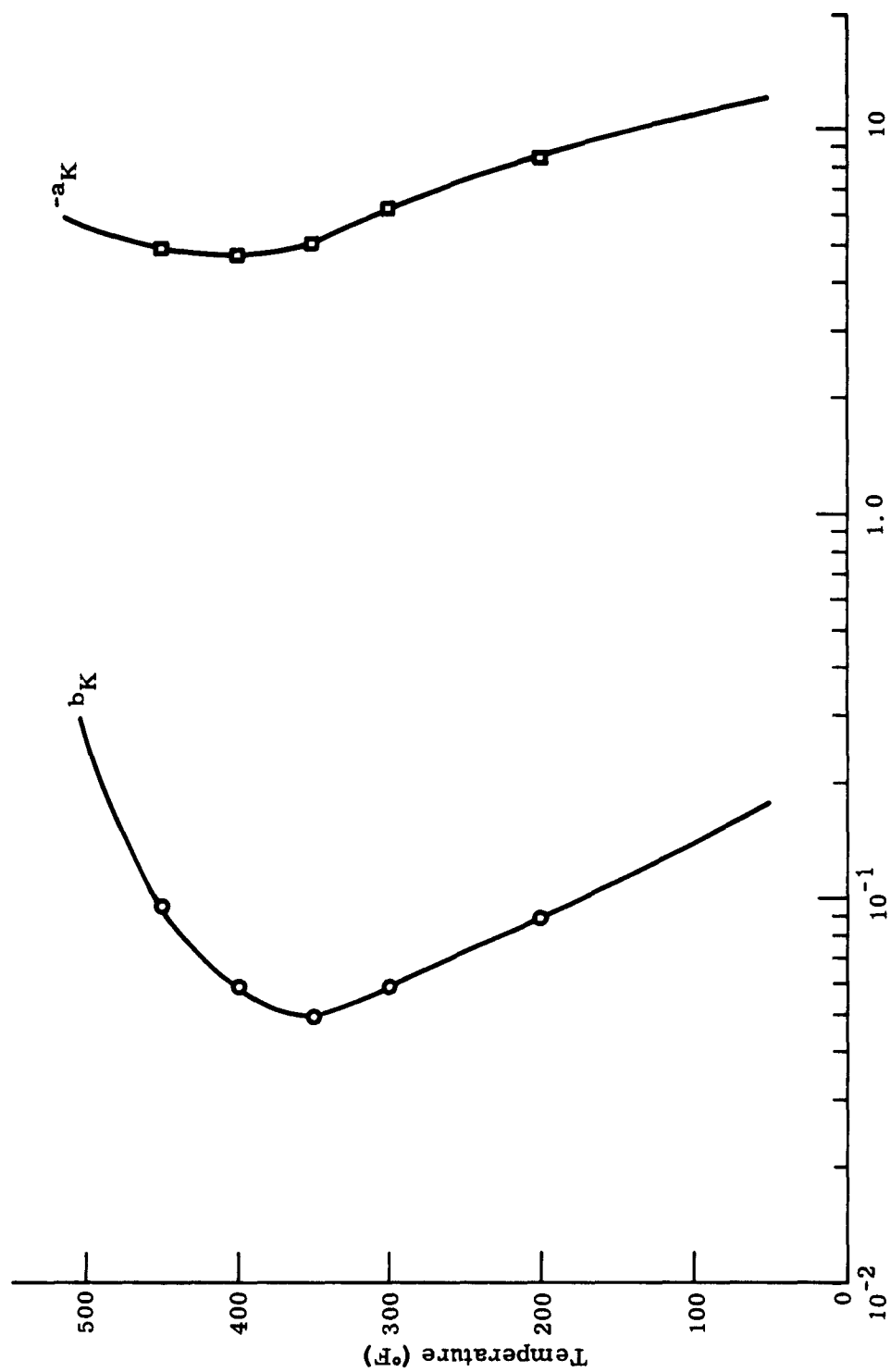


Fig. 40. Primary Creep Parameter K (in./in.)



Auxiliary Parameters (b_K) and ($-a_K$)

Fig. 41. Coefficients in $\log K = a_K + b_K a$

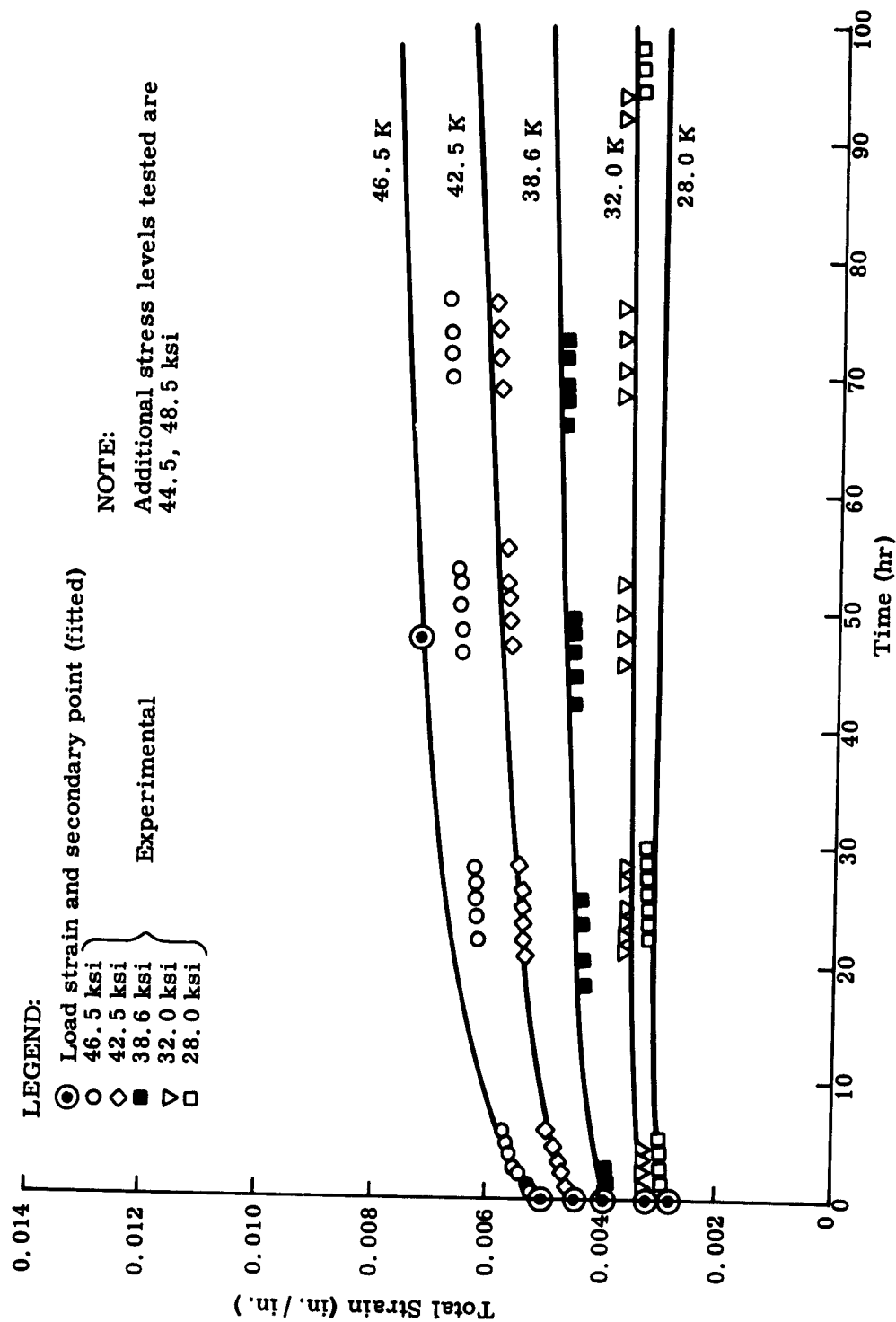


Fig. 42. Spectral Creep Curves for 2024-T4 Bare Aluminum Alloy (300° F)

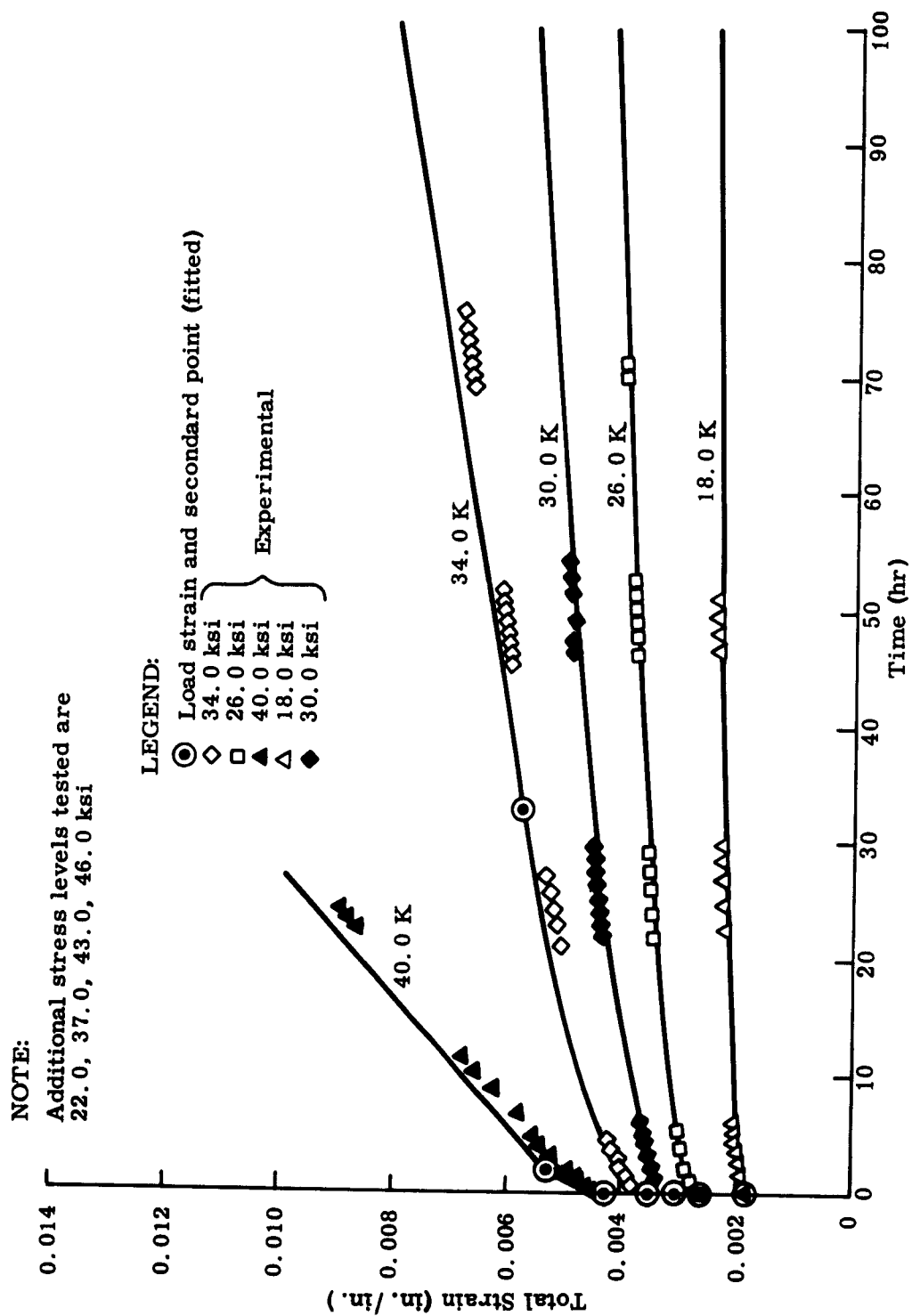


Fig. 43. Spectral Creep Curves for 2024-T4 Bare Aluminum Alloy (350° F)

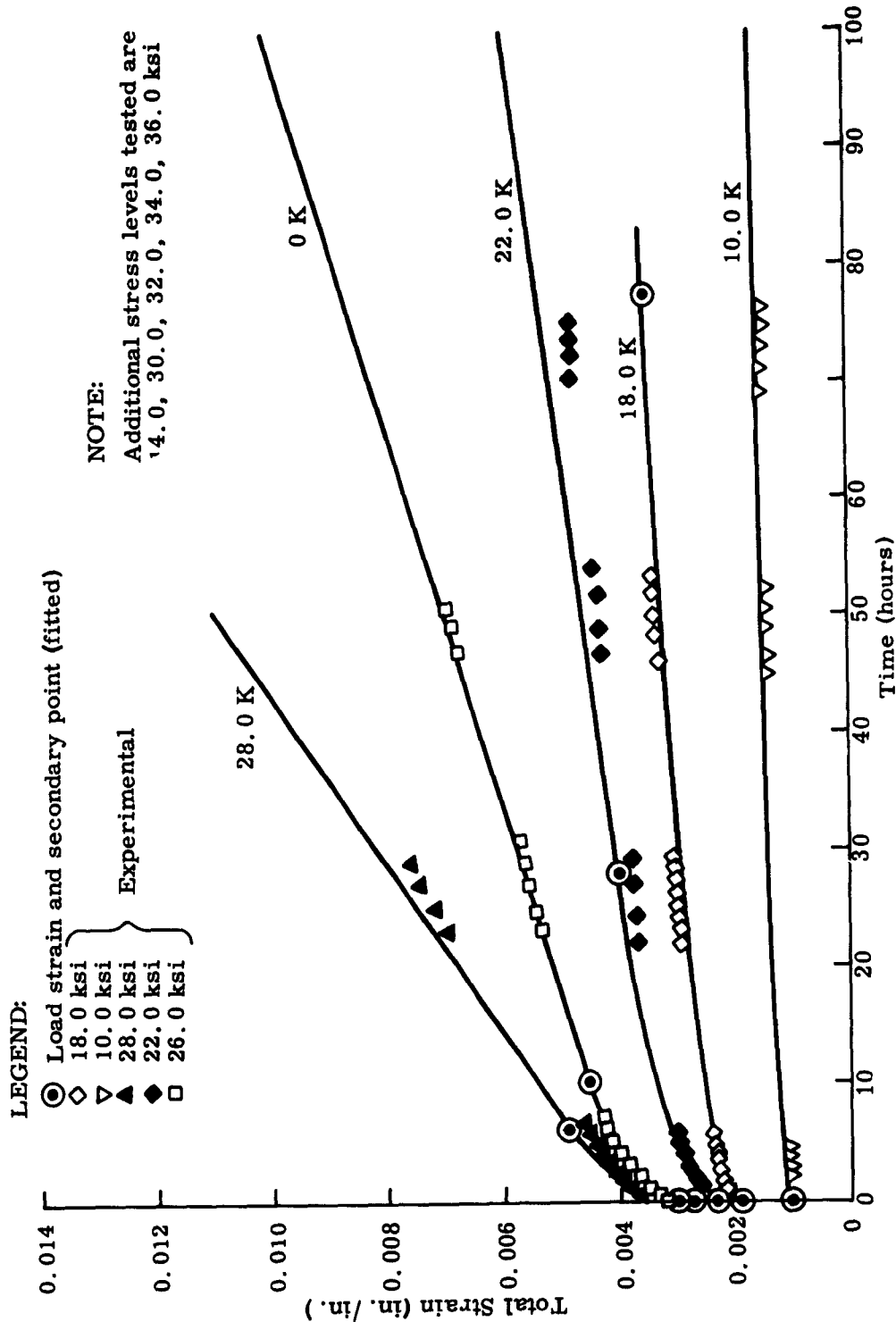


Fig. 44. Spectral Creep Curves for 2024-T4 Bare Aluminum Alloy (400° F)

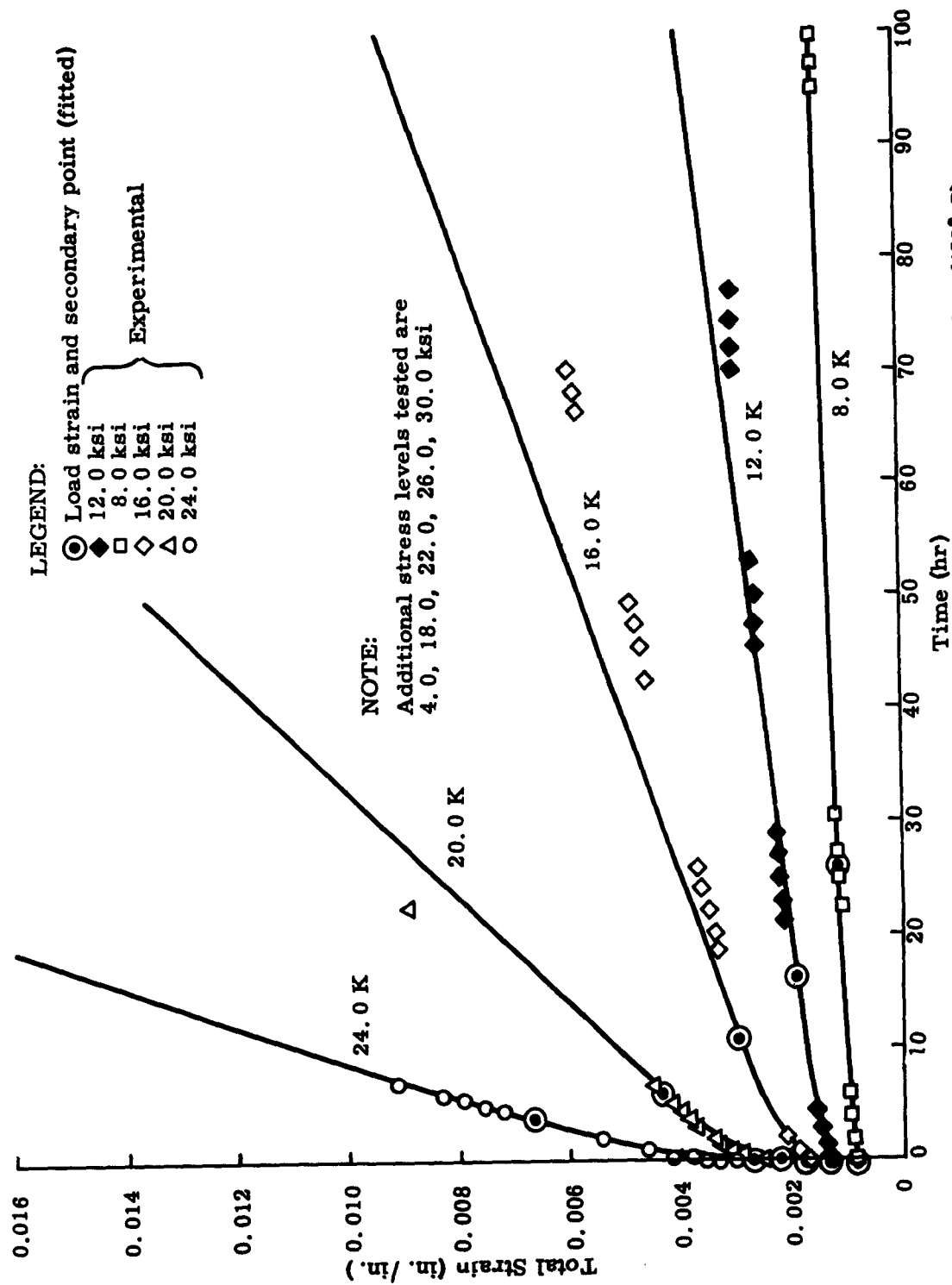


Fig. 45. Spectral Creep Curves for 2024-T4 Bare Aluminum Alloy (450° F)

<p>Aeronautical Systems Division, Dir/Aeromechanics, Flight Dynamics Lab, Wright-Patterson AFB, Ohio.</p> <p>Rpt Nr ASD-TR-61-667, Vol III. ELASTO-PLASTIC ANALYSIS OF STRUCTURES UNDER LOAD AND TWO-DIMENSIONAL TEMPERATURE DISTRIBUTIONS: Experimental Evaluation of the General Time-Dependent Analysis. Final report, Mar 63, 93 p. Incl illus., tables, 6 refs.</p> <p>Unclassified Report</p> <p>This report describes investigations performed to determine experimentally the validity of the time-dependent aspects of a time-dependent, elastoplastic stress and strain analysis method (published in ASD-TR-61-667, Vol. I "Elasto-Plastic Analysis of Structures Under Load and Two-Dimensional Temperature Distributions") for</p> <p>(over)</p>	<p>1. Thermal Stress</p> <p>2. Experimental Data</p> <p>3. Aluminum Alloys</p> <p>4. Plasticity</p> <p>5. Creep</p> <p>I. AFSC Project 1467, Task 146701</p> <p>II. Contract No. AF33(616)7738, BPS No. 241-1367-14002</p> <p>III. Martin Marietta Corp., Balto. Div., Baltimore, Md.</p> <p>IV. R. J. Edwards</p> <p>V. Secondary Rpt Nr RR-35</p> <p>VI. In ASTIA collection</p> <p>VII. Avail fr OTS</p>	<p>Aeronautical Systems Division, Dir/Aeromechanics, Flight Dynamics Lab, Wright-Patterson AFB, Ohio.</p> <p>Rpt Nr ASD-TR-61-667, Vol III. ELASTO-PLASTIC ANALYSIS OF STRUCTURES UNDER LOAD AND TWO-DIMENSIONAL TEMPERATURE DISTRIBUTIONS: Experimental Evaluation of the General Time-Dependent Analysis. Final report, Mar 63, 93 p. Incl illus., tables, 6 refs.</p> <p>Unclassified Report</p> <p>This report describes investigations performed to determine experimentally the validity of the time-dependent aspects of a time-dependent, elastoplastic stress and strain analysis method (published in ASD-TR-61-667, Vol. I "Elasto-Plastic Analysis of Structures Under Load and Two-Dimensional Temperature Distributions") for</p> <p>(over)</p>	<p>1. Thermal Stress</p> <p>2. Experimental Data</p> <p>3. Aluminum Alloys</p> <p>4. Plasticity</p> <p>5. Creep</p> <p>I. AFSC Project 1467, Task 146701</p> <p>II. Contract No. AF33(616)7738, BPS No. 241-1367-14002</p> <p>III. Martin Marietta Corp., Balto. Div., Baltimore, Md.</p> <p>IV. R. J. Edwards</p> <p>V. Secondary Rpt Nr RR-35</p> <p>VI. In ASTIA collection</p> <p>VII. Avail fr OTS</p>	<p>structures exposed to complex load and two-dimensional elevated temperature environments. An experiment specifically designed to evaluate the accuracy of the theoretical method is presented. This consisted of a test of a long flat plate subjected to step functions of load randomly combined with several two-dimensional temperature distributions. Magnitude and duration of the test variables were such that plasticity, creep, and appreciable thermal stress systems were introduced. Comparisons are made of experimental total strains with analytical total strains calculated for conditions identical with the test. The degree of correlation achieved indicates verification of the analysis method within the range of test parameters selected.</p> <p>(over)</p>	<p>structures exposed to complex load and two-dimensional elevated temperature environments. An experiment specifically designed to evaluate the accuracy of the theoretical method is presented. This consisted of a test of a long flat plate subjected to step functions of load randomly combined with several two-dimensional temperature distributions. Magnitude and duration of the test variables were such that plasticity, creep, and appreciable thermal stress systems were introduced. Comparisons are made of experimental total strains with analytical total strains calculated for conditions identical with the test. The degree of correlation achieved indicates verification of the analysis method within the range of test parameters selected.</p> <p>(over)</p>	<p>structures exposed to complex load and two-dimensional elevated temperature environments. An experiment specifically designed to evaluate the accuracy of the theoretical method is presented. This consisted of a test of a long flat plate subjected to step functions of load randomly combined with several two-dimensional temperature distributions. Magnitude and duration of the test variables were such that plasticity, creep, and appreciable thermal stress systems were introduced. Comparisons are made of experimental total strains with analytical total strains calculated for conditions identical with the test. The degree of correlation achieved indicates verification of the analysis method within the range of test parameters selected.</p> <p>(over)</p>	<p>structures exposed to complex load and two-dimensional elevated temperature environments. An experiment specifically designed to evaluate the accuracy of the theoretical method is presented. This consisted of a test of a long flat plate subjected to step functions of load randomly combined with several two-dimensional temperature distributions. Magnitude and duration of the test variables were such that plasticity, creep, and appreciable thermal stress systems were introduced. Comparisons are made of experimental total strains with analytical total strains calculated for conditions identical with the test. The degree of correlation achieved indicates verification of the analysis method within the range of test parameters selected.</p> <p>(over)</p>
---	---	---	---	---	---	---	---